Acoustic Segregation and Structural Timber Production

by

Gregory John Searles

A thesis submitted in partial fulfilment of the requirements of
Edinburgh Napier University for the award of

Doctor of Philosophy

April 2012

Abstract

Concerns about changes in the quality of the maturing British spruce resource (principally stiffness) have raised doubts about maintaining strength grading pass-rates. Acoustic (or stress wave) instruments provide a non-destructive measurement of stiffness and are increasingly used to classify/segregate forests, trees and logs. A fundamental assumption in the use of acoustic instruments is that of constant density, yet there is little understanding of density variation within the British spruce resource. Understanding this variation is essential for understanding the accuracy of acoustic instruments, which can affect how and when they should be used. The extent of variation in density was determined experimentally from a range of sites with contrasting silviculture and environments, and trees within-site were chosen to reflect the extremes of growth rate. Variation within tree (important for log resonance measurement) was found to depend both on dominance class (*i.e.* relative diameter) and height within the tree. The density in the outer part of a tree (important for standing tree time of flight measurement) was found to vary with dominance class, distance in from the bark and season. Mean green density profiles of the outer part of the tree show that density ceases to be constant between dominance classes after 10 mm in from the bark. The effect of this variation could not be quantified because the propagation behaviour of the stress wave within a tree is not fully understood. An examination of wave propagation showed that it did not conform to behaviour as described in the literature and interaction with both density variation within the tree and with the tree's boundaries is likely to affect the accuracy of this technique. The utilisation of these instruments was also examined within a sawmill simulation study, to provide an alternative to simply diverting low stiffness logs to lower value, non-structural products. Exploiting the predictable within-tree stiffness variation and adjusting cutting patterns to avoid the lower stiffness core of lower stiffness logs allowed production of consistently higher stiffness battens. A reduction in twist and knot severity was also observed, but not at significant levels until the juvenile zone (first ten years) was completely excluded. All batten properties improved with increasing cambial age (number of growth rings from the pith). Alternative cutting patterns

had no effect on the recoverable batten volume from within a log and showed considerable potential to improve value to sawmills.

Table of Contents

List of Tables

List of Figures

Acknowledgments

Author's declaration

I, the author, declare that the work presented here is my own, except where information and assistance obtained has been acknowledged. This thesis has not been submitted for any previous application for a degree.

……………………………………………….

Gregory John Searles

February 2012

Common terms and abbreviations

Term	Description
Acoustic velocity	Used synonymously with stress wave velocity, it is the speed at which an impulse travels within a tree or log
Billet	Small length of log
Dilatational wave	A stress wave within an infinite three-dimensional body (*i.e.* a wave with no boundary interactions)
DMOEsort	A group of logs that has been sorted using acoustic velocity and density in the dynamic MOE equation.
Dynamic MOE	The MOE measured using stress wave velocity
Fibre saturation point (FSP)	Is the point at which the cell walls of wood are saturated with water
Green density	The density of a freshly felled or undried wood which contains a moisture above the fibre saturation point
JWCsort	A group of logs that has been sorted using acoustic velocity and density in the dynamic MOE equation and accounts for the size and location of the juvenile core.
Log recovery	The proportion of the log that has been converted into battens
Log sweep	Is a description of how a log deviates from being completely straight
Microfibril angle (MFA)	The helical winding angle relative to the vertical cell axis of the cellulose microfibrils in the secondary cell wall

MOE	Modulus of Elasticity (MOE) is the stiffness of the material
Oven dry density	The density of a wood sample with 0% moisture content
Plane wave	A wave with an equal distribution of strain over the cross section such that all elements of the cross section move identically and parallel to the sides of the rod
Resonant velocity	The acoustic velocity is derived from the resonant frequency of the specimen being tested. The velocity is controlled by the volume weighted average stiffness of the entire specimen.
Static MOE	The MOE derived from a four point bending test
Stress wave	The propagation of energy through a material caused by external excitation
TOF	Time of Flight
TOF velocity	The stress wave velocity determined by measuring the time it takes for the stress wave to travel a certain distance
Value recovery	The value of the battens produced from a log
Velsort	A group of logs that has been sorted using acoustic velocity only and assuming density is constant.
Volume recovery	Same as log recovery

1 Introduction

1.1 *Overview to this study*

Sitka spruce (*Picea sitchensis* (Bong.) Carr.) is the main species used in the production of solid wood products within the UK, with approximately 692,000 hectares of plantations (Forestry Commission 2010). Over 75% of this plantation area is in Scotland or Northern England. Norway spruce (*Picea abies* (L.) Karst.), which consists of approximately 9% of the spruce forests in the United Kingdom and Ireland, is combined with Sitka spruce and recognised as "British spruce" in EN14081:1-2005 (CEN).

Wood production from Scottish forests is expected to increase to 10 million m^3 by 2020 (SFIC 2004) yet there is great concern that the quality of the round timber reaching maturity in the next 15-20 years is lower than that of the current resource due to changes in silvicultural practices (Macdonald and Hubert 2002). Any reduction in the quality of the resource is detrimental to timber processors within the UK as markets for non-structural timber such as pallets, packaging and fencing are saturated or likely to become saturated in the near future (McIntosh 1997). One of the key components of quality is stiffness, or modulus of elasticity (MOE). Stiffness is usually the mechanical property which limits the grade that British spruce can attain under EN338 (CEN 2003) (Moore *et al*. 2009b). Therefore, processors in the UK are facing a difficult challenge; increasing the proportion of higher quality construction timber from a resource that is probably becoming less suitable for the task.

In the United States, New Zealand and Australia, the use of stress wave (or acoustic) instruments, described in section 2.2, are commonly used to segregate between low and high stiffness material (*e.g*. Wang *et al*. 2001, 2002, 2003; Tseheye *et al*. 2000, Matheson *et al*. 2002, Dickson *et al*. 2004). These instruments provide a fast, direct measurement of stiffness (Huang *et al*. 2003) yet in doing so rely on an assumption of constant, uniform density for trees and

logs. Any deviation away from constant density will result in a proportional error in the measurement of stiffness using this technique.

Within the last five years the use of acoustic instruments has become more common in the UK, being used by both industry and research (*e.g.* Mochan *et al.* 2007, Auty and Achim 2008, Moore *et al.* 2009b). If these instruments can be proven to be accurate for British spruce, then this technique would enable foresters to determine the proportion of the resource that is potentially suitable for producing structural timber (Moore *et al.* 2009b) and allow processors to ensure that log quality can be matched to production and user requirements.

This thesis aims to establish the reliability of these instruments in British spruce by measuring the variation in the density of trees and logs and an examination of the wave propagation behaviour and how it can affect accuracy. The industrial application of these instruments was also examined to determine whether a more sophisticated approach than simply segregating low stiffness logs could be shown to provide extra value to sawmillers. A more sophisticated approach is required as the increased proportion of low stiffness logs expected over the coming years and the expected saturation of the non-structural market, means that simply segregating low stiffness logs to non-structural applications is unlikely to benefit the industry. Utilising the within-log stiffness variation that occurs within plantation grown conifers, such that higher value battens can be extracted from high stiffness areas within the log with alternative cutting patterns, potentially offers a more efficient approach to sawmilling low stiffness logs. The viability of this technique in terms of its effect on sawmill processing and its effect on yield and value needs to be established.

A field work and laboratory approach was undertaken to fulfil these aims as it was necessary to better understand the fundamental causes of error in acoustic instruments and how they may be utilised more efficiently. Further numerical/analytical modelling can follow on but this thesis focuses on the error and application of these instruments.

Ten sites were chosen (see section 3.2) to establish the variation in density of both logs and the wood nearest the bark in trees. These sites were from a contrasting range of environments, yield classes and silvicultural treatments, to provide a broad range of tree growth rates and wood properties. Further, within each site, test trees were chosen to reflect the variation in dominance class to again, examine the broadest range of wood properties that may affect the assumption of constant density for acoustic instruments.

To examine the effect of alternative cutting patterns, 155 British spruce logs were divided into four equal size and equal stiffness sample groups and used in a sawmill simulation experiment. Each of the four groups were cut according to specific rules based on the assumed level of knowledge about the wood properties of the logs within the group. The effect of each of the specific cutting rules on batten MOE was then compared. Also examined was the effect of the cutting rules on distortion and knots, two of the other major causes of battens being downgraded. This approach was chosen because whilst there are a range of theoretical and experimental results in the literature concerning either the ability of acoustic instruments to segregate logs based on stiffness or the pith to bark variation in stiffness, a study which examines the economic and processing viability of combining the two has not been explored previously.

1.2 Thesis Aims

The objectives of this thesis are:

1. Investigate the potential causes of error when using acoustic instruments to measure stiffness of standing trees and logs, examining effects such season, dominance class and silviculture.
2. Compare the accuracy of standing tree instruments to predict log velocity with other indicators such as live crown ratio and slenderness.
3. Simulate a standing tree acoustic measurement, examine the wave propagation behaviour and compare results with fundamental theories

presented in the wood science literature and qualitatively examine the possible interaction with variation in density of the outer part of a tree.

4. Determine if alternative cutting patterns based on log acoustics could be a viable way of maintaining the viability of sawmilling in the face of declining timber quality.

1.3 Thesis outline

Chapter 2 contains a general introduction to the relevant literature, explaining how resource quality has been affected, how acoustic instruments work to measure stiffness and how they might be implemented.

Chapter 3 shows an examination the effect of season on standing tree acoustics and the relationship between tree and log velocity over a range of sites, environments and silviculture, all without considering the effect of density. Seasonal sampling of standing tree velocity was undertaken in the summer and winter. A proportion of winter sampling corresponded to periods of freezing temperatures and its possible effects on standing tree acoustics are examined. Values of log velocity are compared with standing tree velocity, stem slenderness and live crown ratio. The proportion of the variation in log velocity that was explained by standing tree velocity was quite poor and led to the development of a set of assumptions implicit in the use of standing tree instruments that need to be met to obtain accurate measurements.

Chapter 4 re-examines the data from Chapter 3, this time with the inclusion of density in the analysis. Log velocities were adjusted for changes in density and its relationship with standing tree velocity, slenderness and live crown ratio were re-examined. Also considered is the proportion of juvenile wood at breast height between trees of different dominance class and its possible effect on processing. The green density profiles of the wood nearest the bark were examined across dominance classes and season and were found to vary for both. However, the effect of the variation in density of wood in the outer part of standing trees for standing tree measurements was hard to determine. Using the density of the outer 30 mm of the tree to adjust the standing tree velocity resulted in no

improvement in the relationship with log velocity. This opened up another avenue of investigation since it was realised that the exact path/trajectory of a stress wave in a standing tree acoustic measurement is unknown and is only assumed to travel in the outer portion of the tree. Chapter 5 examines this problem in more detail.

Chapter 5 reports the result of an experiment where the stress wave arrival times in three different diameter test logs are mapped over a cross section at 0.5 m and 1 m from the stress wave initiation point. The original premise behind this experiment was to identify if the variation in the outerwood density profile observed in Chapter 4 between dominance classes had a measureable effect on the speed of the stress wave. However, further investigation in the experimental results of this chapter and the results of a very limited number of other research papers examining stress wave behaviour in standing trees, showed inconsistencies with the generally accepted theory. The basic fundamental concepts and theory behind wave mechanics are discussed and a distinction is found between what aspects of wave propagation in trees are covered by the theory and which are not. The implications of these findings on the accuracy of standing tree stress wave instruments is also discussed.

Chapter 6 examines the effect of trying to improve the mean stiffness of structural battens produced at a sawmill by altering the cutting patterns from those that would typically be used to produce construction grade timber. This experiment was undertaken in an attempt to find solutions to the fundamental problem facing processors outlined earlier; trying to increase the proportion of higher quality construction timber from a resource that may be becoming less suitable for the task. This is a sawmill simulation study which combined a number of factors, not previously considered simultaneously, to estimate the potential value of alternative cutting patterns to a sawmill. The key aspects of this experiment that differentiate it from other studies are its utilisation of the pith-to-bark variation in stiffness to adjust cutting patterns and the examination of the effect these patterns have on other major quality aspects such as knots and twist. Further, the effect of alternative cutting patterns on log volume recovery and value recovery as well as practical implications for their implementation to

processors is discussed. The experiment also examines the effect that different levels of knowledge about the log have on the quality of the battens. Levels of knowledge range from knowing only the size and shape of the log, *i.e.* as per typical sawmill operation; knowing its acoustic velocity; knowing its acoustic velocity and density; and knowing its acoustic velocity, density and size and location of the juvenile core.

2   Introduction to the literature

The chapter contains a general introduction to the literature concerning:

- The effects of forest practices on the quality of the resource and why it is expected to be in decline.
- How acoustic velocity is measured within the forest industry and the assumptions required for their use.
- How acoustic tools might be implemented to improve batten quality.

2.1   Effect of forest practices on resource quality

Wood quality is defined by its fitness for purpose (*e.g.* Johansson *et al*. 1994). In this case quality is defined as the mechanical properties and the tree growth characteristics that have the greatest effect on the use of wood for structural applications. These include; knots, stem straightness, taper, density, grain angle, dimensional stability (*i.e.* distortion), Modulus of Elasticity (MOE or stiffness) and Modulus of Rupture (MOR or strength).

The quality of the British spruce resource is perceived to be declining due to a number of factors:

- A reduced rotation length due to advances in tree breeding is resulting in trees reaching merchantable size at younger ages (Macdonald and Hubert 2002)
- An increased proportion of plantation forests are being established on exposed upland sites, where there is a high risk of wind damage once trees reach a critical height and require felling before wide spread damage can occur (Rollinson 1987, Macdonald and Hubert 2002).
- A move to wider planting spacing in order to reduce establishment costs (Wardle 1967).
- A no-thinning policy in plantations where either the risk of wind damage is too high (Rollinson 1987, Malcolm 1997), or where financial surplus on early selective thinnings is not possible (Cameron 2002).

Factors such as stem straightness and taper do not just affect the recoverable yield from a log but also influence the quality of sawn battens. For example, consider Figure 2.1 obtained from PowerSAW (SAATECH Systems Pty Ltd) sawing simulation software, which shows a typical sawmill cutting pattern on a highly tapered log.
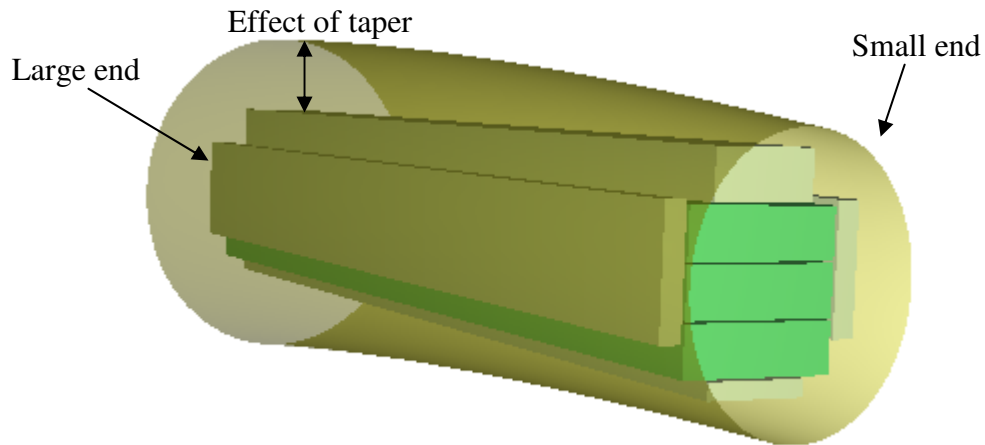
Figure 2.1. Example cutting pattern in highly tapered log.

When logs are processed into battens, saws run in straight lines relative to any distortion or flaring. This results in battens which have inclined grain and variation in grain angle from end to end because a batten's cross section which starts near the bark at the small (or top) end of the log may be much closer to the centre of the log at the large (or bottom) end. These battens are therefore less stiff, weaker and more likely to distort (Brazier and Mobbs 1993).

A tree's mechanical and physical properties, including straightness and taper, are influenced by the environment, silviculture and genetics of the plant stock (Lassere *et al*. 2009). The choice of environment is limited by the availability of land, *e.g.* in the UK, forest planting has taken place on low fertility soils at higher elevations in order maintain land for agricultural use (Malcolm 1997), yet tree breeding programmes and a range of silvicultural options are available to forest managers in order to manage the quality of the final crop. The financial and practical limitations placed on forest managers to enact these options are

discussed later in this section. What follows is a brief discussion on how rotation length, spacing and thinning all affect the suitability of Sitka spruce in the UK for structural purposes. Also discussed is some of the history of forest management in the UK and how the difficult job of trying to obtain greater yields at lower costs and shorter rotations has been administered when all mechanical properties tend to improve with age, slower growth and are adversely affected by the greater wind speeds typical at higher altitudes.

2.1.1 Rotation Length

The genetic improvement of Sitka spruce began in 1963 (Lee 1999) and since then there have been significant improvements in growth rate and stem straightness. Consequently, trees are reaching acceptable volumes for processing at younger ages and resulting in shorter rotations. The main effect of any reduction in rotation length in plantation conifers, is an increased proportion of juvenile wood. The juvenile core consists of the first 10-20 growth rings from the pith and is characterised by a lower percentage of late-wood, lower density, shorter tracheids with larger microfibril angle and grain angle (Dinwoodie 2000, Larson *et al*. 2001, Macdonald and Hubert 2002, Burdon *et al*. 2004). The presence of juvenile wood has been suggested as one of the greatest causes of variation in wood properties of conifers (Saranpaa 2003) and has a serious deleterious effect on the strength, stiffness and dimensional stability of any resulting battens cut from this portion of the log.

Cameron *et al*. (2005) showed that if forests were harvested at the time of maximum mean annual increment or at a set mean tree diameter, there would be a higher proportion of juvenile wood in fast growing progenies and that the quality of the juvenile wood, *i.e*. the effect on stiffness and stability, would be more detrimental compared with slower grown trees. Similarly, if trees are grown on exposed, upland sites where the risk of wind throw is high, stands will be harvested before they reach a critical height. Rollinson (1987) showed that the harvest age for sites at high risk of wind throw ranged from 33 years to 51 years, which will have a significant effect on the proportion of juvenile wood within the stem and therefore batten quality.

The increase in forest cover in Great Britain from around 3% in 1920 to the current 12% has been mostly achieved by afforestation on upland sites (Malcolm 1997, Mason 2007). Therefore the combination of growth rate and risk of wind throw is a major governing factor in determining the harvest age (or rotation length) and therefore the proportion of juvenile wood entering sawmills.

2.1.2 Spacing

The space available for a tree to grow affects its form and vigour. Control of spacing, either through planting distance or thinning, is one of the main ways a forester can control wood formation and quality in a crop (Brazier and Mobbs 1993, Larson *et al.* 2001, Moore *et al.* 2009). When Sitka spruce was first being planted in the UK in the 1920's, spacings of 0.9 m – 1.2 m were common. This was to achieve early competition between stems in order to encourage straightness of growth, natural pruning (*i.e.* reduced branch and therefore knot size) and weed control (Wardle 1967, Malcolm 1997). Close initial spacing also has the added benefits of reducing the size of the juvenile core and increasing its stiffness due to increased competition, resulting in slower radial growth and a greater allocation of resources to height growth (Watt *et al.* 2006), *i.e.* reducing taper (increasing slenderness). Whilst this may indeed be the optimal spacing for improved timber quality, several very practical constraints have severely limited this as a technique to be used by foresters:

- Closer plant spacing results in much higher establishment costs. Wardle (1967) calculated that there was a 30% reduction in establishment costs if spacing was increased from 1.6 m to 2.4 m with only a 2 – 10% estimated reduction in final yield.
- Either proximity to buyers or poor market conditions mean that a financial surplus on early selective thinnings is not possible (Cameron 2002, Mason 2007). Whilst Cameron (2002) argued that such short term economic savings through the reduction in thinning costs would have detrimental effects on the value of the final crop, it was a policy that was

in place and the consequences still need to be dealt with by today's processors.

- Thinning is not practical on sites where the risk of wind damage is too high (Rollinson 1987, Malcolm 1997). Macdonald and Hubert (2002) report that upwards of 50% of forests managed by the Forestry Commission are on a no-thin regime.

- Shallow soils and/or high winter water tables combined with the inability of Sitka spruce roots to handle anaerobic conditions, mean that wide, lateral spreading of the roots is the only way to maintain stability. This can only be achieved with wide spacings (Malcolm 1997). This has the other stabilising benefit of lowering the trees' centre of gravity by increasing stem taper and having a deeper live crown (Cameron 2002).

One of the most influential studies for Sitka spruce in the UK regarding initial spacing and its effect on wood quality was carried out by Brazier and Mobbs (1993). The authors found that increased spacing severely affected the structural performance of the sawn wood by increasing knot size and reducing stiffness due to a larger proportion of juvenile wood. The main recommendation of the report was to have a maximum planting spacing of 2.0 m for stands that were to remain unthinned in order to obtain an acceptable yield of structural timber. Initial spacing also has an effect on stem straightness and taper: Stirling *et al.* (2000) reported a decrease in stem straightness with increased planting distance and elevation in an extensive survey of stem straightness across southern Scotland. Given that Brazier and Mobbs (1993) made comment in the paper that plant spacings had been widened to 2.4 m and occasionally 2.7 m, this highlights the concern that timber quality is in decline. Simpson and Denne (1997) after revisiting a site used in the Brazier and Mobbs study 7 years later when the trees were 52 years old, found that the differences in the amount of juvenile wood between spacing plots was less marked. The study suggested that self thinning in closely spaced stands (a process by which dominant, larger trees out-compete smaller trees for nutrients and light) effectively kills trees that didn't have a competitive advantage from a very early age. However, it is likely that the variation in diameters within a site at harvest age remains large: Moore *et al.*

(2009b) in an examination of Sitka spruce in 64 sites with ages ranging from 35-50 years across Scotland and northern England, found the range of diameter at breast height (DBH) in live trees varied from 79 mm to 555 mm with an average of 230 mm. The age range examined in Moore *et al*. (2009b) was the typical harvest age of Sitka spruce plantations in the UK of between 35-50 years. This indicates that the self thinning effects of competition are unlikely to have fully set in and that the proportion of juvenile wood is likely to vary significantly from tree to tree within a typical site.

Lassere *et al*. (2005, 2009) assessed the impact of two different spacings, 833 stems ha^{-1} and 2500 stems ha^{-1}, on the wood properties of 11 year old radiata pine (*Pinus radiata* D. Don) in New Zealand. Lassere *et al*. (2005, 2009) found that high initial stocking density had more of an effect on dynamic stiffness measured using non-destructive acoustic instruments on standing trees, than genotype with a 34% and 15% improvement, respectively. There was no effect on density or tree height but there was a significant effect on (DBH), with a 32% reduction for the closer spacing. Waghorn *et al.* (2007) performed a similar experiment across a wider range of spacings; from 209 stems ha^{-1} to 2551 stems ha^{-1}, again with radiata pine in New Zealand but this time with 17 year old trees. Waghorn *et al.* (2007) found a similar trend of increasing dynamic stiffness with increased stocking, yet when comparing results to equivalent spacings in Lassere *et al*. (2005, 2009) found only a 6% improvement. This was attributed to the differences in age between experiments (17 years versus 11 years). The reason for increased stiffness with greater stocking described by Watt *et al*. (2006) was the result of greater inter-tree competition which produces trees that are more slender. To accommodate for increased slenderness, trees must produce stiffer material to reduce the risk of stem buckling (Watt *et al*. 2006). A similar relationship between slenderness and stiffness was also reported for loblolly pine (*Pinus taeda* L.) by Roth *et al*. (2007). Waghorn *et al.* (2007) also reported an increase in distance to the live crown from the base of the tree for closer spacings, which indicates that there is both a reduction in knot size due to earlier shading of branches and that the knots are confined to the centre of the log for those coming from the lower part of the tree. Similarly, Simpson and Denne

(1997) found an increase in distance to the crown for Sitka spruce in the UK as initial spacing was reduced.

2.1.3 Thinning

Thinning of forest stands affects the amount of light, nutrients and water available to the remaining trees. Therefore, trees on thinned sites will have more growing space and will reach a bigger diameter over a given rotation length than unthinned stands (Macdonald and Hubert 2002). This section contains a very brief summary of the environmental and economic factors that affect the timing and intensity of the thinning operation and the selection criteria used, as they are the main factors that affect tree quality (Cameron 2002).

The benefits of thinning in terms of growth promotion are many but the negative effects must also be recognised and balanced against the positive (Larson *et al.* 2001). Full descriptions of the advantages and disadvantages of various thinning regimes can be found in Cameron (2002) and Macdonald and Hubert (2002).

The threat of wind damage is often the most important factor determining thinning policy (Rollinson 1987). As summarised in Cameron (2002), recently thinned stands are less stable than unthinned stands and susceptibility to wind damage can last several years after thinning takes place. This is because in mature, closely spaced unthinned stands, trees are more slender (Cameron 2002, Watt *et al.* 2006, Brüchert and Gardiner 2006) with less lateral spreading of roots (Cameron 2002). Slender trees have a higher centre of gravity which, when combined with a smaller root system, results in a greater susceptibility to wind damage if suddenly exposed to greater winds after thinning. Trees respond to increased wind loads by reducing height growth and increasing diameter growth in the lower part of the stem, *i.e.* increasing taper, and developing a more supportive root system (Cameron 2002). This is an example of a trade-off decision a forester must make: increase a trees' volume production, risk wind damage and reduce the mechanical properties of resulting battens by increasing taper and branch size or produce smaller trees with better mechanical properties.

The decline in the price of small round wood and pressure to make a profit from thinning operations (Rollinson 1987, Cameron 2002) have meant that thinning strategies, in some cases, have had to be modified. It has been argued that the economic case for thinning over the rotation length of the stand depends largely on whether the first thinning was profitable (Grayson 1981, in Cameron 2002). A typical modification to improve profitability is to delay first thinnings by 5 or 10 years and then to adopt a systematic thinning procedure such as line or row thinning. This has the benefit of an increase in volume of the removed trees and cheaper operational costs over selective thinning. Unfortunately, these actions not only result in a greater risk of wind damage (as the remaining trees will have a poorly adapted root systems and a high centre of gravity), they also do nothing to improve the mean stem straightness of the stand (Rollinson 1987). In fact, this type of thinning is associated with an asymmetric crown and an irregular stem form (Cameron 2002).

2.2 Description of acoustic instruments for measuring wood stiffness

Given the considerable site-to-site and tree-to-tree variation in the physical and mechanical properties of harvested wood, not all wood produced from managed forests is suitable for products such as structural timber where mechanical properties, particularly bending strength and stiffness, are important. Historically, the segregation of trees and logs has often been made on the basis of external characteristics, *e.g.* diameter, taper and sweep. While this generally provides valuable information on the volume of timber that can be recovered, it is not a good indicator of the mechanical properties of the log (Wagner *et al*. 2003). However, in recent years the use of acoustic (or stress wave) based instruments for segregating material based on wood properties, particularly modulus of elasticity, has become more common. Stress wave instruments are capable of being used on logs and trees. This makes them potentially extremely useful for processors as the strength grading of battens usually occurs at the end of the production process, *i.e.* the processing costs such as cutting, drying and

planing have been incurred. Battens rejected at the strength grader are sold at a reduced price.

The use of acoustics in the forestry sector has increased, particularly in countries such as New Zealand (*e.g*., Walker and Nakada 1999, Tseheye *et al*. 2000), Australia (*e.g*., Dickson *et al*. 2004, Raymond *et al*. 2008), the United States (*e.g*., Wang *et al*. 2000, 2001, 2002, 2004) and Canada (*e.g*., Achim *et al*. 2010). This technology is beginning to be used more by researchers and industry in the UK (*e.g*. Auty and Achim 2008, Mochan *et al*. 2009, Moore *et al*. 2009a,b).

Acoustic instruments work on the principle that following an excitation from an external source, *e.g*. hammer blow or ultrasonic pulse, the speed of transmission of the disturbance through the test specimen is affected by the stiffness and density of the material. If the disturbance travels as a plane wave in a rod like structure, *i.e*. there is a uniaxial and uniform distribution of strain (Graff 1975) such that all elements of the cross section move identically and parallel to the sides of the rod (Andrews 2002), then the stiffness or modulus of elasticity (MOE) can be calculated by the one-dimensional wave equation (2.1):

$$E_d = \rho V^2 \hspace{3cm} [2.1]$$

Where:
- E_d is the dynamic MOE
- ρ is the density of the test specimen
- V is the stress wave velocity

The term "dynamic MOE" is used because the loading of the specimen from a stress wave consists of rapid stretching and contraction of the material. The term "static MOE" is used for stiffness derived from standard bending tests.

2.3 Measuring Acoustic Velocity

Instruments for measuring stress wave velocity in the forest products industry
fall into two classes: resonance or stress wave timers (Chauhan *et al*. 2006).

Resonance instruments work by the impulse excitation of a beam or rod-like
structure in which the length is much greater than the diameter. When the
impulse is applied, the structure will vibrate at its natural frequencies, *i.e.* its
fundamental frequency and associated harmonics, where the second harmonic is
two times the fundamental frequency and the third harmonic is three times the
fundamental frequency, *etc*. The resonant speed is then calculated by equation
(2.2):

$$V = \frac{2 f_i L}{i} \qquad\qquad [2.2]$$

Where:

- V is the stress wave velocity
- f_i is the frequency of the *i*th harmonic.
- L is the length of the specimen
- i is the harmonic number; 1, 2, 3, *etc*.

Stress wave timers, commonly called TOF instruments, are mostly suitable and
more commonly used for measuring the acoustic speed in a standing tree. There
are a number of variations but generally they work by hammering at least two
probes into the same side of a tree a known distance apart, then initiating a stress
wave at one probe, *i.e.* striking it with a hammer, and timing how long the stress
wave takes to reach the other probe. The speed is then calculated by simply
dividing the distance between the two probes by the transit time.

The main advantage of resonance based instruments is that their measurements
are more accurate than stress wave timers because as Chauhan *et al*. (2005)
showed that "*resonance speed obeys the law of mixtures and is the volume
weighted average stiffness of the whole section under test*". This is because,

when the log resonates due to an externally applied excitation, the wave front forms a constant strain over the whole cross section, *i.e.* it is a plane wave. Therefore the wave speed is affected by the wood properties of the entire cross section.

The main advantage of using stress wave timers is that they are a far less destructive form of measurement, *i.e.*, the tree does not have to be cut down for it to be measured. The only damage comes from inserting the probes approximately 20 mm – 30 mm into the side of a tree. However, TOF instruments are less accurate as the stress wave speed is assumed to only be affected by the wood properties in outer portion of the tree, directly between the two probes (Huang *et al.* 2003). Also, each impulse applied to the tree or specimen is one measurement, whereas the accuracy of resonance instruments are improved over TOF instruments by the averaging of hundreds of reverberations of the test specimen per excitation. Therefore, whilst stress wave TOF instruments are capable of being used on logs or battens, the convenience and accuracy of the resonant technique means that they are mostly used on standing trees.

The mechanics of wave transmission in standing trees are also more complicated as the stress wave is not plane and does not conform to the one-dimensional wave equation (Wang *et al*. 2007). Rather, it is an expanding wave with a tri-axial state of stress (Graff 1975, Meyers 1994, Cremer *et al.* 2005). To explain what this means, consider a plane wave travelling longitudinally through a slender rod (or log). If there are no constraints placed on the external surface of the bar, then as the wave propagates, the bar is free to contract in response to the axial extension caused by the stress wave (see Figure 2.2).
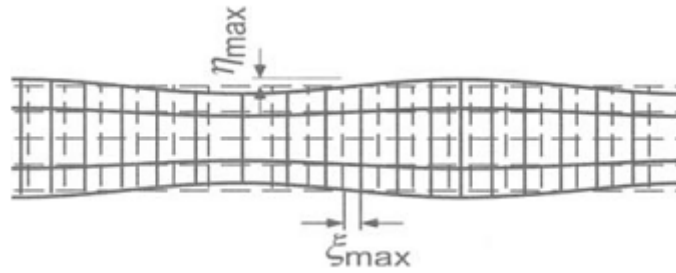
Figure 2.2. The lateral contraction, η_{max}, due to the axial extension, ξ_{max}, caused by the passing stress wave (from Cremer et al. 2005).

The ratio of this relative contraction (η_{max}) to relative expansion (ξ_{max}) is called the Poisson's ratio (υ). Because there is no constraint on the external surface, there is no stress present except for that of the passing wave travelling along the longitudinal axis of the bar (Cremer *et al*. 2005). This is a uni-axial state of stress.

Now consider a wave initiated in a standing tree, it is predominantly travelling in the longitudinal direction but it is not yet plane, *i.e.* strain is not equal over the entire cross section of the tree and it is still spreading outward in three dimensions (Graff 1991). Zhang *et al*. (2011) found that a plane wave will form approximately 10 times the diameter from the point of stress wave initiation in a standing tree measurement. A majority of distances between initiation and detection probes reported in the literature lie between 1 m and 2 m (*e.g*., Wang *et al*. 2003, Lassere *et al*. 2005, Moore *et al*. 2009b, Chauhan *et al*. 2006, Weilinga *et al*. 2009). Also most testing is on commercial size trees with diameters greater than 0.2 m which means that the wave is still most likely to be in a state of expansion over the entire test distance. This means that material directly adjacent to the leading edge of the expanding wave front is partially constrained by the volume of wood beside it, inducing stresses in the specimen (tree) perpendicular to the stress wave. These stresses correspond to the contractions that would have occurred if the cross section was unconstrained and result in a tri-axial state of stress (Cremer *et al.* 2005). The additional stresses act to reduce the displacement in the longitudinal direction caused by the passing wave. Because stiffness is a measure of how far something is displaced for a given force, any forces acting to reduce the displacement will cause an apparent

increase in stiffness and therefore the speed of sound. This is called a dilatational wave. Equation 2.3 gives the ratio of dilatational velocity to the plane wave velocity in a finite beam or rod:

$$\frac{V_d}{V_l} = \sqrt{\frac{(1-\upsilon)}{(1+\upsilon)(1-2\upsilon)}} \qquad\qquad [2.3]$$

Where:

- V_d is the velocity of the dilatational wave.
- V_l is the velocity of a plane wave.
- υ is the Poisson's ratio.

Wang *et al.* (2007) achieved excellent correlations ($R^2 = 0.95$) between standing tree TOF velocity at breast height and resonant velocity on the bottom log, by modelling the standing tree velocity as a dilatational wave and resonant log velocity as a plane wave. This was achieved independent of stand age and tree diameter after adjusting the standing tree velocity to account for the different wave propagation mechanisms only. However, the correlations by species were already very good before adjustment, with R^2 values ranging from 0.71 to 0.93. A study in the UK by Moore *et al.* (in press) showed an R^2 correlation of 0.6 between resonant log velocity and TOF velocity measurements on trees. This indicates a reduction in the predictive ability of standing tree tools in British spruce compared with other species. The assumption of constant density in the outer part of a tree or the whole log when using the dynamic MOE equation may be responsible.

2.4 Density in the Dynamic MOE equation

The assumption made when estimating wood stiffness from velocity measurements on standing trees and freshly felled logs is that wood density has a constant value of 1000 kg m^{-3}. The extent of the variation in green density (*i.e.* the density of freshly felled wood) within and between Sitka spruce trees is unknown and thus the validity of this assumption has not been tested. The green

density of a freshly felled log is controlled by the density of the wood and the proportion of heartwood to sapwood. Figure 2.3 shows the proportions of heartwood and sapwood in discs of Sitka spruce and Scots pine (*Pinus sylvestris* L.).
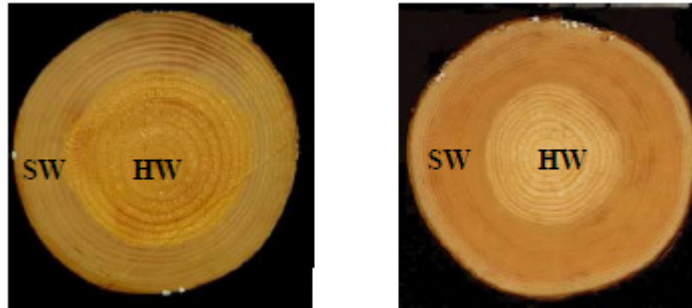
Figure 2.3. From Beauchamp (2011). Left. Sitka spruce and, Right. Scots pine heartwood (HW) and sapwood (SW).

Sapwood is the conductive tissue for water in the stem which contains some living (parenchyma) cells used for the storage of food. Heartwood is the inner layer of wood which contains no living cells (Hillis 1987, USDA 1999). During the conversion of sapwood to heartwood there is a reduction in moisture content and (depending on species) the wood can become impregnated with chemical extractives, including resinous and phenolic compounds, to protect it from degradation (Hillis 1987). There is a significant amount of variation in proportions of heartwood and sapwood between species (USDA 1999) and between trees depending on their growth history and environment (Beauchamp 2011). For the purposes of this thesis, the only aspect of heartwood that is considered is that of its reduced moisture content and its possible effect on the assumption of constant density. A simple diagram of how heartwood percentage can vary with height in a tree is shown in Figure 2.4 by assuming a constant sapwood depth. The figure also shows how the proportions of heartwood and juvenile wood interact with height. Note that this figure does not account for changes in the wood properties of the juvenile core with changes in tree maturation as explained by Burdon *et al*. (2004).
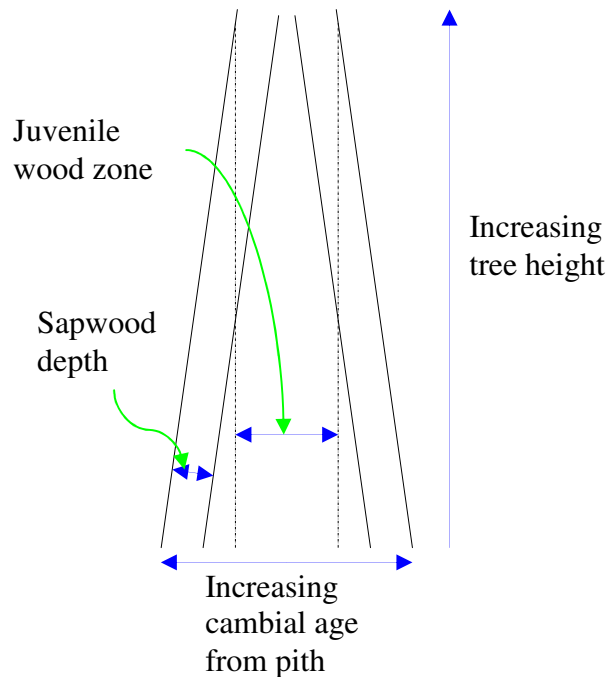
Figure 2.4. Illustration of how sapwood depth, and therefore heartwood percentage, can change with height in the tree and how it interacts with juvenile wood.

For radiata pine growing in New Zealand, the green densities of sapwood and heartwood are virtually constant at 1100 kg m^{-3} and 600 kg m^{-3} respectively, so that the average green density of logs depends on the proportion of heartwood (Cown 1992). The difference in green density between heartwood and sapwood in trees or freshly felled logs is predominantly due to differences in moisture content. Given the relatively young felling age for radiata pine trees (typically 25 – 30 years), the heartwood percentage is often quite low and therefore the overall green density of logs may be close to 1000 kg m^{-3}. The variation in heartwood percentage for Sitka spruce in the UK may be higher/lower as typical felling ages are between 35 and 45 years (Moore 2011).

Achim *et al.* (2009) and Jones and Emms (2010) found that the inclusion of density in the calculation of dynamic MOE improved the relationship with the static MOE of the battens from an R^2 of 0.41 to 0.69 and from 0.49 to 0.68, respectively. The variability in density was mostly due to differences in sapwood depth. Sapwood depth is also an important consideration for standing

tree instruments. Whilst the fastest path of a stress wave is assumed to travel in the outer part of the tree directly between the start and stop probes (Huang *et al.* 2003, Wielinga *et al.* 2009), these probes are generally inserted 20-30 mm into the side of the tree. If the sapwood-heartwood boundary is within this vicinity then the assumptions of constant density for standing tree tools may also be brought into question. To illustrate this, Chalk and Bigg (1956) showed that moisture content profiles of the outer 50 mm of a tree in UK Sitka spruce varied considerably between dominant, co-dominant and suppressed trees. Moore *et al.* (2009b) showed a large diameter range between trees at harvest age, indicating that these instruments would be required to work across a mix of dominance classes. If there is a large variation in the sapwood depth and therefore heartwood percentage, the accuracy of the technique may be affected by invalidating the assumption of constant density.

2.5 Using acoustics to measure stiffness

Acoustic instruments provide a fast, direct measure of stiffness (Huang *et al.* 2003) and significant, positive relationships have been found between acoustic velocity[2] on logs and batten stiffness in New Zealand and Australia on radiata pine (Ridoutt *et al.* 1999, Tseheye *et al.* 2000, Matheson *et al.* 2002, Dickson *et al.* 2004, and Jones and Emms 2010), in the USA and Canada on jack pine (*Pinus banksiana* Lamb.), red pine (*Pinus resinosa* Ait.), loblolly pine and white spruce (*Picea glauca* (M.) Voss*)*, (Wang *et al.* 2000, 2002, 2004, Mora *et al.* 2009 and Achim *et al.* 2010) and in the UK on Sitka spruce (Achim and Carter 2005 and Moore *et al.* in press).

These reports have shown the utility of acoustic instruments to be able to segregate logs based on stiffness. However, while the variation in average log stiffness can be measured easily, there still remains a very large degree of stiffness variation within a log due to normal physiological growth patterns in plantation conifers. Variation in wood properties within the stem is the rule rather than the exception (Burdon *et al.* 2004) with whole log data (*e.g.* log acoustic velocity) disguising an enormous range of wood properties from pith to bark (Huang 2003). For radiata pine, Xu and Walker (2004) found that battens

taken from near the bark were, on average, 50% stiffer than battens taken from the pith. Also for radiata pine, Grabianowski *et al*. (2006) constructed "Russian doll" models of pith to bark stiffness from 8, 16 and 26 year old trees and showed that the acoustic velocity-squared measured with a standing tree, TOF tool was approximately 100% higher in the oldest trees than the youngest. Moore *et al*. (2009a, c) have shown that greater than 50% of the variation in MOE of battens was due to within-log variation and Moore *et al*. (in press) showed that 37% of the variation in global MOE was due to intra-tree variation for UK Sitka spruce. This natural variation in stiffness allows scope for cutting higher stiffness, higher value structural battens from logs that are lower in overall stiffness when averaging the whole cross section. For example, consider the cutting pattern in Figure 2.5 for a 260 mm diameter log. This cutting pattern represents a typical sawmill cutting pattern, targeting structural dimensions and designed to optimise for volume recovery. In this example, structural battens are those labelled "153x49" and "103x49".
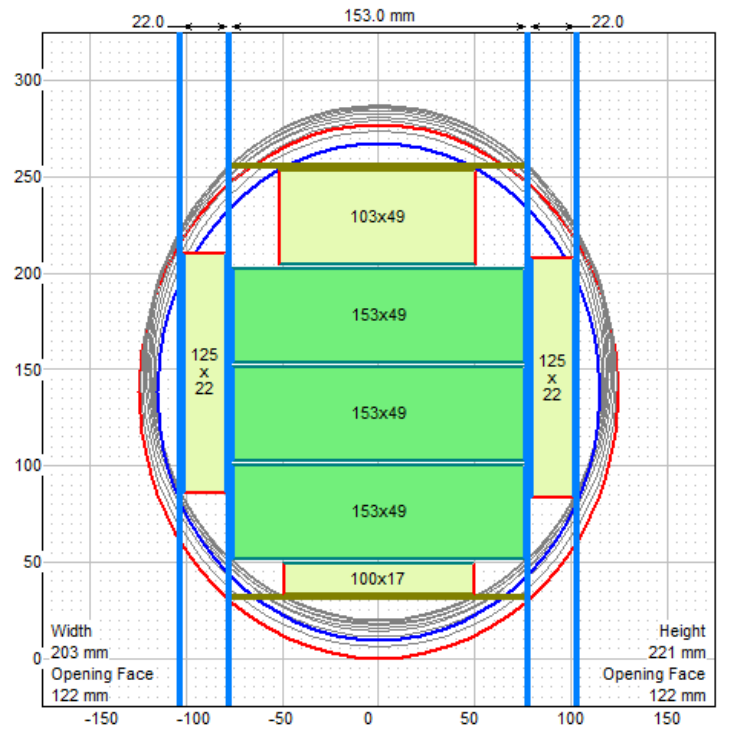
Figure 2.5. Typical sawmill cutting pattern.

Whilst this approach to extracting rectangular sections from round logs is the most efficient in volume recovery, it results in the potential for the structural battens to contain a large proportion of juvenile wood. This is shown in Figure

2.6 a and b, where the proportion of juvenile wood was assumed to be 5% and 20% of the cross section, respectively and overlaid on top of the cutting pattern in Figure 2.5

a.   b.
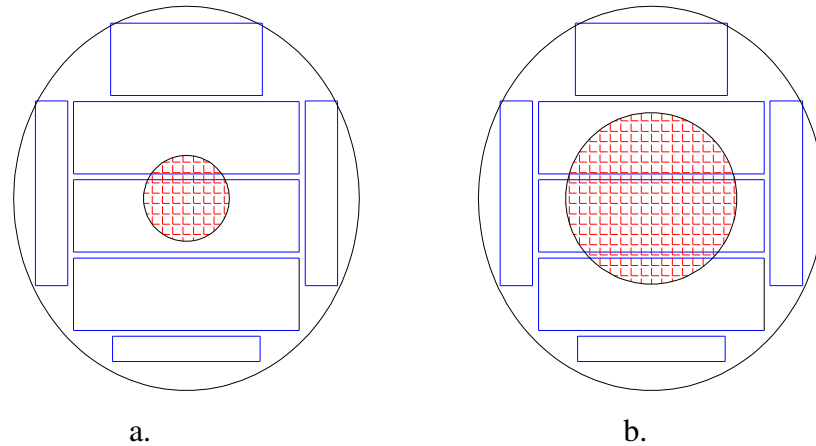
Figure 2.6. The proportion of juvenile wood in structural battens when JW takes up a) 5% and b) 20% of the cross section.

Therefore, alternative patterns designed to avoid the juvenile wood and its associated adverse affects on wood quality should improve batten stiffness. However, there may be some expense in volume recovery.

2.6 Summary

The rapid expansion of British forests from the 1920's till the present day has required that many plantations occur on exposed sites with poor soils, which, in addition to financial constraints, have either precluded or modified forest management practices that can produce high yields and improve the quality of the final crop. Since these interventions were either not possible financially or practically, the target was to produce high volumes only. Further, tree breeding programmes have resulted in improved vigour and straightness, meaning that trees are reaching merchantable sizes at younger ages. The net effect of these factors is to increase the proportion of juvenile wood within a stem at harvest age. With at least half of Forest Commission plantations managed on a no thin regime and a lack of published data about the proportion of stands planted at

various spacings and at various growth rates make it hard to evaluate how far the quality of the resource is falling relative to historic norms. The best statement that can be said about the future of the resource is that the quality will be highly variable but generally poorer.

With the advent of portable, easy to use acoustic tools, it is possible to measure the variability of stiffness in the resource and direct logs to their most appropriate end use. However the combined effects of variations in site environment and management may have resulted in differences in the proportions of heartwood and sapwood between sites and between trees within sites. This may affect the accuracy of both standing tree TOF measurements on trees and resonant velocity measurements on logs.

Finally, the use of acoustics to date, when applied to sawmilling, has looked at establishing the quality of the relationship between log velocity squared and the average MOE of the resulting battens. The utility of these tools to perform this task has been largely established across a wide number of species and countries. The next step is to match the between-log MOE measured with acoustics, to the within-log variation. This will allow the higher stiffness regions of logs with poor average overall stiffness to be converted to higher value structural battens, improving the overall value of the log to the processor than if it were diverted to purely non-structural applications.

3 Measuring the Variation of Stand Quality in Scotland

3.1 Introduction

This chapter contains an examination of the effect of season on standing tree acoustics and the relationship between tree and log velocity over a range of sites, environments and silviculture, all without considering the effect of density. Seasonal sampling of standing tree velocity was undertaken in the summer and winter. A proportion of winter sampling corresponded to periods of freezing temperatures and its possible effects on standing tree acoustics are examined. Values of log velocity are compared with standing tree velocity, slenderness and live crown ratio.

3.1.1 Objectives

The objectives of this chapter are:

1   To examine the relationship between standing tree and log acoustic measurements.
2   To examine the effect of season on TOF measurements.
3   To examine the relationship between acoustic measurements and tree level measurements such as slenderness and live crown ratio.
4   To add to the body of knowledge concerning the variation in stand quality in Scotland.

3.1.2 Background

This chapter follows on from the extensive work reported in papers by Moore *et al*. (2009b and in press) which examined 64 sites around Scotland and northern England, measuring stem straightness and standing tree and log velocities. The purpose of these studies was to model the effect of site and stand factors on wood quality, this chapter uses some of the conclusions from Moore *et al*. (2009b), to

select a number of sites that contain a contrasting range of wood properties and focus on the accuracy of acoustic instruments to measure this variation.

A description of acoustic instruments commonly used in the forestry industry and how they work is described in section 2.2. Density is commonly assumed to be constant when measuring acoustic velocity in standing trees or logs and stiffness is calculated by velocity^2. The variation in density of logs and the outerwood of trees and its effect on the accuracy of acoustic tools will be examined in Chapter 4, so the term E_d or dynamic stiffness, will not be used in this chapter. Instead, results will be labelled 'standing tree velocity^2' or 'log velocity^2' and have the units: $km^2 \, s^{-2}$. Note: log velocity is not the logarithm of velocity but the acoustic velocity of a log.

The utility of using TOF instruments on mature standing trees for predicting whole log stiffness has been examined in a number of papers, however very few have examined the effect of different silviculture and/or environment on the relationship. Factors such as initial spacing, thinning regime, felling age and growing environment will affect the relative proportions of juvenile wood (JW) and mature wood (MW) between trees (MacDonald and Hubert 2002, Larson *et al*. 2001, Cameron 2002, Cameron *et al*. 2005, Beauchamp 2011). Raymond *et al*. (2008) provides a very good illustration of the effect of silviculture on the relationship between velocity measured by TOF instruments and log velocity obtained from resonance. Raymond *et al*. (2008) specifically looked at the relationship between log velocity^2 and standing tree velocity^2 measurements for 28-43 year old, thinned and unthinned radiata pine. The authors found that the coefficient of determination (R^2) reduced from 0.56 to 0.31 for thinned and unthinned stands, respectively and concluded that it was very difficult, if not impossible, to extrapolate data collected from the outer part of the stem to the whole log or tree for unthinned sites. Other studies looking at the relationship between standing tree velocity and resonant log velocity for radiata pine in New Zealand and Australia include; Grabianowski *et al*. (2006) for 8-11 year old trees, $R^2 = 0.92$; Chauhan and Walker (2006) for 8, 16 and 25 year old trees found R^2 values of 0.89, 0.91 and 0.75, respectively. Wang *et al*. (2007) studied a range of species and ages from New Zealand and the United States, including

Sitka spruce western hemlock (*Tsuga heterophylla*), jack pine, ponderosa pine (*Pinus ponderosa* Dougl. ex Laws) and radiata pine. The study found R^2 values for each species ranged from 0.71 to 0.93. Also in the United States, Mora *et al.* (2009) found and R^2 of 0.81 for loblolly pine for trees ranging from 14-19 years old. In the UK, Moore *et al.* (in press) studied 120 trees from 12 sites across Scotland and northern England to examine the effect of site and stand factors on sawn timber properties of Sitka spruce. Sites ranged from 35-50 years old and gave an R^2 of 0.61 for standing tree velocity versus resonant log velocity.

Matheson *et al.* (2002) also examined the relationship between standing tree and log velocity for 27 year old thinned radiata pine and reported an R^2 of 0.58. However, this study collected standing tree velocity measurements by placing the receiver probe on the opposite side of the tree to the starter probe, whereas all other studies summarised here had the receiver on the same side of the tree as the starter probe. Therefore, this result by Matheson *et al.* (2002) will not be included in the general comparison of standing tree and log velocity[2].

In addition to acoustic measurements on standing trees to measure stiffness, there are also tree level properties such as slenderness (ratio of tree height to diameter at breast height, HD) and live crown ratio (ratio of the length of the live crown to tree height, CR) that can provide an estimate of tree stiffness. Lassere *et al.* (2009), states that there is a growing body of literature from spacing trials that show a strong relationship between MOE and slenderness. The mechanistic explanation given for this relationship is that under increased competition for light, trees will sacrifice diameter growth for height. This in turn creates a higher water potential gradient between the roots and the crown, requiring a greater specific conductivity, which means longer tracheid lengths to reduce the number of bordered pits (the connections between individual tracheids) that water must pass through. Longer fibre lengths were also positively correlated with stiffness in Lassere *et al.* (2009) who goes on to explain that "the goals of maintaining stability and hydraulic needs are not antagonistic". Therefore, secondary wall formation, which begins at the end of the cell extension phase, produces higher stiffness material to avoid buckling (Lassere *et al.* 2009) as described by Watt *et al.* (2006). Standing tree acoustic measurements need to be better than crown

ratio and slenderness to be worthwhile using, so a comparison will be made between the methods later in the chapter.

To date, Moore *et al*. (in press) and Raymond *et al*. (2008) are the only studies to explicitly examine the relationship between standing tree and log velocity for mature stands across a range of silvicultural treatments and they are the two studies with the worst correlation between standing tree and log velocity[2]. All other studies quoted here are either very young (Grabianowski *et al*. 2006), thinned (Chauhan and Walker 2006, Mora 2009) or undefined (Wang *et al*. 2007). Given the large variability in stand management and environmental conditions for Sitka spruce forests in the UK, there is the potential that standing tree tools will not provide an accurate measurement of tree stiffness. Therefore it would be beneficial to examine not just the relationship between tree and log velocity, but the relationship between log velocity and other tree level properties. This would allow forest managers a greater understanding of the errors inherent in the various methods for measuring standing tree stiffness.

3.2 Method and Materials

3.2.1 Site Selection

Moore *et al*. (2009b) in an investigation of 64 Sitka spruce sites around Scotland and northern England, found that standing tree stiffness, measured with TOF tools, was most strongly affected by age, yield class and elevation. Latitude and initial spacing, as well as interactions between almost all parameters also had an impact on standing tree velocity, though lesser in magnitude. Therefore, to obtain the broadest possible variation in values between trees and seasons in Scotland, 10 sites were chosen from a wide range of geographical locations and silvicultural regimes (see Table 3.1). The sites ranged through Argyll, Galloway, Inverness, Aberdeenshire and Tayside (Figure 3.1) with elevations ranging from 32 – 450 m above sea level and moisture deficits and accumulated temperature ranging from 32 – 120 mm and 790 – 1431 degree days >5.6°C, respectively. Furthermore, the sites were divided up into six high yield class (YC>18) and four low yield class (YC=12), with 4 sites that had been thinned and 6 unthinned.

Sites were selected on the basis that they were of harvestable age, but won't be felled within the next 12 months to ensure the seasonal variation in green density could be measured. The experimental procedures described in the following section were undertaken at the same sites in both the summer (June-August, 2009) and winter (December-March, 2009-2010).

Table 3.1. Summary characteristics of the ten sites measured.

Site Number	Site Code	Location	Altitude (m)	Age (yrs)	Yield Class m^3/ha/yr	Initial Spacing (m)	Thinning
1	AB11L	Aberdeenshire	265	50	12	1.7 x 1.7	Thinned
2	AB21L	Aberdeenshire	398	65	12	1.7 x 1.7	Thinned
3	AB26H	Aberdeenshire	276	65	18	1.7 x 1.7	Thinned
4	AR11H	West Argyll	101	40	18	1.5 x 1.5	Unthinned
5	AR31L	West Argyll	59	48	12	1.5 x 1.5	Unthinned
6	GA32H	Galloway	103	38	20	1.5 x 1.5	Unthinned
7	GL31L	Galloway	127	50	12	2 x 2	Unthinned
8	IN23H	Inverness	289	59	20	2 x 2	Thinned
9	TA23L	Tay	450	46	18	1.5 x 1.5	Unthinned
	TR11H	Cowal &					
10		Trossachs	143	39	20	2 x 2	Unthinned
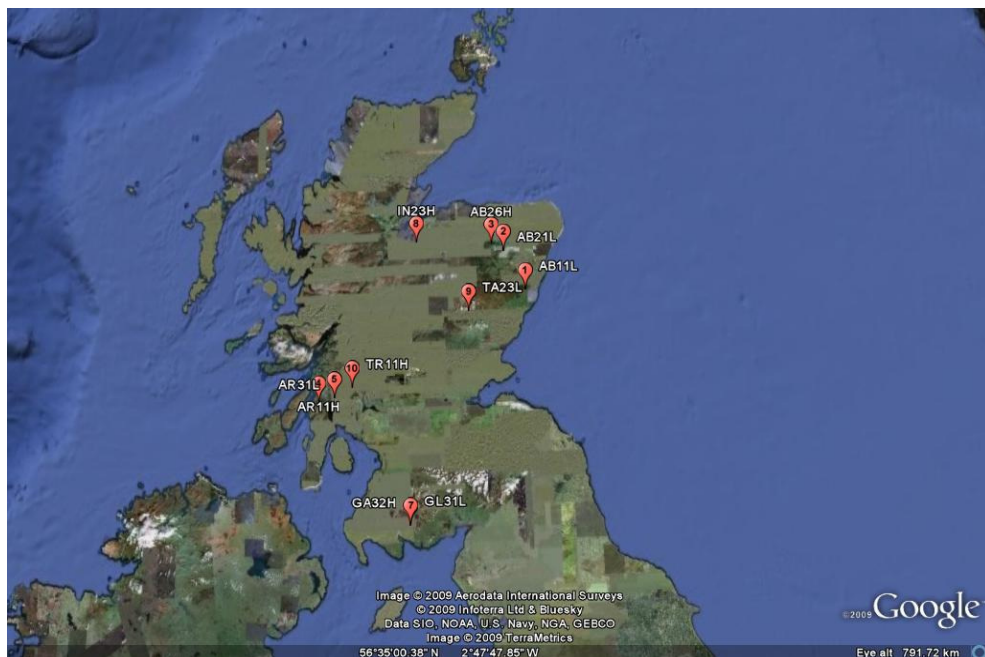
Figure 3.1. Location of the ten sites sampled. Site names correspond to those given in Table 3.1.

3.2.2 Experimental Procedure

At each site a plot centre was chosen at random to give a representative sample of the site and the first 60 live trees were selected radiating outwards from this point. Their diameter at breast height (DBH) was measured with DBH tape and the stem form (straightness) of each of these trees was assessed visually using the seven-point scoring system developed by Macdonald *et al*. (2001). Of these 60 trees, at least 40 were required to have a DBH $\geq$ 200 mm and a stem straightness score > 2, *i.e*., could produce at least one 3 m long log. If 60 trees were not enough, then more were added to the plot until 40 were obtained. The stress wave velocity was measured on both the north and south sides of the suitable trees using the IML Hammer (Instrumenta Mechanic Labor GmbH, Germany). Two probes were hammered into the side of a tree 1 m apart, at an angle of approximately 30˚ to the trunk (Figure 3.2). The bottom probe was then struck with an impulse hammer linked to the IML processor, to initiate the timer. A piezoelectric sensor was screwed into the top probe which detected the stress wave and stopped the timer. The speed is then simply the distance between the two probes divided by the transit time. An average of three measurements was obtained for each side of the tree. The location at which the probes were inserted into the tree was marked with paint so that when the sites were revisited in the winter, TOF measurements were made in exactly the same location.
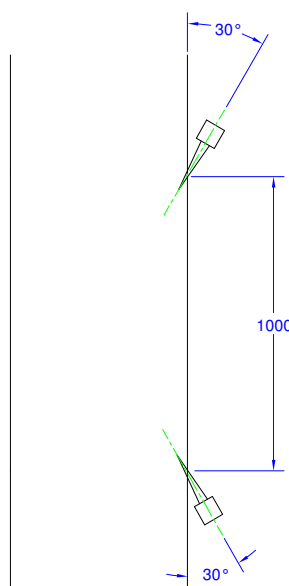
Figure 3.2. IML probe setup.

From the range of suitable trees, 3 were felled and measured with the Director HM200 (Fibre-gen NZ) to obtain the resonant log velocity. The trees chosen for felling were the smallest (with DBH $\geq$ 200 mm), median and largest within the plot to get the broadest possible range of heartwood and juvenile wood proportions. The stiffness of both logs and trees was calculated using equation 1.1, assuming a constant density of 1000 kg m^{-3} (section 2.4). In this chapter, the smallest tree from each site that was felled has been labelled suppressed; the median tree, co-dominant; and the largest, dominant. Trees were only felled in the summer.

Across the ten sites a total of 779 trees were assessed, *i.e*., their DBH was recorded and stem straightness measured according to the stem straightness protocol (Macdonald *et al*. 2001). Of these, 434 (56%) had a straightness score greater than 2 and a diameter $\geq$200 mm and were therefore capable of producing at least one saw log, 3 m in length. The stress wave velocity was measured on all 434 of these trees using the IML Hammer and 30 trees were felled and had their resonant acoustic velocity measured with the Director HM200 (Fibre-gen NZ).

3.2.3 Data Analysis

Data were analysed using the R open-source statistical package (R Development Core Team 2010). Comparison of means was undertaken using *t*-tests. The box and whisker plots have the following features: the horizontal line in the middle of the box is the median value, while the upper and lower horizontal lines of the box define the first and third quartiles. The extent of the whiskers on each box is one-and-a-half times the inter-quartile range, or approximately two standard deviations.

3.3 Results

A summary of the tree and stand level measurements is given in Table 3.2.

Table 3.2. Summary of the tree and stand level attributes of the 10 sites sampled. Standard deviations of the attributes are given in parentheses after the mean.

Attribute	Level	Minimum	Maximum	Mean
DBH (mm)	Tree	200	633	334 (79)
Height (m)	Tree	19	33.7	25.8 (4.3)
Standing tree (ST) velocity (km s^{-1}) in Summer	Tree	2.21	3.55	2.87 (0.2)
Standing tree (ST) velocity (km s^{-1}) in Winter	Tree	2.33	3.90	3.02 (0.28)
ST Velocity^2 in Summer (km^2 s^{-2})	Tree	4.87	12.63	8.28 (1.2)
ST Velocity^2 in Winter (km^2 s^{-2})	Tree	5.43	15.21	9.1 (1.84)
Log Velocity^2 (km^2 s^{-2})	Tree	7.18	17.89	11.76 (2.14)
% of trees producing sawlogs	Stand	38	85	56 (17)
Stem straightness*	Stand	2.71	5.68	3.96 (0.93)
Standing tree velocity (km s^{-1}) in Summer	Stand	2.73	2.97	2.88 (0.07)
Standing tree velocity (km s^{-1}) in Winter	Stand	2.8	3.24	3.02 (0.16)
ST Velocity^2 in Summer (km^2 s^{-2})	Stand	7.45	8.82	8.3 (0.39)
ST Velocity^2 in Winter (km^2 s^{-2})	Stand	7.82	10.47	9.1 (0.97)
Log Velocity^2 (km^2 s^{-2})	Stand	9.74	13.57	11.76 (1.12)

*Indicates all trees within each stand

Site average values of standing tree velocity^2 ranged from 7.45 to 8.82 km^2 s^{-2} with an overall average of 8.28 km^2 s^{-2} (COV=14%). This range was less than that observed in the original study by Moore *et al*. (2009), where site average values ranged from 6.09 to 9.50 km^2 s^{-2} with and overall average of 7.72 km^2 s^{-2} (COV=9.6%).

Similar to Moore *et al*. (2009b), there is no relationship between stem straightness and standing tree velocity^2 (Figure 3.3). In Figure 3.3, a stem straightness score of '3' means a tree is capable of producing one 3 m long log, while a stem straightness score of '7' means a tree is capable of producing at least one 6 m long log.
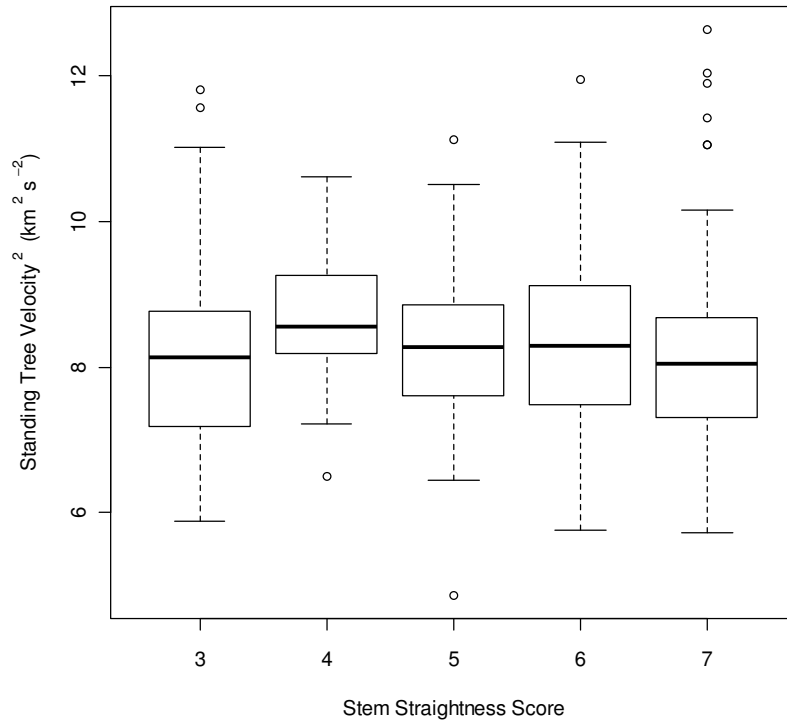
Figure 3.3. Standing tree velocity^2 with stem straightness

The distribution of DBH for trees capable of producing logs ≥200 mm in thinned and unthinned sites is shown in Figure 3.4a and b, respectively.
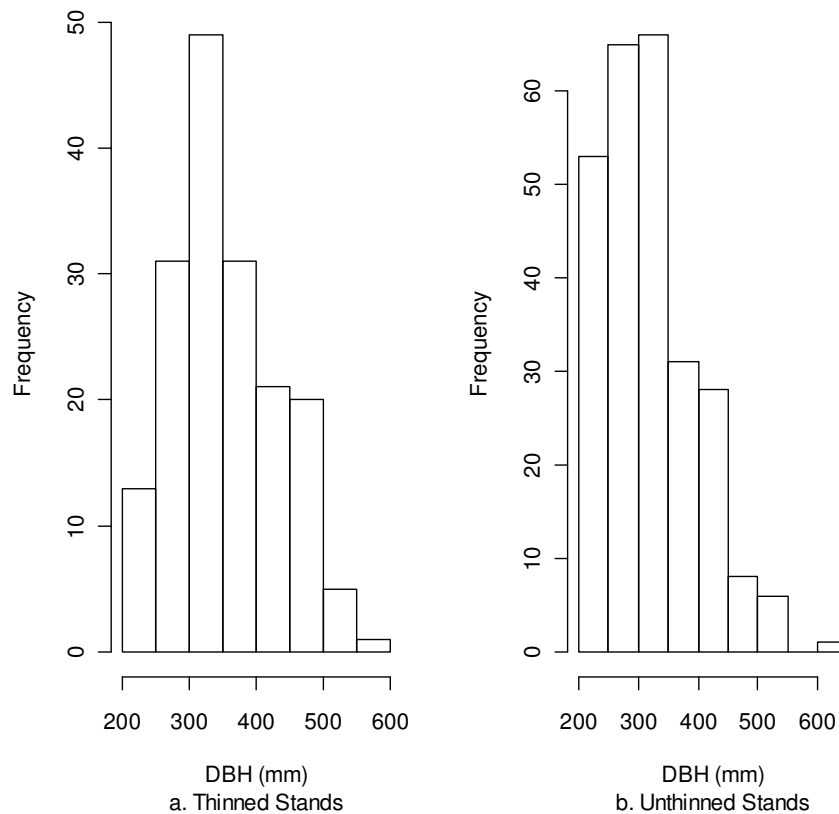
Figure 3.4. Distribution of DBH for a) Thinned, and b) Unthinned stands.

The overall mean and standard deviation for both thinned and unthinned stands was 334 mm and 79 mm, respectively (COV = 23.7%). The DBH of both could be characterised by a normal distribution, with various proportions of its tail being cut off by the 200 mm minimum diameter requirement. The mean DBH for thinned stands is 356 mm with a maximum of 575 mm. The distribution of unthinned stands shows that a significant proportion of the sample population had a DBH less than 200 mm (Figure 3.4b). The mean DBH for unthinned stands was 320 mm, however the maximum DBH for unthinned stands was larger than for thinned stands, at 633 mm.

Although trees on thinned sites will have more growing space and will reach a bigger diameter over a given rotation length than unthinned stands (Macdonald and Hubert 2002), the smaller mean DBH for unthinned stands is not due solely to increased competition at these sites; stand age also influenced the results, with unthinned stands having a mean age of 43.5 years and thinned stands a mean age

of 59.8 years. Other confounding factors such as variations in altitude and initial spacing may also affect the comparison of thinned and unthinned stands. However, this was a conscious decision in the experiment design as the aim was to obtain a contrasting range of sites to test the accuracy of acoustic instruments.

3.3.1 Effect of season on standing tree velocity

The relationship between summer and winter standing tree velocity was poor with $R^2 = 0.47$ (Figure 3.5). Average winter standing tree measurements were greater than summer measurements by 5.6% ($p<0.01$ using t-test).
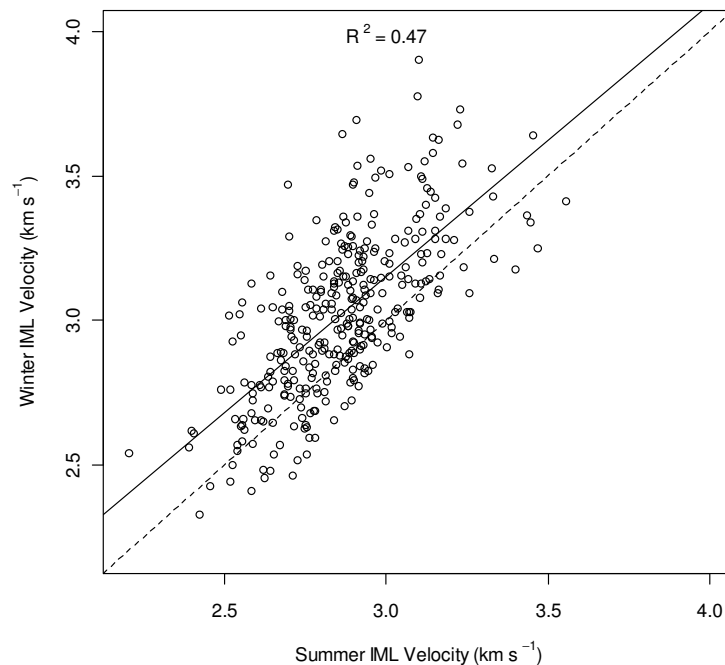
Figure 3.5. Relationship between standing tree velocity in summer and winter.

Although there was an overall increase in mean standing tree velocity from summer to winter, if the results for each site are analysed by the month they were re-sampled in winter, a more interesting picture emerges (Table 3.3).

Table 3.3. Site by site comparison of average standing tree velocity^2 measurements between summer, winter and winter sample month.

Site Number	Site ID	Summer ST Velocity^2	Winter ST Velocity^2	% Difference	Sample Month
1	AB11L	8.30 (1.3)	7.86 (1.1)	-5.1	Dec
2	AB21L	8.54 (0.9)	8.90 (1.1)	4.1	Dec
3	AB26H	8.22 (1.4)	8.90 (1.6)	8.2	Dec
4	AR11H	8.50 (1.3)	9.82 (1.5)	15.5	Feb
5	AR31L	8.75 (1.0)	10.25 (1.4)	17	Feb
6	GA32H	8.17 (1.0)	8.33 (1.2)	1.8	Dec
7	GL31L	8.13 (1.0)	9.11 (1.5)	11.7	Dec
8	IN23H	8.86 (1.2)	10.20 (1.3)	15.2	Mar
9	TA23H	7.47 (0.8)	7.93 (1.3)	5.7	Dec
10	TR11H	7.95 (0.9)	10.54 (1.8)	28.7	Feb

Sampling in February and March consistently resulted in a much higher winter standing tree velocity than sampling in December. These months also coincided with the coldest conditions. Analysing the results for February and March separately show that there is a 21% difference in summer and winter measurements ($p<0.01$ using t-test). The difference between summer and winter measurements for December only, show a difference of 5.2% ($p<0.01$ using t-test).

3.3.2 Relationship between standing tree and log velocity

The relationship between standing tree velocity^2 and bottom log velocity^2 (Figure 3.6) is $R^2 = 0.46$ compared with $R^2 = 0.60$ for Moore *et al.* (in press).
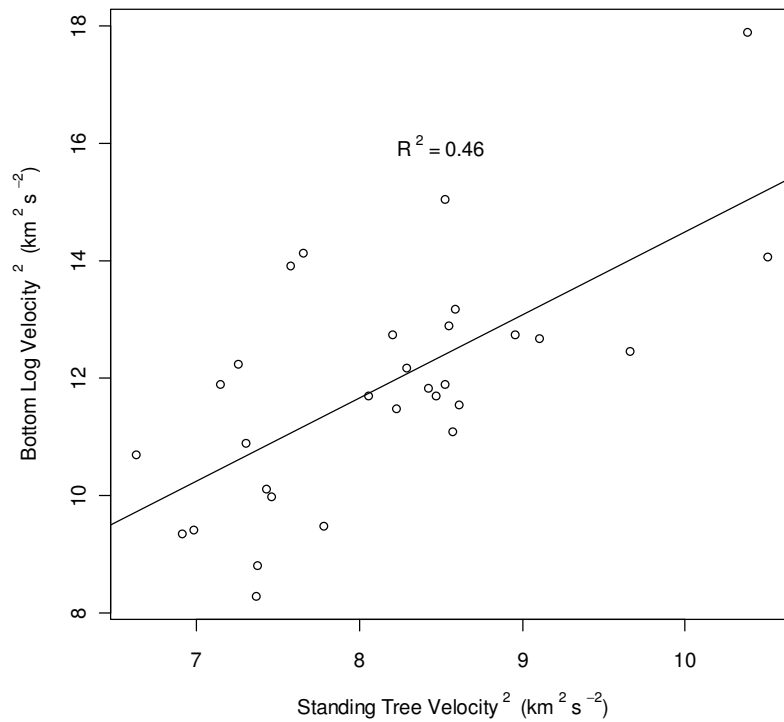
Figure 3.6. Relationship between standing tree velocity^2 and bottom log velocity^2.

The relationship between standing tree velocity^2 and bottom log velocity^2 for thinned and unthinned stands, as well as by dominance class is shown in Figure 3.7 and Figure 3.8. The overall relationship for the 30 tree measured in this study is relatively poor, R^2=0.46. If thinned and unthinned stands are analysed separately, R^2 values change to 0.74 and 0.36, respectively (Figure 3.7a and b)
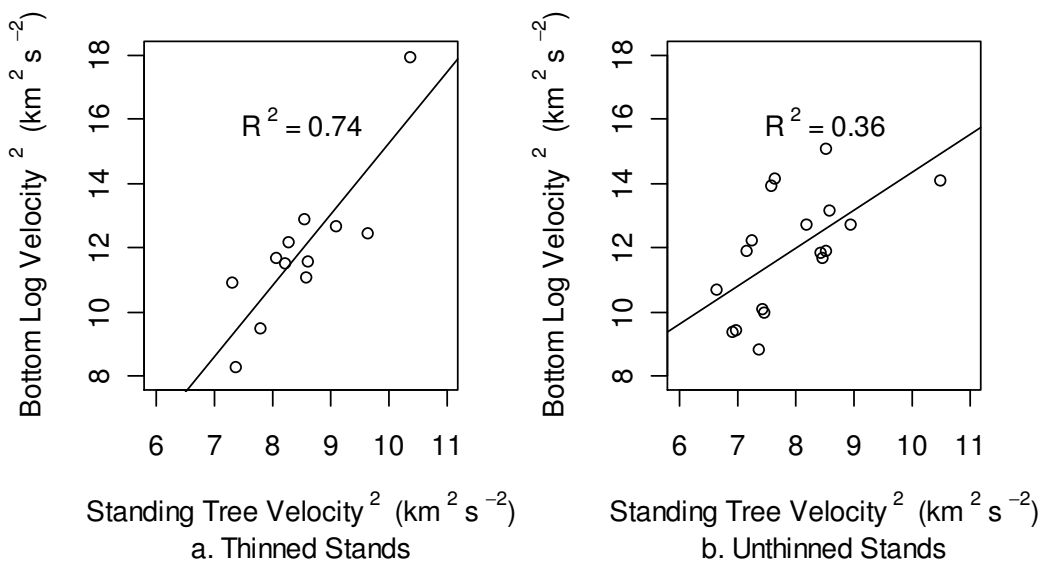
Figure 3.7. Relationship between standing tree velocity^2 with the bottom log velocity^2 for thinned and unthinned stands.

The relationship between bottom log velocity^2 and standing tree velocity^2 for thinned stands is highly leveraged by one point and its removal changes the R^2 relationship from 0.74 to 0.53.
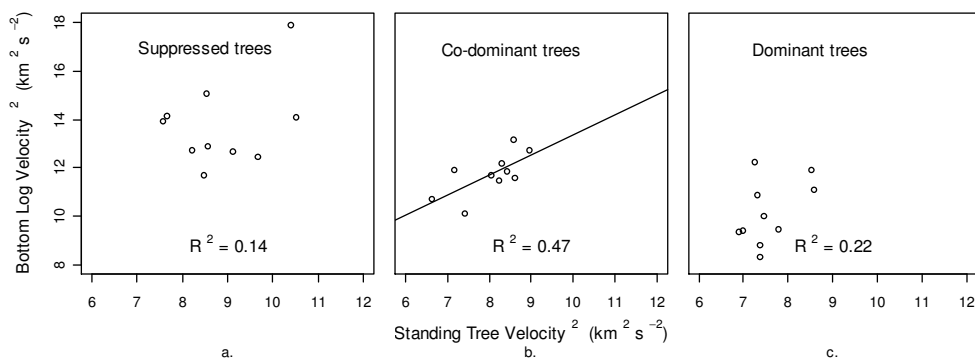
Figure 3.8. Relationship between standing tree velocity^2 with the bottom log velocity^2 for a) suppressed, b) co-dominant and c) dominant trees.

If analysed by dominance class, R^2 values are 0.14, 0.47 and 0.22 for suppressed, co-dominant and dominant trees, respectively. Unfortunately, there are not enough samples to make any definite conclusions but as an initial investigation, it would seem that the strength of the relationship is affected by thinning treatment and dominance class. This is possibly due to varying proportions of

both heartwood to sapwood and juvenile wood to mature wood between trees. These relationships will be re-examined in Chapter 4 with the inclusion of density in the calculation of tree and log stiffness.

Another point worth noting is the inverse relationship between dominance class and log stiffness. The average values of bottom log velocity^2 for suppressed, co-dominant and dominant trees are 13.6, 11.6 and 10.2 km^2 s^{-2} respectively. There is no difference between the average stiffness of thinned and unthinned stands (p=0.72 using t-test). These results should be viewed with caution as sampling was not random, *i.e.* only the smallest, median and largest trees within a site were selected.

3.3.3 Relationship between tree level measurements and log acoustic velocity

The relationships between bottom log velocity^2, standing tree velocity^2 and various tree level measurements for thinned and unthinned stands are shown in Figure 3.9a, b and c and summarised in Table 3.4. The R^2 values shown on the graphs and reported in Table 3.4 were calculated after the effect of the highly leveraging point identified in section 3.3.2 was removed.
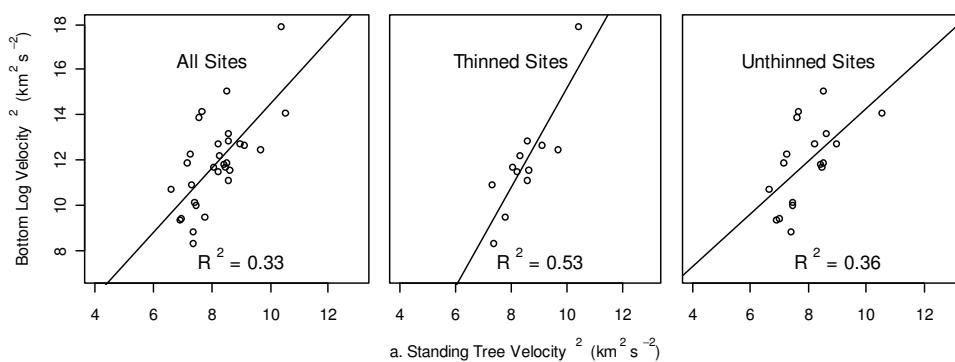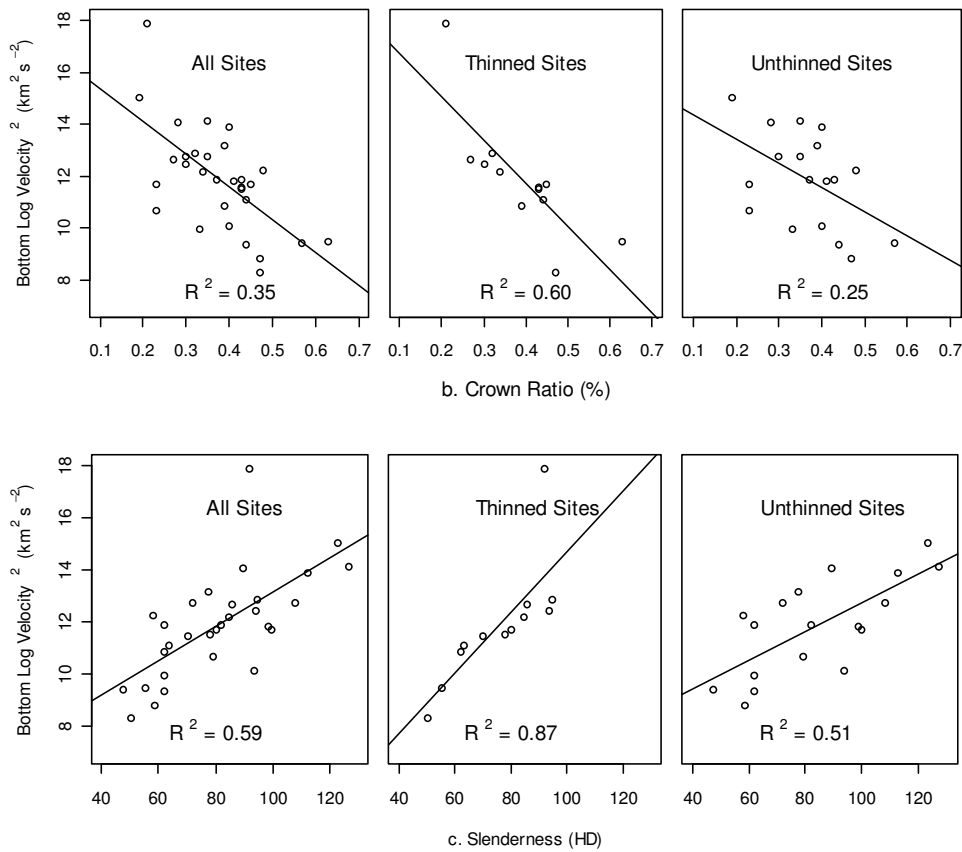
Figure 3.9. Relationship between bottom log velocity^2 with a) standing tree velocity^2, b) crown ratio and c) slenderness.

Table 3.4. R^2 values for the relationship between bottom log velocity^2 and various tree level measurements calculated with the highly leveraging point removed. The number in brackets indicates the number of samples used in the analysis.

Attribute	All Sites	Thinned	Unthinned
Standing Tree Velocity^2	0.33 (29)	0.53 (11)	0.36 (18)
Live crown ratio (CR)	0.35 (29)	0.60 (11)	0.25 (18)
Slenderness (HD)	0.59 (29)	0.87 (11)	0.51 (18)

Overall, it would appear that slenderness is far more accurate than standing tree velocity^2 in predicting bottom log stiffness across all sites, with R^2 values of 0.59 and 0.33, respectively. This is also true in thinned and unthinned (or possibly younger and older) stands. Overall, using CR gives much the same result as using standing tree velocity^2, however it performed slightly worse in unthinned stands.

The ability of standing tree velocity to estimate bottom log stiffness in unthinned stands is less than in thinned stands with R^2 values of 0.36 and 0.53, respectively. In general, this appears to confirm the conclusion by Raymond *et al.* (2008) that outerwood properties are poor predictors of whole log or tree stiffness for unthinned sites. Slenderness and bottom log velocity^2 also appear to be a function of dominance. Figure 3.10 shows the overall relationship of HD to bottom log velocity^2, highlighting each dominance class separately.
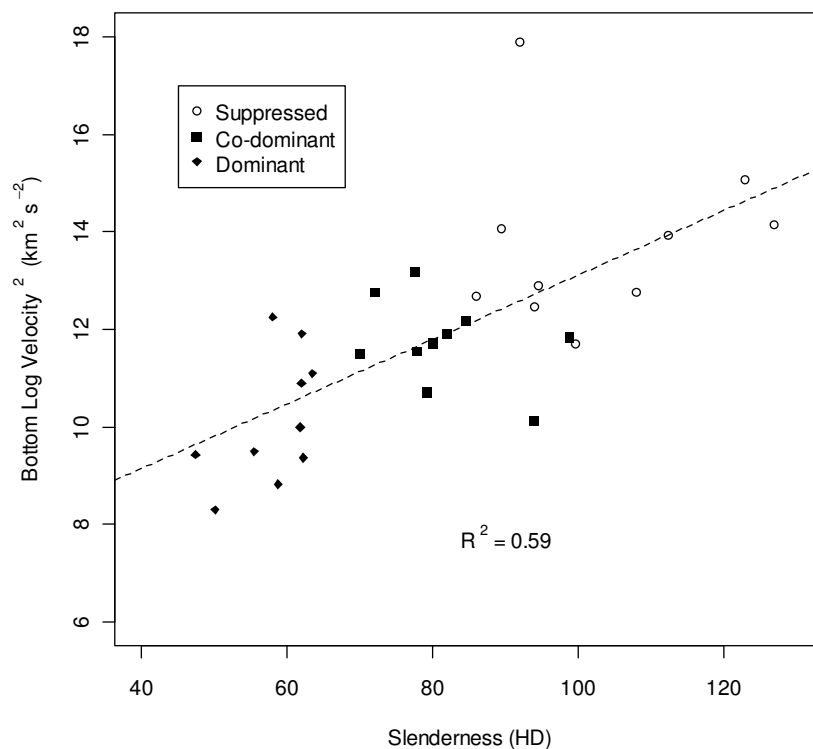
Figure 3.10. Relationship between slenderness and bottom log velocity^2, highlighting the effect of dominance.

The equation for the regression line in Figure 3.10 is:

$$\text{Bottom log velocity}^2 = 0.0066 \times \text{Slenderness} + 6.480$$

3.4 Discussion

3.4.1 Effect of temperature on standing tree velocity

Studies by Bächle and Walker (2006) and Chan *et al*. (2009) as well as a review by Bucur (2006) have all examined the change in the speed of sound through wood at various temperature ranges and moisture contents. They have all shown an abrupt increase in the speed of sound at 0˚C for wood above the fibre saturation point. This occurs as the free water within the lumen changes from a liquid to a solid state (*i.e*. it freezes), increasing the rigidity of the tree/specimen and therefore increasing the speed of sound (Bucur 2006). Bächle and Walker (2006) estimated that the magnitude of the discontinuity at 0˚C in freshly felled logs was 960 m s^{-1}. Chan *et al*. (2009) showed that the magnitude of the increase in velocity at 0˚C depended on the moisture content of the specimen; velocity changed by 138 m s^{-1}, 465 m s^{-1} and 725m s^{-1} for wood that was just above the fibre saturation point (42% moisture content), partially saturated (84% moisture content) and saturated (154% moisture content), respectively. Additionally, Silins *et al*. (2000) showed that the stiffness and strength of standing lodgepole pine (*Pinus contorta* var. *latifolia* Engelm.) was 50% greater in winter than in spring when conducting a tree pulling experiment. Sapwood temperatures in Silins *et al*. (2000) were from -16˚C to -3.5˚C in winter and from 0˚C to 16.7˚C in spring.

It is possible that increase in velocity is due to the experimental procedure of using the same probe location for both seasons: if probes were hammered into the tree a further 10 – 20 mm at an insertion angle of 30˚, the distance between the probes will have reduced by between 1.7% and 3.5%. This would correspond to an increase in velocity^2 between 3.4% and 7.1% - similar in magnitude to that seen for average December sampling measurements, *i.e.* sampling months unaffected by freezing temperatures. However, the range of the difference between summer and winter measurements in December (-5.1% to 11.7%) would suggest that other factors are affecting wave speed. Seasonal variation in density is a possibility and will be examined in Chapter 4.

3.4.2 Effect of silviculture and dominance on accuracy of standing tree acoustic instruments

Whilst the number of samples was limited and it is difficult to draw any firm conclusions, the results reported in this chapter indicate that the relationship between standing tree and log velocity deteriorates when considering unthinned sites and at the extreme diameter ranges within each site, *e.g.* suppressed or dominant trees. There is some complication due to the difference in mean site age between thinned and unthinned sites, yet this observation can be supported by results from Raymond *et al.* (2008) and Moore *et al.* (in press) who examined sites with varied silvicultural treatments and obtained weaker statistical relationships than other studies (*e.g.*, Chauhan and Walker 2006, Wang *et al.* 2007, Mora *et al.* 2009). Considering that there is a poorer relationship between standing tree and log velocity due to variations in age or silviculture and dominance class, it would be useful to identify the factors that cause the inaccuracy. This discussion should then highlight some of conditions required for the accurate assessment of log stiffness with standing tree acoustic instruments.

Essentially, the utility of using TOF instruments on mature standing trees for predicting whole log stiffness depends on the consistency of the relationship between wood near the bark and whole log properties. This relationship can be affected by a number of factors: Firstly, the ratio of the stiffness of wood near the bark to juvenile wood stiffness needs to be consistent between trees. Xu and Walker (2004) found that battens taken from near the bark in radiata pine (*Pinus radiata* D. Don) were about 50% stiffer than those taken from the pith. However, local variations in stiffness within the TOF test span due to grain deviation around knots or compression wood can skew the relationship (Wang *et al.* 2000). Additionally, Grabianowski *et al.* (2006) showed that the variation in velocity between different sides of the tree can increase as trees get older. Therefore, to improve the TOF accuracy, it has been recommended to perform measurements from two sides of a tree, normal to the prevailing wind direction and perpendicular to any lean in the stem (Toulmin and Raymond 2007).

Secondly, the ratio of the volume of low stiffness juvenile wood to mature outerwood needs to be consistent between trees. Section 2.1 gives an overview of how the genetics, environment and silviculture can affect the proportion of juvenile wood in mature trees at harvest. Generally speaking, the push toward shorter rotations will increase the proportion of the juvenile core within the stem. This can be compounded by planting improved stock for faster growth rates, resulting in trees reaching merchantable sizes at younger ages (Macdonald and Hubert 2002, Cameron *et al*. 2005). Financial constraints and/or an unacceptable risk of wind damage can affect the initial planting distance between trees and preclude or restrict the use of thinning as a means of managing the growth rate, and therefore the size of the juvenile core on some sites (Rollinson 1987, Cameron 2002). Inevitably, given the range of sites/environments on which Sitka spruce plantations are established in the UK, an equally broad range of silvicultural treatments and planting distances has followed:

- In the UK, approximately 50% of Forestry Commission plantations are managed under a no-thin regime (Macdonald and Hubert 2002).
- Brazier and Mobbs (1993) refer to initial plant spacings of up to 2.4 m and 2.7 m square. Moore *et al*. (2009) examined sites with initial plant spacings ranging from 1.12 m to 3.21 m square.
- Systematic thinning operations such as row or line thinning are regularly employed to make first thinnings more profitable (Rollinson 1987).

Consequently, mature wood from unthinned stands experience a dramatic reduction in growth rate after canopy closure compared to a thinned stand where there is less competition for light and nutrients, resulting in different proportions of juvenile to mature wood. Brazier and Mobbs (1993) examined the effect of initial planting distance between trees on the quality of the resulting saw logs and battens. The study concluded that the increase in diameter of the tree was due to the increase in growth rate of the juvenile wood and after this point, growth rate for bottom logs was similar regardless of initial spacing for unthinned stands. The proportion of juvenile wood as a percentage of the largest square cant that can be cut from the log increases from approximately 50% in a 200 mm log to

75% in a 300 mm log. Additionally, Cameron *et al*. (2005) showed that the proportion of juvenile wood for fast grown progenies was higher than for slow grown trees. Also, consideration needs to be made of the variation in quality of the juvenile core due to variation of initial plant spacing. Watt *et al*. (2006) and Lassere *et al*. (2009) both describe how increased competition can increase the stiffness of the tree by simultaneously increasing fibre length to aid water conduction and producing small microfibril angle (MFA) to reduce the risk of buckling.

Lastly, the ratio of heartwood to sapwood needs to be consistent between trees. The proportion of heartwood is expected to vary between trees and sites due to differences in rotation length and dominance class. As outlined in Chapter 2 (section 2.1.1), rotation length is affected by the environment and genetics of the planting stock; both greater exposure to wind at higher elevations and faster growing trees result in reduced rotation lengths (Rollinson 1987). Moore *et al*. (2009) reported diameters of living trees between 79 mm and 555 mm for trees between 35 and 50 years of age. The maximum DBH measured in this study was even larger, at 633 mm. Given that typical felling age of Sitka spruce in the UK is 35-50 years, the diameter range reported in Moore *et al*. (2009) indicates a very broad range of dominance classes at the time of harvest.

Heartwood is not the same as juvenile wood (*e.g*. see Figure 2.4). Juvenile wood is the zone of wood, approximately 10-20 years worth or growth, extending outward from the pith where wood characteristics undergo rapid and progressive changes in successively older growth rings (Larson *et al*. 2001). Heartwood (for the purposes of this study) is a region in the centre of the tree that is characterised by a reduced moisture content. Therefore, variations in heartwood will manifest as variations in green density of the log or tree. For radiata pine growing in New Zealand, the green densities of the sapwood and heartwood are virtually constant at 1100 kg m^{-3} and 600 kg m^{-3}, respectively, so that the average green density of logs depends on the proportion of heartwood (Cown, 1992). Therefore, depending tree age and the size of the crown, it is possible for trees to have a saturated juvenile core, or, a heartwood area that extends well into the mature wood zone. Chalk and Bigg (1956) have shown that the sapwood moisture

content (as a percentage of oven dry weight) and saturation percentage vary considerable between suppressed and dominant trees. Chalk and Bigg studied Sitka spruce in 4 sites across the UK with stand ages ranging from 23 to 37 years old and found that dominance is quite clearly related to higher moisture content in the outer wood closest to the bark, with average sized and suppressed trees containing progressively less water than dominant trees. Some of the results from Chalk and Bigg (1956) indicate that the heartwood area for suppressed trees may extend into the region 20 – 30 mm in from the bark which could affect the assumption of constant density for standing tree measurements.

Season and drought may also have an important effect on the amount of water in a stem. Chan (2007) conducted a study over a period of 17 months on the same sites to examine the effects of season on standing tree measurements. The period of measurement happened to coincide with a long drought in the region and a significant reduction in tree moisture contents was found during that time. Chan (2007) found that there was a 19.7% and an 11.9% increase in standing tree velocity[2] compared to a 6.9% and an 8.3% decrease in green density, respectively for 2 sites of radiata pine in Australia. In the absence of abnormal water stress, it is generally agreed that tree moisture content is lowest in the middle or toward the end of a growing season and highest in winter (Chalk and Bigg 1956). An increased moisture content of the sapwood in winter would translate to a slower acoustic velocity. However this is not apparent in the results, with only one site showing a decrease in velocity in winter.

3.5 Conclusions

The ability of standing tree tools to accurately predict whole log stiffness from outerwood properties in mature stands depends on three assumptions. These are:

- Consistent relationship between the stiffness of wood nearest the bark and juvenile wood stiffness.
- Consistent ratio of mature wood to juvenile wood.
- Consistent ratio of heartwood to sapwood, *i.e.* tree density.

All these factors are affected by environment, genetics, silviculture and tree age, all of which are known to vary widely within the Sitka spruce population in the UK. Studies by Raymond *et al*. (2008) and Moore *et al*. (2009b) have shown a poorer relationship between standing tree and whole log acoustics for radiata pine in NZ and Sitka spruce in the UK respectively, compared to other studies by sampling across a range of silvicultural managements and environments.

This study further examined the relationship between standing tree velocity and bottom log velocity and found the same conclusion as Raymond *et al*. (2008): properties of wood nearest the bark are a poor predictor of whole log properties for unthinned stands. There also seems to be an effect of dominance class on accuracy. This indicates that one or all of the requirements for accurate measurement with TOF tools in standing trees is not being met for some stands, or some trees within stands. The extent of green density variation in the wood nearest the bark and the relative proportions of heartwood to sapwood and juvenile to mature wood will be examined in the next chapter.

Lassere *et al*. (2009) states that there is a growing body of research that shows a good relationship between slenderness and whole tree stiffness. Slenderness in this study was shown to be more consistent than standing tree velocity in measuring bottom log stiffness when measuring thinned and unthinned stands.

The accuracy of standing tree velocity^2 in measuring stiffness can also be affected by freezing weather with up to a 28.7% difference in values between summer and winter, when winter temperatures were below zero. When winter temperatures were above zero, there was no effect of season between sites that could not be explained by using the same probe location for repeated tests. However, this will be examined further in Chapter 4 to see if there is any change in density affecting TOF measurements.

4 Effect of Green Density, Heartwood and Juvenile Wood Proportions on Acoustic Measurements

4.1 Introduction

The density profiles of the wood nearest the bark at breast height and the variation in density with height in the tree were examined to determine the possible range in error of acoustic measurements of stiffness in standing trees and logs due to the assumption of uniform constant density. Log and standing tree velocities were adjusted for changes in density to obtain dynamic MOE and its relationship re-examined. The relationship between the dynamic MOE of logs with slenderness and live crown ratio were re-examined. The proportion of juvenile wood at breast height between trees of different dominance class and its possible effect on the accuracy of standing tree instruments was also examined.

4.1.1 Objectives

The objectives of this chapter are to:

1. Examine the variation in the density of wood closest to the bark in standing trees within the immediate vicinity of the stress wave path and examine its effect on the dynamic MOE calculation.

2. Examine the variation in density of wood closest to the bark in standing trees between sites and seasons

3. Examine the variation in heartwood/sapwood proportions between trees of different silvicultural regimes and dominance classes.

4. Examine the variation in juvenile wood percentage between trees of different silvicultural regimes and dominance classes.

5. Examine the use of effective density in the standing tree dynamic MOE calculation.

6. Examine the variation in density with height in a tree.

4.1.2 Background

As outlined in Chapter 3, the ability of standing tree tools to accurately predict whole log stiffness from the properties of wood nearest the bark in mature stands depends on a number of factors. These include:

- Consistent relationship between the stiffness of wood nearest the bark and juvenile wood stiffness.
- Consistent ratio of mature wood to juvenile wood.
- Consistent ratio of heartwood to sapwood, *i.e.* green density of the log or tree.

The poorer correlation between standing tree and log acoustics when sampling across a varied range of environments and silvicultural treatments for UK Sitka spruce indicates that at least one, if not all of the requirements listed above is not being met.

When testing standing trees and logs, density is assumed to be constant and uniform, such that the dynamic MOE depends only on the stress wave velocity. The extent of the variation in green density for UK Sitka spruce has not been established for logs.

Chalk and Bigg (1956) showed that the sapwood depth (the radial distance from the bark toward the pith which contains the sapwood) at breast height can vary between trees of different dominance classes. The sapwood depth can sometimes only extend 20-30 mm into the tree, a similar depth to which the probes in a standing tree instrument are placed which may affect the assumption of constant density. The variation in sapwood depth between trees and with increasing height in a tree is also expected to have an effect on overall log density. Beauchamp (2011) found that there was less variability in sapwood area with height in the tree than sapwood depth. This suggests that sapwood depth changes with sapwood height to maintain a sapwood area to supply the needs of the branches and canopy of the tree above that point. As trees taper from wide at the base to narrow at the top, a (relatively) constant sapwood area up the stem would

result in an ever decreasing proportion of heartwood. Much higher moisture contents in sapwood will result in increased density further up the stem. If the density increases significantly, the assumption of constant density for the calculation of dynamic MOE will produce a proportional error.

The green density of a tree or log consists of wood fibres, water and air. The relative proportions of these components affect the speed of a propagating stress wave. Water exists in two states within the tree. The first, bound water, is water hydrogen bonded to the cell walls and will constitute approximately 30% of the oven dry mass of wood fibre. The level at which fibres are completely saturated is called the fibre-saturation point (FSP). As the moisture content drops below the FSP, which does not happen in a living tree, there is an increase in strength and stiffness and the specimen begins to shrink. At moisture contents above the FSP, water contained within the cell cavity or lumen is called free water (Dinwoodie 2000).

Free water is unable to bear stress (Wang and Chuang 2000) and as such, contributes nothing to the strength or stiffness of the specimen. Whilst the mechanical stiffness off wood remains almost constant above the FSP, the dynamic stiffness has been shown to vary by a number of authors over a range of species as the moisture content increases (*e.g.*, Gerhards 1975, Wang and Chuang 2000, S. Wang *et al*. 2002, 2003, Ilic 2001, Goncalves and Costa 2008, Chan *et al*. 2009). The change in dynamic stiffness above FSP appears to depend on the stress wave method used to determine the velocity:

- Ilic (2001) and Chan *et al*. (2009) show a pattern of decreasing dynamic MOE with increasing moisture content using the resonant velocity method.
- Wang and Chuang (2000) show an increasing dynamic MOE with increasing moisture content using a stress wave TOF method.
- Gerhards (1975), Sobue (1993), Wang and Chuang (2000), S. Wang *et al*. (2002, 2003) and Goncalves and Costa (2008) all show an increasing

dynamic MOE with increasing moisture content using ultrasound TOF methods.

Ultrasound, stress wave TOF and resonant techniques show a pattern of decreasing velocity with increasing moisture content. However, it is the rate of decrease in velocity with increasing moisture content that drives the difference in dynamic MOE between methods; using ultrasound, the magnitude of the velocity gradient is not as great as with resonant acoustics:

- Using ultrasound; Wang and Chuang (2000), S. Wang *et al.* (2002, 2003) and Goncalves and Costa (2008) report drops in velocity of between 5.3 and 7.4 m s^{-1} for every percent increase in moisture content (MC)
- Using resonance; Chan *et al.* (2009) and Ilic (2001) report drops of between 10 and 13 m s^{-1} for every percent increase in moisture content, although in Chan *et al.* (2009) the gradient did decrease to 6 m s^{-1} per percent increase in MC when MC was greater than 84%.
- Using stress wave TOF; Wang and Chuang (2000) report a drop of 7.8 m $^{-1}$ for every percent increase in MC.

The behaviour of ultrasonic waves in wood above FSP has led to the concept of 'the mobility of free water'. First proposed by Sobue (1993), this is an empirical value between 0 and 1 and represents the ratio of the weight of free water that vibrates in phase with the wood substance to the total weight of water. The mobility of free water, *k*, is used to calculate an effective density, given by equation (4.1):

$$\rho^* = \rho\left\{1 - \frac{(1-k)(MC-MC_{FSP})}{100+MC}\right\} \qquad [4.1]$$

Where:
- $\rho*$ is the effective density
- ρ is the green density
- *k* is the value for the mobility of free water

- *MC* is the moisture content of the material
- MC_{FSP} is the moisture content at fibre saturation point

The value of free water mobility varies with species and possibly ultrasound frequency, with values ranging from 0.33 in cupiúba (*Goupia glabra* Aubl.) tested at 45 kHz by Goncalves and Costa (2008) to 0.78 in Japanese cedar (*Cryptomeria japonica* (L.f.) D.Don) tested at 200 kHz by Sobue (1993). There is only one value reported for stress wave TOF velocity, 0.6 by S. Wang and Chuang (2000), also in Japanese cedar.

For resonant velocity measurements by Chan *et al*. (2009) on radiata pine, the negative velocity gradient is almost matched to the increase in bulk density (*i.e.* the density of wood plus water). This is due to increasing moisture content such that E_d, calculated using equation 2.1, is only slightly lower at high moisture contents than at FSP (*i.e.* bulk density is inversely proportional to velocity^2). This led Chan *et al*. (2009) to conclude that (at temperatures above freezing and moisture contents above FSP), although there was some variation in E_d, this was of low magnitude and agreed with the idea that mechanical properties are unaffected by free water in the lumens. This would indicate that all the free water was vibrating in phase with the wood and that the mobility of free water is equal to 1. However, Ilic (2001), also using resonant velocity but testing *Eucalyptus regnans* (F. Muell.) showed that the dynamic MOE always decreased as MC increased above the FSP. The results from Ilic (2001) show that the negative velocity gradient was larger than the corresponding increase in bulk density due to increasing MC. To put this in terms of the concept of mobility of free water, this would imply that more than 100% of the free water was vibrating in phase with the wood substance, clearly a physically impossible condition. There would appear to be underlying complications due to species and/or velocity measurement method. Attempting to resolve these complications is beyond the scope of this work. It has merely been highlighted as another potential source of error in the comparison of standing tree TOF and log resonant velocity; *e.g.* even with the assumption of constant density between trees, resonant velocity on logs may underestimate and stress wave TOF on trees may

overestimate the dynamic stiffness. This overestimate on standing trees would be over and above that due to dilatational wave speeds (explained in Section 2.3). Mora *et al*. (2009) successfully adjusted the stress wave standing tree TOF velocity on 14-19 year old loblolly pine to account for both the dilatational wave speed and the mobility of free water to form a 1:1 relationship between static and dynamic MOE values. Therefore, it would be interesting to see if the same result can be obtained with UK Sitka spruce.

4.2 Methods

The data were collected from the same sites that were used in Chapter 3 (Table 3.1).

4.2.1 List of equations to determine density, saturation percentage and moisture content

Green density is given by:

$$G_{Density} = \frac{G_{Wt}}{G_{Vol}} \qquad\qquad [4.2]$$

Saturation percentage is given by:

$$Sat(\%) = \frac{Sat_{Wt}}{G_{Vol}} 100\% \qquad\qquad [4.3]$$

Oven dry density is given by:

$$OD_{Density} = \frac{OD_{Wt}}{G_{Vol}} \qquad\qquad [4.4]$$

Moisture content is given by:

$$MC(\%) = \frac{GW - OD_{Wt}}{OD_{Wt}} 100\% \qquad\qquad [4.5]$$

Where:

- G_{Wt} is the green weight of the sample, *i.e*. directly after extraction from the tree
- G_{Vol} is the green volume of the sample

- Sat_{Wt} is the weight at saturation

- OD_{Wt} is the oven dry weight

4.2.2 Variation in density of wood nearest the bark

Following the standing tree velocity measurements on at least 40 trees with a DBH >200 mm and a stem straightness score >2 at each site (*i.e.* capable of producing one straight 3 m log), three trees were selected from each of the lower, middle and upper regions of the diameter range. As with elsewhere in this thesis, trees from the lower, middle and upper regions are called suppressed, co-dominant and dominant, respectively. In summer, increment cores 60 mm long were taken from the north side of 9 trees using a 12 mm diameter hand corer. Each core was immediately broken up into 10 mm lengths using a chisel and weighed with a battery powered laboratory balance (accurate to ±0.02g or ±0.02cc or a measurement error of approximately 0.35%). The volume of each section was measured using the water displacement method. Each section of core was labelled 1 to 6 (1 for the sample closest to the bark and 6 for the sample closest to the pith as per Figure 4.1) and placed in a sealed plastic bag for return to the lab.
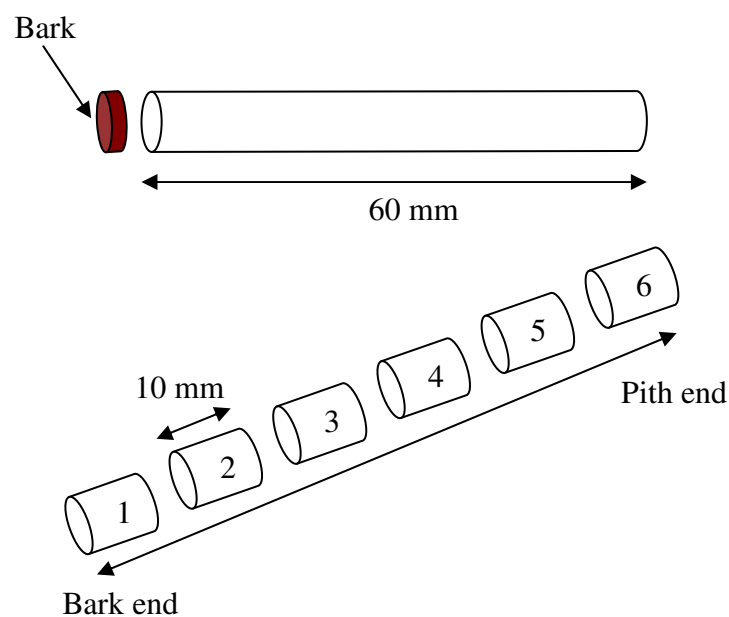
Figure 4.1. 60 mm long increment core before and after being broken up into 10 mm lengths for density measurement.

Great care was taken with the field measurements to ensure the balance was level and the batteries were fully charged to ensure accuracy. All measurements were performed inside a tent to remove any effect of wind or rain.

In order to obtain saturation, samples were immersed in water and placed in a vacuum chamber for an hour. To guarantee full saturation, samples were then placed in containers full of water and left to soak until two subsequent measurements, taken at least a week apart, had a weight difference of less than 2%. Once samples were saturated, they were weighed and placed in an oven at 103˚C until completely dry and re-weighed to obtain oven dry density and moisture content.

In winter, a different set of trees were selected for coring. Again, 3 trees were selected from each of the lower, middle and upper regions of the diameter range and cores were obtained to measure green density, saturation percentage, moisture content and oven dry density as per the procedure above.

4.2.3 Pith-to-bark density profile and heartwood/sapwood percentage

In order to; verify the accuracy of the density measurements on wood nearest the bark taken with the hand corer; and obtain an estimate of heartwood percentage, a disc approximately 50 mm thick, was cut from breast height (1.3 m) directly above the core location. The discs were obtained from 3 trees at each site. These were the smallest (with a DBH >200 mm), median and largest trees and were the same used for the bottom log velocity measurements in Chapter 3. Each disc was firstly cut in half from east to west through the pith, then a strip 50 mm wide from pith to bark, directly above the core location (north side) using a chainsaw, as per Figure 4.2.

Figure 4.2. Marking of 50 mm wide strip that was extracted from the breast height disc to verify corer density measurements.

The strip was cut into 10 mm lengths from pith-to bark with a chisel and immediately weighed on a balance. Volume, saturation percentage, oven dry density and moisture content were obtained with the procedure described for the increment cores.

Heartwood/Sapwood percentages were estimated by (arbitrarily) designating all material with a saturation percentage >80% to be sapwood and the remainder to be heartwood.

Total disc area, A_{Tot}, was calculated with equation 4.6.

$$A_{Tot} = \pi \left(\frac{DBH}{2} \right)^2 \qquad [4.6]$$

The area of heartwood was calculated with equation 4.7.

$$A_{HW} = \pi (Rad_{HW})^2 \qquad [4.7]$$

Where:

- Rad_{HW} is the radius of the heartwood determined by counting the number of segments obtained from the pith-to-bark strip that were at less than 80% saturation.

The sapwood area was calculated with equation 4.8.

$$A_{SW} = A_{Tot} - A_{HW} \qquad [4.8]$$

The volume of water in the sapwood is calculated with equation 4.9 and is expressed as litres of water per unit length (L m^{-1}).

$$V_{Water} = A_{SW}(G_{DensitySW} - OD_{DensitySW}) \qquad [4.9]$$

Where:

- $G_{DensitySW}$ is the green density of the sapwood
- $OD_{DensitySW}$ is the oven dry density of the sapwood

This method of heartwood area measurement may suffer from inaccuracy due to:
- Poor resolution as the heartwood/sapwood boundary is only accurate to ±5 mm and completely ignores any transition area.
- Only one slice 50 mm wide from pith to bark will ignore any effect of stem eccentricity.
- Rectangular instead of wedge shaped samples means that for smaller trees with higher ring curvature near the heartwood/sapwood boundary are likely to have a mixture of both.

Therefore, to confirm accuracy, heartwood area measured with this method will be compared to models of heartwood area for Sitka spruce developed by Beauchamp (2011). The heartwood area model is given by equation 4.10:

$$MOD\ A_{HW} = a\pi\left(\sqrt{DiscArea/\pi} - b\right)^2 \qquad [4.10]$$

Where a and b are constants with the values of 0.4362 and 0.8080, respectively.

4.2.4 Calculating dynamic MOE with effective density

As per Mora *et al.* (2009) the dynamic MOE using the effective density is calculated using equation 4.11.

$$MOE_{eff} = \rho^* \text{ x } STVel^2 \qquad\qquad [4.11]$$

Where:

- ρ^* is the effective density from equation 4.1.
- $STVel^2$ is the standing tree velocity^2.

4.2.5 Juvenile wood percentage

The other half of the breast height disc was weighed in the field and then taken back to the lab where a larger set of scales was required to measure the volume using the water displacement method. Once the volume was measured, the half-discs were placed in the oven at 103˚C until completely dry and re-weighed to obtain oven dry density and moisture content. The samples were then scanned analysed with WinDENDRO (Regent Instruments Inc, 2004; Quebec, Canada) to measure the radial distance from pith-to-bark in 5-year increments. To try and account for any eccentricity of the disc, measurements were taken at least twice and averaged. The juvenile wood percentage was calculated from the ratio of the area of the first 10 growth rings from the pith to the total disc area, A_{Tot}. The cambial age at breast height was also measured to try and remove the effect of age variation between sites, as was identified between thinned and unthinned stands in Chapter 3.

4.2.6 Variation in density with height in the tree

In addition to the breast height disc, discs were taken every 3 m up the stem for each felled tree until a top diameter of approximately 160 mm. Each disc was weighed in the field with a battery powered laboratory balance and transported back to the lab to measure its volume via the water displacement method. The discs were placed in the oven at 103˚C until completely dry and re-weighed to obtain oven dry density and moisture content.

4.2.7 Data analysis

Data were analysed using the R open-source statistical package (R Development Core Team 2010). The box and whisker plots have the following features: the horizontal line in the middle of the box is the median value, while the upper and lower horizontal lines of the box define the first and third quartiles. The extent of the whiskers on each box is one-and-a-half times the inter-quartile range, or approximately two standard deviations. Linear models were examined in ANCOVA to determine the relationship of juvenile wood proportion with age at breast height, dominance class and thinning regime (*i.e.* thinned or unthinned). Linear models were also examined in ANOVA to determine any significant difference in bottom log dynamic MOE between dominance classes. Unless otherwise stated, standard *t*-tests were used to compare means.

4.3 Results and Discussion

Across the 10 sites, a total of 30 trees were measured destructively to obtain pith to bark green density, saturation percentage, moisture content and dry density. Density variation along each of the 30 felled trees was obtained from 164 discs. The density profile of the wood nearest the bark of 180 trees (half in summer, the other half in winter) were obtained through 60 mm long increment cores.

To establish the accuracy of the density measurements on wood nearest the bark made with the 12 mm diameter hand corer, the average green density for each 10 mm increment in from the bark was compared to the equivalent position in the pith-to-bark density profiles obtained from the breast height disc. The average density profiles of wood nearest the bark obtained from increment cores and pith-to-bark slices is shown in Figure 4.3 for suppressed, co-dominant and dominant trees.
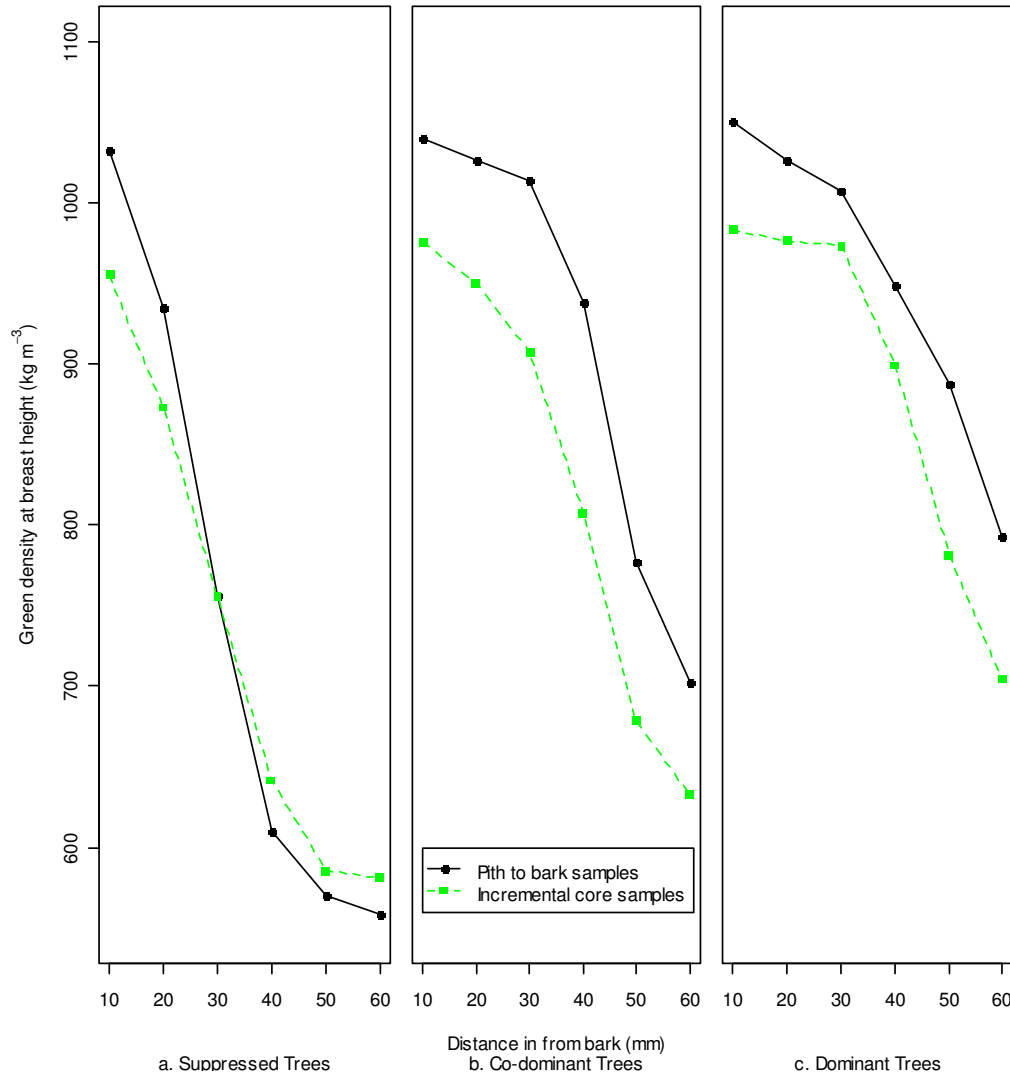
Figure 4.3. Comparison of mean green density at each position in from the bark for destructive pith to bark and incremental corer methods.

The variation in density at each position for pith to bark and summer incremental core samples is shown by the box-plots in Figure 4.4.

Pith to bark   **Incremental core**

Green density (kg m^{-3})

1000
900
800
700
600
500
400

10 20 30 40 50 60

a. Suppressed trees

Distance in from bark (mm)

Pith to bark   **Incremental core**

Green density (kg m^{-3})

1000
900
800
700
600
500
400

10 20 30 40 50 60

b. Co-dominant trees

Distance in from bark (mm)
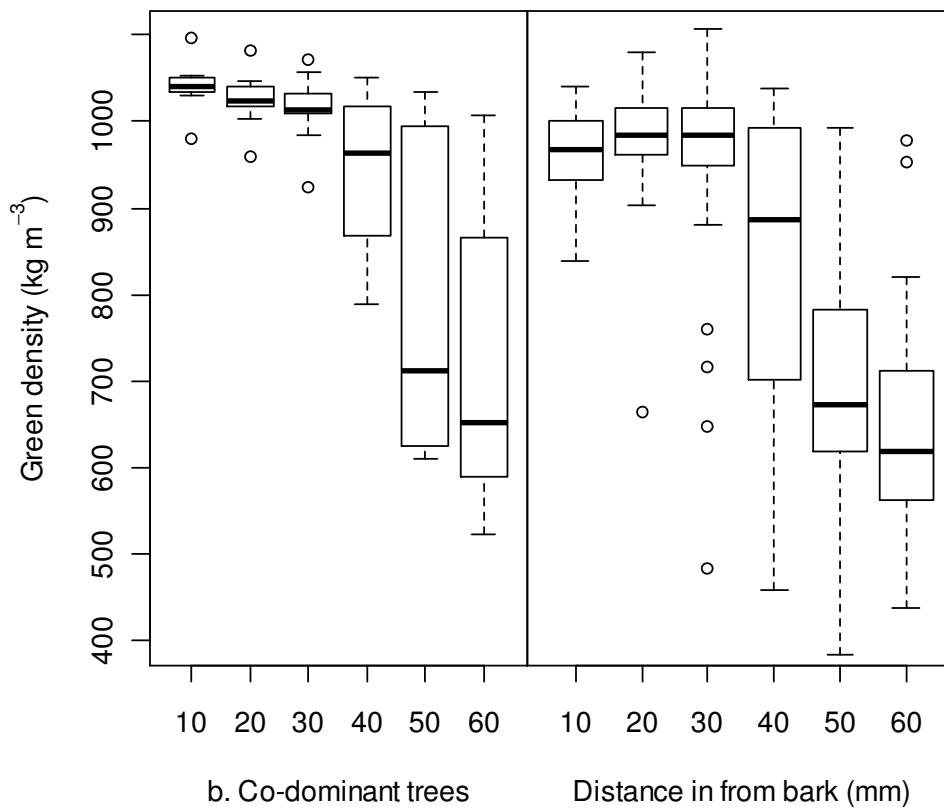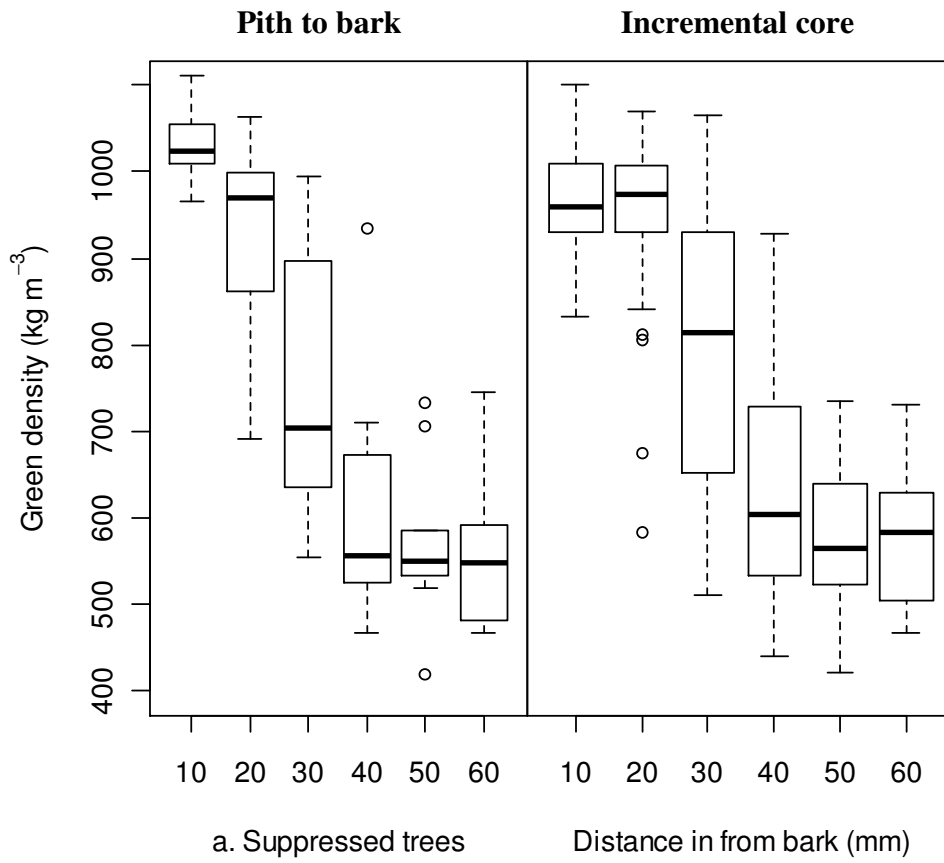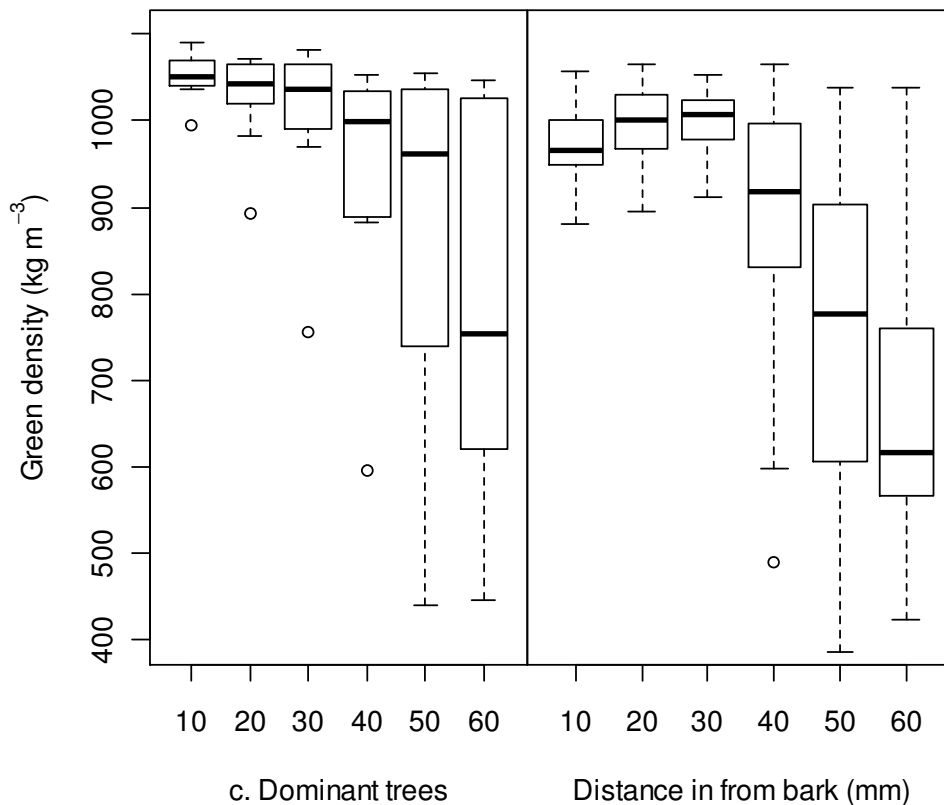
Figure 4.4. Box and whisker plots showing the variation in green density measurements with distance in from the bark between destructive pith to bark and incremental core methods. a. Pith to bark and incremental core for suppressed trees, b. Pith to bark and incremental core for co-dominant trees, c. Pith to bark and incremental core for dominant trees. There were 10 pith-to-bark samples at each position for each tree and 30 incremental core samples at each position for each tree.

The pith to bark samples are on average, greater in density than the increment corer measurements for all dominant and co-dominant trees. There is a high between-tree variation in green density moving inwards from the bark, indicated by the range of the box plots. The variation is smallest near the bark where all wood is sapwood and increases moving into the tree. This is due to differences in the transition zone between sapwood and heartwood within the same dominance class. At positions 50 mm and 60 mm in from the bark, the suppressed trees show a decreasing variation as the core moves into pure heartwood for all trees.

Despite the general differences in average green density, there is a good overall relationship between incremental core and pith-to-bark density measured on the same trees ($R^2 = 0.85$), shown in Figure 4.5.
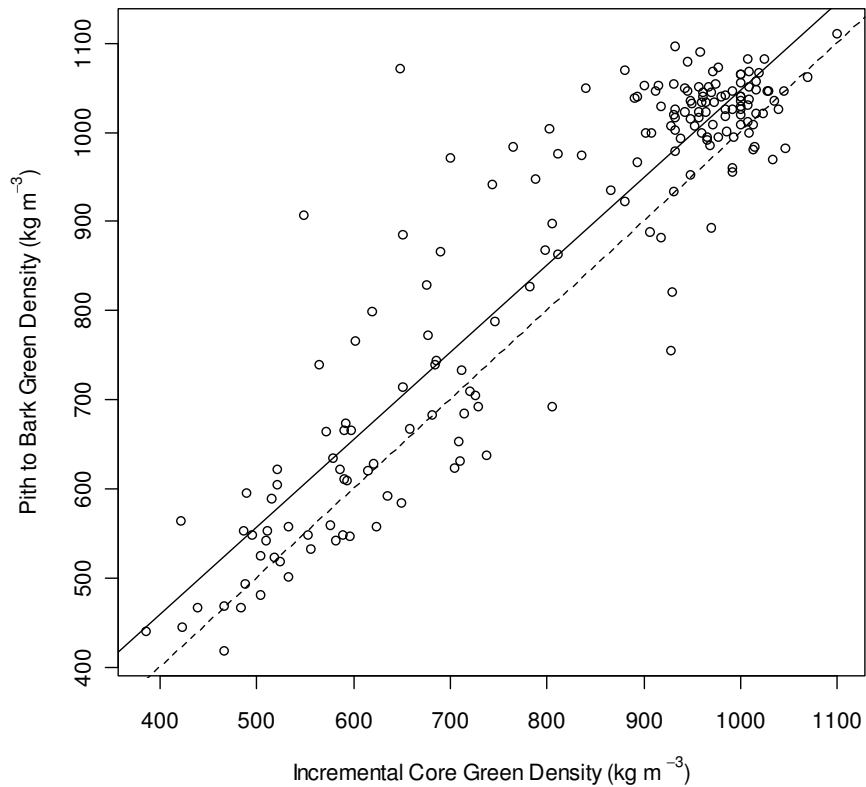
Figure 4.5. Relationship between incremental core and pith to bark green density. The dotted line represents the 1:1 relationship between the two variables and is parallel with the calculated regression line.

The amount of moisture lost per sample for using the increment corer over destructive measurements is estimated by the intercept of the regression line, 64 kg m^{-3}.

4.3.1 Variation in density of wood nearest the bark between trees

There is very little published data into the extent of the variation in outerwood green density and the best measurement method. Chan (2007) provides the most comprehensive discussion on the effects of measurement method on accuracy. Chan (2007) found that when comparing 12 mm increment cores with destructive samples, the average density was significantly lower in increment cores and the variability was much greater. Samples obtained with the corer are typically lower in density as moisture is squeezed from the samples by the pressure of the corer (Chalk and Bigg 1956, Chan 2007). Chan (2007) recommended soaking cores for 24 hours to provide a good approximation of destructive sampling by replacing lost moisture and reducing the variation. For this experiment, increment core samples were not soaked for 24 hours as it was feared this would introduce unpredictable errors as heartwood is less permeable and therefore likely to soak up water at a different rate to sapwood. Instead, samples' weight and volume were measured in the field immediately after collection to try and minimise error due to moisture loss in storage and transportation. The results shown in Figure 4.3 would suggest that incremental cores underestimate green density by between 7.5% and 14% within the sapwood region for all trees. This is deemed acceptable here as the difference between the two methods does very little to change the shape of the density profile. Also, a visual analysis of the variation for each successive position in from the bark in Figure 4.4 showed that the variation in increment core measurements was almost always mirrored by the variation of the destructive pith-to-bark measurements. This implies that the between tree variation in green density is greater than any variation due to measurement method in Sitka spruce. Therefore, further analysis on increment cores alone will provide a good relative measure of density variation and its effect on standing tree acoustics.

The average green density profile of outer 60 mm of wood nearest the bark of each dominance class for all 180 trees measured is shown in Figure 4.6. It is very similar in shape to the profiles shown in Figure 4.3.
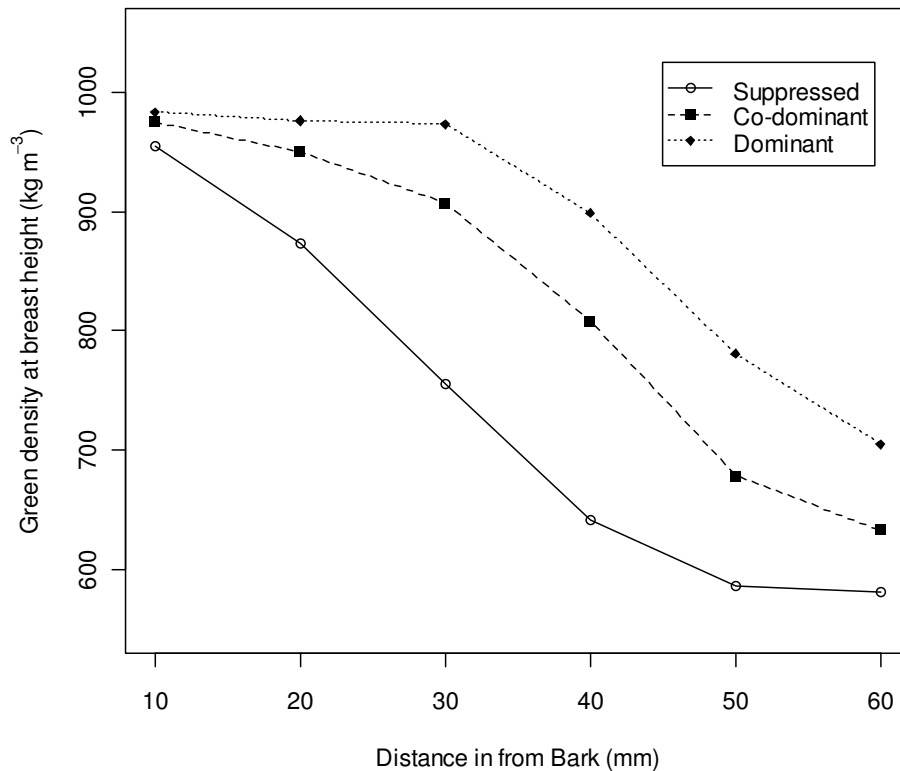
Figure 4.6. Mean green density profile of outer 60 mm of wood nearest the bark obtained by increment core method for suppressed, co-dominant and dominant trees.

The outermost 10 mm was almost constant between all trees. However, the density of the remaining samples changed depending on the dominance class of the tree measured. Dominant trees averaged 8.8% higher density across the whole 60 mm than the overall average due to their larger sapwood content. Suppressed trees averaged 10.2% lower density across the whole 60 mm than the overall average due to their greater heartwood content.

Therefore, the validity of the assumption of constant density when calculating stiffness from standing tree velocity depends on the path the stress wave takes between the start and stop probes. It is generally assumed that the path the wave takes is the shortest distance between the ends of the two probes which, if inserted 30 mm into the tree at an angle between 30-45° relative to the trunk, will penetrate horizontally to a depth of 15 mm and 21mm, respectively. This places

within the region of density variation between dominance classes in Figure 4.6. However, the actual extent to which this wavefront interacts with the density variation is unknown. The stress wave is unlikely to remain unaffected by material from outside this area directly between the probes as Graff (1991) explains about the behaviour of stress waves;

"T*he interaction of one part of the system to the next is the interaction of one differential element on the next. Instead of the simple push pull motion along a series of springs and masses, the disturbance spreads outward in a 3-dimensional sense. A wavefront will be associated with the outward spreading disturbance.*"

The extent to which this wavefront extends into the tree over a normal TOF test span and the effect of the variation in density is examined in Chapter 5.

4.3.2 Variation in density of wood nearest the bark between seasons

The density profile of the outer 60 mm of wood nearest the bark in nine trees was collected at each site in summer and winter. The same trees were not used for both seasons as it was feared that after taking a core in summer, subsequent measurements would affected. Instead, an average site density was obtained for each season and compared to the average site change in standing tree velocity. It was expected that any significant change in site density would result in a measureable and proportional change in velocity[2].

As with the incremental core samples in summer, there is large variation in green density within and between dominance classes. This is shown in the box plots of summer and winter incremental core densities by distance in from the bark and dominance class in Figure 4.7.

Summer Winter

Green density (kg m^{-3})

10 20 30 40 50 60

a. Suppressed trees

Distance in from bark (mm)

Green density (kg m^{-3})

10 20 30 40 50 60

b. Co-dominant trees

Distance in from bark (mm)
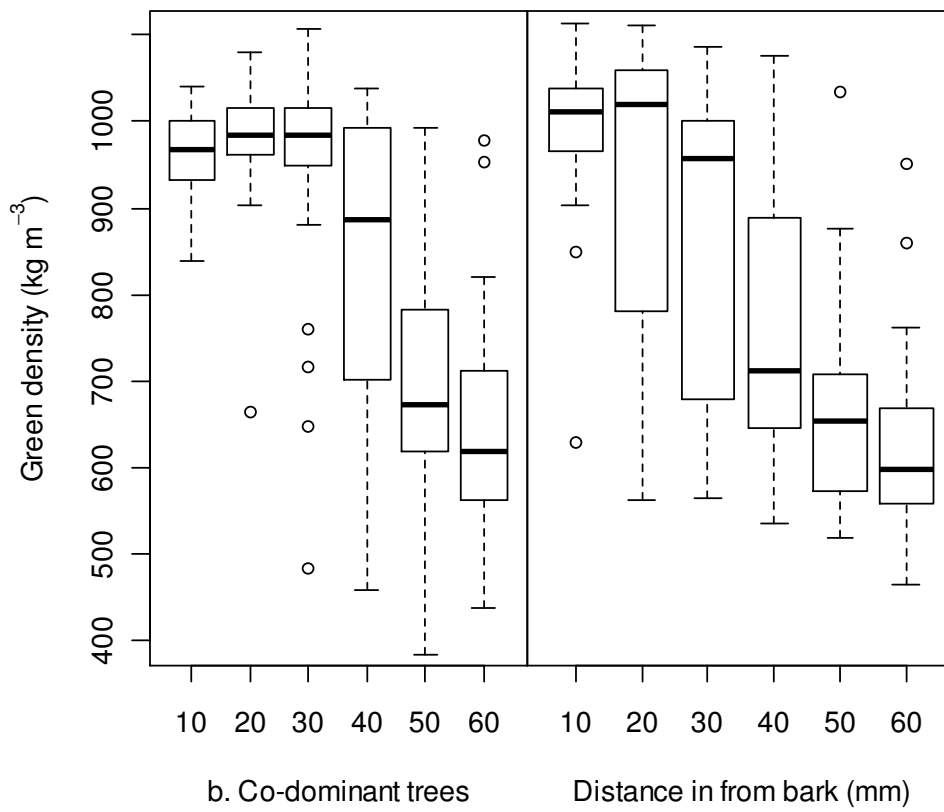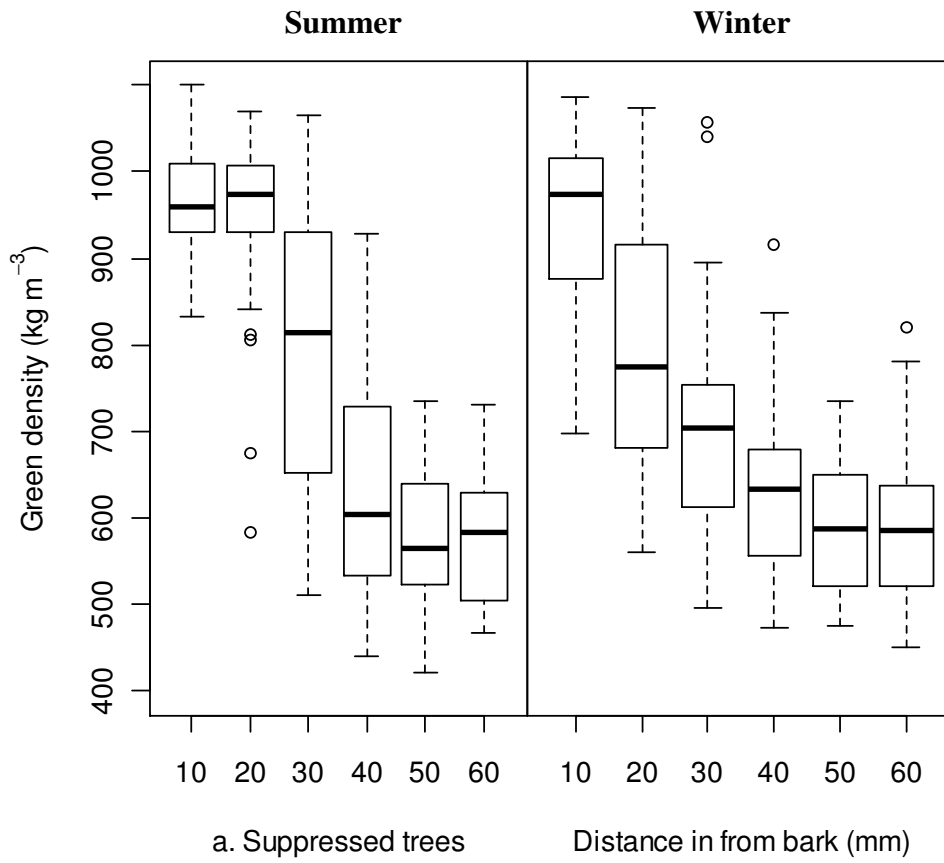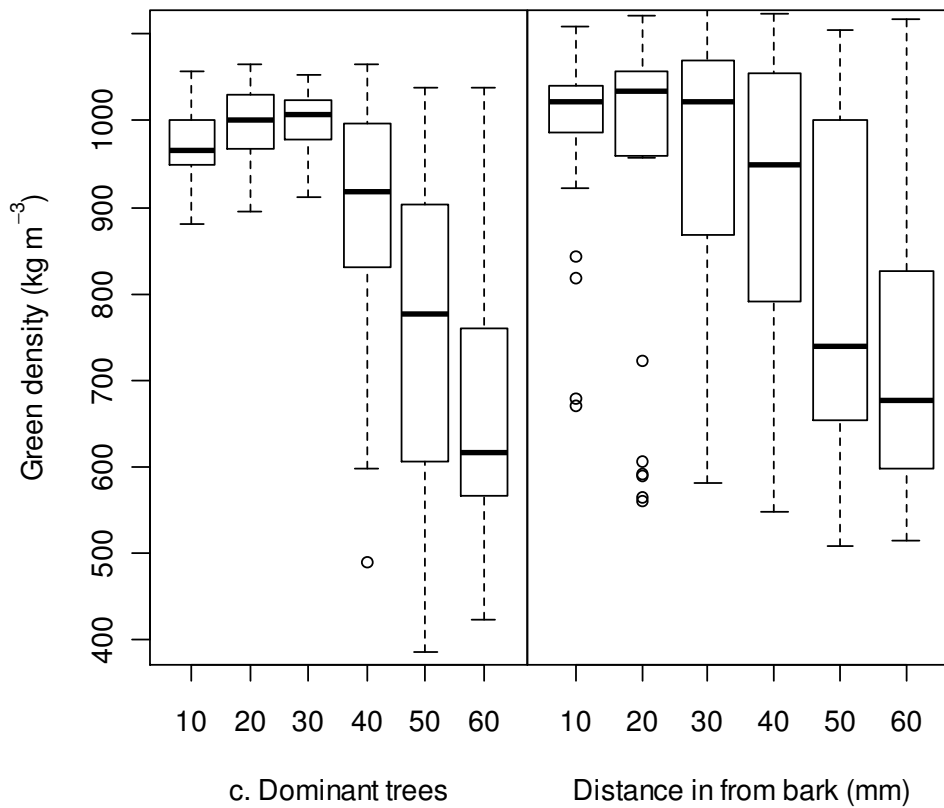
Figure 4.7. Box and whisker plots showing the variation in green density measurements with distance in from the bark between summer and winter incremental cores. a. summer and winter variation for suppressed trees, b. Summer and winter variation for co-dominant trees, c. Summer and winter variation for dominant trees. There were 30 samples for each position in each dominance class for both summer and winter.

Figure 4.7 shows that the variation in green density is greater in winter than summer and that the mean green density is likely to be lower in winter. Table 4.1 shows the change in mean green density for each site alongside the change in standing tree velocity[2] between seasons.

Table 4.1. Site by site comparison of average standing tree velocity measurements and fresh density of the outer 30 mm between summer, winter and winter sample month.

Site Number	Site ID	Summer ST Velocity^2	Winter ST Velocity^2	% Difference	Sample Month	% Change in Density
1	AB11L	8.30 (1.3)	7.86 (1.1)	-5.1	Dec	6.4
2	AB21L	8.54 (0.9)	8.90 (1.1)	4.1	Dec	-7.2
3	AB26H	8.22 (1.4)	8.90 (1.6)	8.2	Dec	-2.8
4	AR11H	8.50 (1.3)	9.82 (1.5)	15.6	Feb	-3.7
5	AR31L	8.75 (1.0)	10.25 (1.4)	17.0	Feb	4.8
6	GA32H	8.17 (1.0)	8.33 (1.2)	1.8	Dec	-23.0
7	GL31L	8.13 (1.0)	9.11 (1.5)	11.7	Dec	-16.4
8	IN23H	8.86 (1.2)	10.20 (1.3)	15.2	Mar	4.8
9	TA23H	7.47 (0.8)	7.93 (1.3)	5.7	Dec	-2.1
10	TR11H	7.95 (0.9)	10.54 (1.8)	28.7	Feb	-12.2

The mean site density was calculated from the outermost 30 mm, the assumed path of the stress wave in a standing tree acoustic measurement. There is no correlation between change in density and change in velocity^2 and correlations did not improve if mean site densities were calculated using only the first 10 mm or the entire 60 mm of the density profile of wood nearest the bark. From equation 2.1 (page 2-9), it is expected that an inverse relationship would exist between density and velocity^2 but this was not reflected in the results. The frozen condition of the trees in February and March confounds the expected relationship by increasing the velocity even when overall density increases, *e.g.* 3 sites had an overall increase in mean density and the two sampled in freezing conditions (site numbers 5 and 8) showed an increase in velocity while site 1, sampled in non-freezing conditions, showed a decrease in velocity. Unsurprisingly, freezing conditions also increase the velocity over and above what would be expected from a decrease in density alone, *e.g.* sites that had a mean decrease in density in non-freezing conditions (sites 3, 7 and 9) showed an 8.2%, 11.7% and 5.7% increase in velocity^2 for a 2.8%, 16.4% and 2.1% decrease in density, respectively. Whereas sites samples in freezing conditions (sites 4 and 10) showed a 15.6% and 28.7% increase in velocity^2 for a 3.7% and

12.2% drop in density, respectively. Of course, there is one site (site 6) that defies explanation by exhibiting a 1.8% increase in velocity^2 for a 23% reduction in mean site density. This anomalous result possibly indicates that the range of densities was not adequately represented by the nine trees measured in summer, at least for this site. It is the complication associated with not measuring the change in density and velocity on the same tree between seasons, making it very hard to separate the effects of density, experimental procedure and temperature.

Interestingly, the sites with the greatest drop in density (site numbers 6 and 7) were the sites with the greatest soil moisture deficit as given by the Forestry Commission Ecological Site Classification (ESC). However, two other sites (Sites 1 and 5) with only slightly smaller soil moisture deficits showed an increase in density from summer to winter. The other mechanism for dehydration or desiccation in stems when lack of precipitation is not a factor, is caused by freezing conditions. Sakai (1970) and Herrick *et al*. (1990) explained that winter desiccation is possible in sites with frozen soil, where solar heating of needles above air temperatures result in transpiration and therefore water loss from the stem. Whilst February and March experienced freezing air temperatures at time of sampling and would have resulted with ice in the stem, there was often snow lying on the ground when sampling in December, even though air temperatures were not freezing.

Regardless of the mechanism of density loss, there are much larger variations in green density of the outer 30 mm in from the bark in winter compared to summer. Additional effects of freezing temperatures forming ice within the tree further complicate the relationship between standing tree velocity^2 and tree MOE. Therefore it is recommended that acoustic tools not be used in freezing or near freezing conditions to avoid the risk of overestimating MOE. Additionally, further work needs to be undertaken to ascertain whether density profiles of wood nearest the bark for winter shown here are normal, or were subject to a greater degree of winter desiccation by lower than normal temperatures. This is possible as Chalk and Bigg (1956) state that in the absence of abnormal water stress, it is generally agreed that tree moisture content is lowest in the middle or toward the end of a growing season and highest in winter.

4.3.3 Variation in Juvenile Wood and Heartwood Percentage Within and Between Trees

4.3.3.1 Heartwood Variation

From the 30 trees felled, 26 of the breast height discs were analysed for heartwood (HW) and juvenile wood (JW) percentage (4 discs were damaged too much for measurement) as per the method outlined in sections 4.2.3 and 4.2.5. The proportion of JW ranged from 3% to 21% of disc area with a mean of 11%. The proportion of HW ranged from 38% to 83% with a mean of 62%. Corresponding green densities were 652.8 kg m^{-3} and 952.4 kg m^{-3} with a mean of 766.6 kg m^{-3} (COV=11.8%). The cambial age (number of growth rings) of the discs ranged from 29 to 54 years with a mean of 38.7. The difference in cambial age at breast height between dominant and suppressed trees ranged from 1 to 12 years with a mean of 4.9. There was no correlation between JW and HW proportions, shown in Figure 4.8. There was a significant ($p<0.01$) inverse relationship between disc density and heartwood percentage ($R^2 = 0.55$) shown in Figure 4.9.
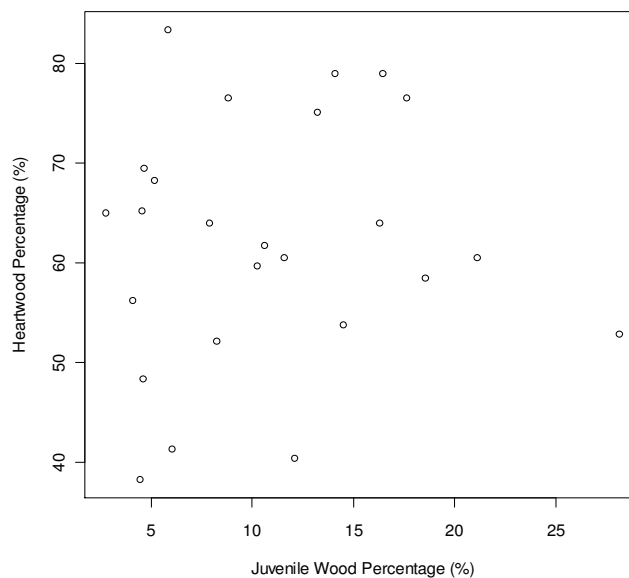
Figure 4.8. Heartwood was plotted against juvenile wood percentage at breast height.
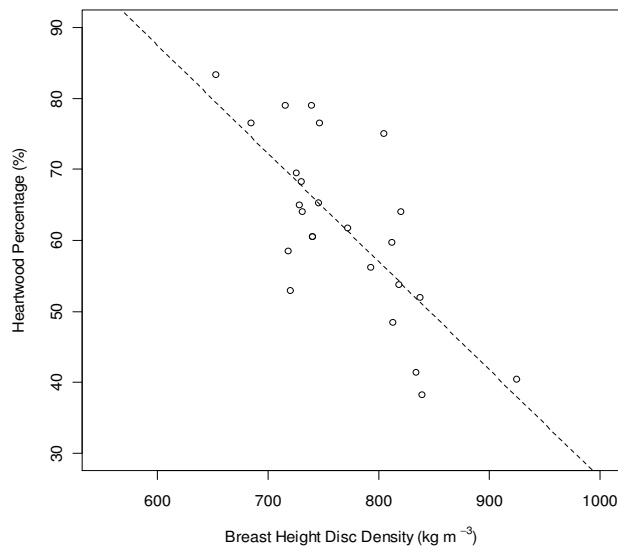
Figure 4.9. Relationship between disc density and heartwood percentage at breast height.

The measured HW area was plotted against the modelled HW area from Beauchamp (2011) (Eq. 4.10) to give Figure 4.10. There is an excellent relationship between the measured and modelled area ($R^2 = 0.92$). Given the uncertainties in the HW area measurement method expressed in section 4.2.3, this result offers enough validation to use the data in further analysis.
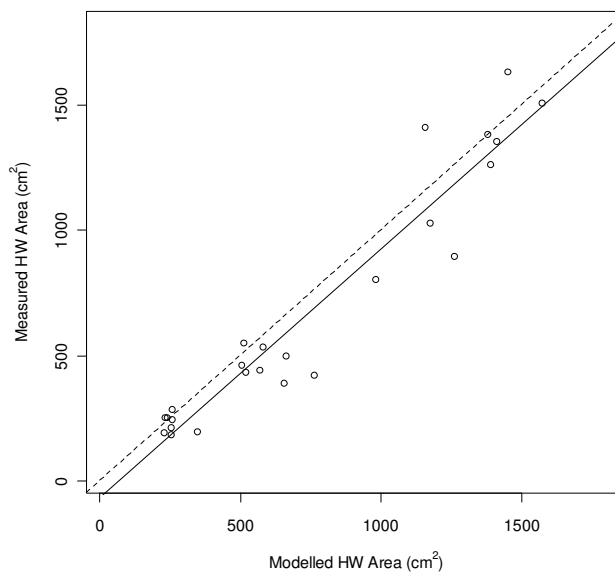
Figure 4.10. Comparison of measured heartwood area against the heartwood area model in Beauchamp (2011).

Figure 4.11 shows the density change with height in the stem by dominance classes compared with the overall mean ±5%.
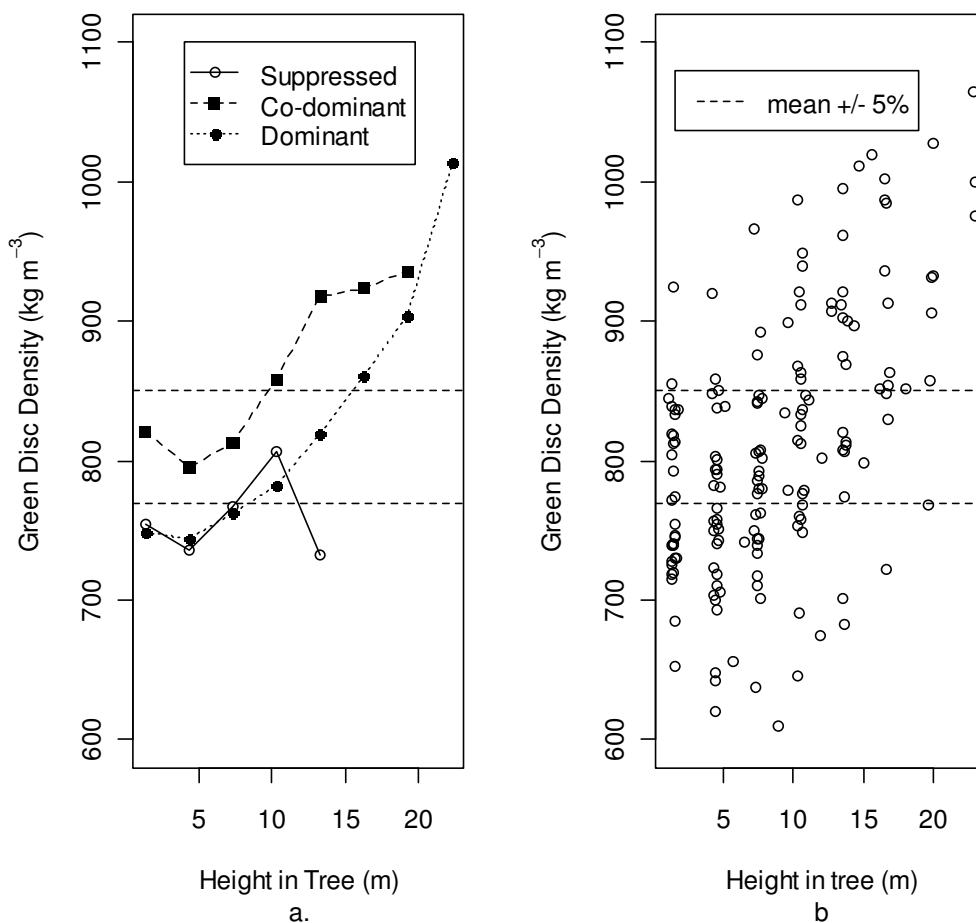
Figure 4.11. a. Mean green density variation with height in the stem by dominance class. b. Scatter plot of all disc densities with height in tree.

The mean overall green density for all discs (from breast height to a top diameter of 160 mm for all trees) is 810 kg m^{-3} (COV=11.2%) with a range of 610 kg m^{-3} to 1064 kg m^{-3}. The green density of 64% of discs exceed 5% and 37% of discs exceed 10% of the overall mean.

Using the mean green density values from Figure 4.11 shows that the following locations were outside the ±5% region:

- For suppressed trees, the bottom 7.3 m and the top disc.

- For co-dominant trees, the top 9 m of the tree.

- For dominant trees, the bottom 7.3 m and the top 6 m of the tree.

Whilst green density does increase with height in the tree, it also varies with dominance class. Comparison of the mean density between dominance classes was undertaken with a Wilcox rank sum test as the distributions were non-normal (Crawley 2007). There was a significant difference between the means of co-domianant and suppressed trees using values up to 10.3 m tree height for both (p<0.001), which corresponds to a difference of 7.0%. There was no significant difference between dominant and suppressed trees over the same height range. Comparing the mean densities of dominant and co-dominant trees up to a tree height of 16.3 m, showed a significant difference between the two (p<0.001), corresponding to a difference of 7.7%.

This result means that co-dominant trees contain consistently less HW percentage than dominant trees. This is due to similar sapwood (SW) depths in dominant and co-dominant trees, shown in Figure 4.12a. However, this still results in a larger SW area in dominant trees and a greater volume of water per unit length in SW (shown in Figure 4.12b) to supply the greater need for water by the branches and canopy of larger trees.
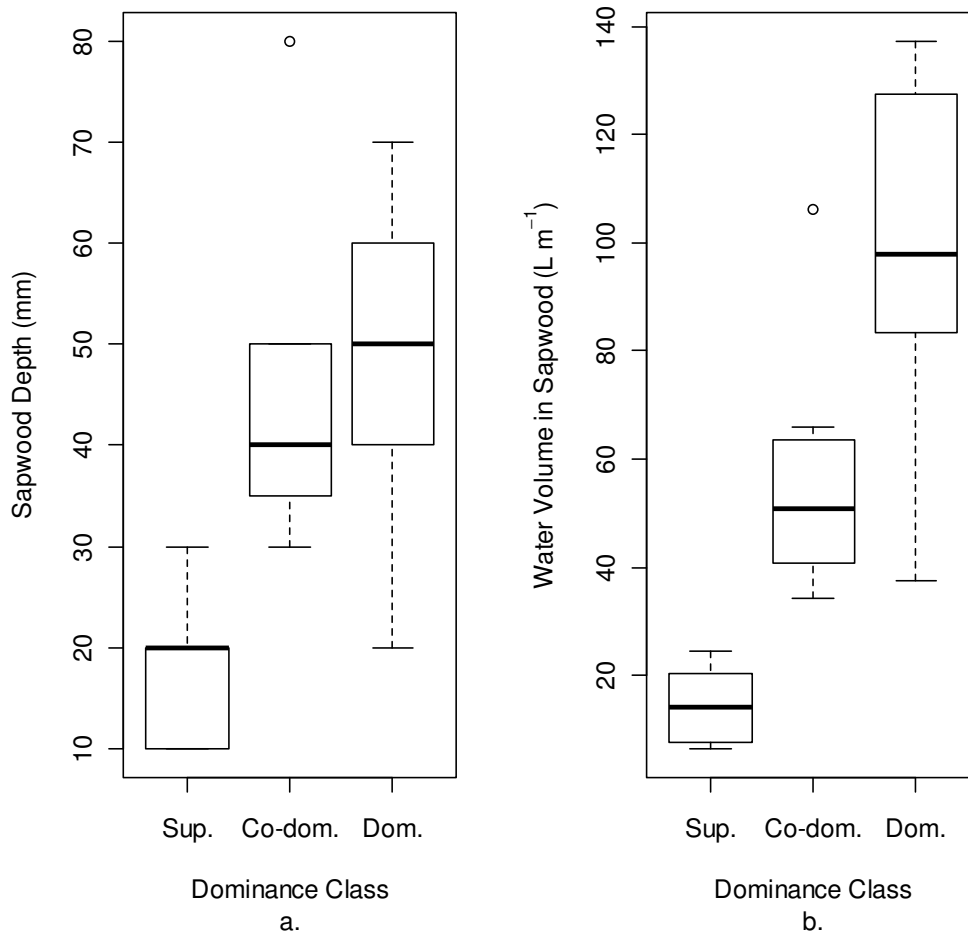
Figure 4.12. Box and whisker plots showing (a) Sapwood depth by dominance class, and (b) Water volume per unit length by dominance class.

A comparison of HW percentage, JW percentage and disc density at breast height is shown in Figure 4.13.
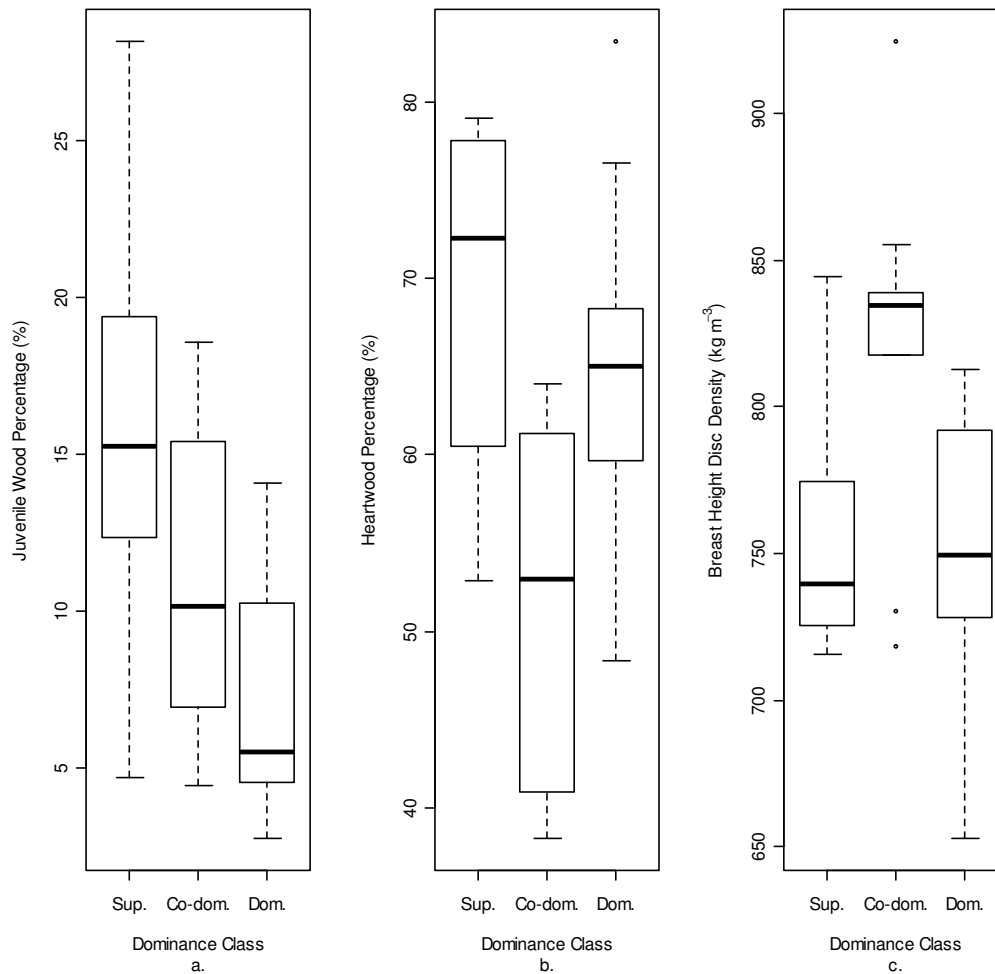
Figure 4.13. Plots showing (a) Juvenile wood percentage, (b) heartwood percentage and (c) green disc density at breast height by dominance class.

The variation in JW percentage for each dominance class (Figure 4.13a) is quite high but there is a clearly visible inverse relationship between dominance and JW percentage. The inverse relationship between HW percentage and green density is shown again in Figure 4.13b and its effect on green density in Figure 4.13c.

The combination of these factors leads to the conclusion that assumptions of constant, uniform green density produce errors of ±5% for almost two-thirds of all discs up to 160 mm top diameter. The question then becomes, how well do these data represent the general population of logs coming into a sawmill? Samples were measured in the forest, directly after felling and there is typically a delay, of varying duration, between harvest, collection of logs from roadside,

storage of logs at a sawmill and processing. It is unknown what effect this has on log density, *i.e.* whether it normalises or amplifies any differences. It may depend on the season logs were harvested, *i.e.* warm, dry, cold or wet. Also, it is important to determine an acceptable margin of error. This is presumably at the point where economic gains still exceed the economic costs associated with misclassification. Does the margin of error presented here warrant the introduction of a log density measurement system or is using velocity^2 still a powerful enough measurement?

There is very little literature discussing the implications of variation in green log density on acoustic measurements. Achim *et al*. (2009) stated that the relationship between the static MOE of battens and the dynamic MOE of logs could be improved from $R^2 = 0.41$ to $R^2 = 0.69$ with the inclusion of log density for white spruce.

Due to the relatively young harvest age, the assumption of constant density in green logs is routinely used in papers from Australia and New Zealand (*e.g*., Tseheye *et al*. 2000, Matheson *et al*. 2002, Dickson *et al*. 2004). However, Jones and Emms (2010) showed that the inclusion of log density provided a significant improvement in the prediction of kiln dried batten MOE measured by a machine stress grader; R^2 improved from 0.49 to 0.68. This study was conducted on the second and third logs in the stem and interestingly showed that the HW varied from 11% to 60% with a mean of 20%, resulting in a green log density variation between 695kg m^{-3} and 1012 kg m^{-3} with a mean of 913 kg m^{-3}. The magnitude of this improvement is similar to that seen in Achim *et al*. (2009), despite the obvious differences in age. Overall, it would appear that HW variation is significant in mature trees for many species of harvest age and green density should be accounted for in the calculation of log MOE.

Chapter 6 will attempt to answer some of the questions presented here by showing the grading results of a sawmill simulation experiment which contained one group of logs sorted by estimated log MOE with log velocity^2 only and another using density and velocity^2.

4.3.3.2 Juvenile Wood Variation

Figure 4.13a shows that the proportion of JW is inversely related to dominance class *i.e*. larger trees have a smaller proportion of JW. Modelling the proportion of JW at breast height with age at breast height (AgeBH) as a continuous variable and dominance class (Status) and thin regime (Thin) as categorical variables, produce the ANCOVA results in Table 4.2. This model has an R^2 of 0.80.

Table 4.2. ANCOVA results for the full model to predict the relationship between JW percentage by age at breast height (AgeBH), dominance class (Status) and thinning regime (Thin).

Term	Df	Sum of Squares	Mean Square	F value	Pr(>F)
AgeBH	1	0.05077	0.05077	39.33	2.05e-5
Status	2	0.01880	0.00940	7.28	0.0068
Thin	1	0.00201	0.00201	1.56	0.2326
AgeBH:Status	2	0.00436	0.00218	1.69	0.2200
AgeBH:Thin	1	0.00298	0.00298	2.31	0.1510
Status:Thin	2	0.00053	0.00027	0.21	0.8146
AgeBH:Status:Thin	2	0.00081	0.00046	0.31	0.7351
Residuals	14	0.01807	0.00129		

Table 4.2 shows that there is no statistical dependence on the proportion of JW with any two or three-way interactions between age at breast height, thinning and dominance class (*p*>0.05). A step-wise model simplification procedure (using AIC) to obtain the minimally adequate model was carried out to remove the non-significant parameters. The results of the model simplification are shown in Table 4.3.

Table 4.3. Simplified, minimally adequate ANCOVA model to predict the proportion of JW by age at breast height (AgeBH) and dominance class (Status).

Term	Df	Sum of Squares	Mean Square	F value	Pr(>F)
AgeBH	1	0.05077	0.05077	38.82	2.86e-6
Status	2	0.01880	0.00940	7.19	0.0040
Residuals	22	0.02877	0.00131		

The R^2 of the simplified model is 0.71 and there is no significant difference between the maximal and simplified models (p=0.22) using an F-test. A summary of the ANCOVA in Table 4.4 is shown in Table 4.4.

Table 4.4. Summary of ANCOVA results for predicting the proportion of JW by age at breast (AgeBH) height and dominance class (Status).

Term	Parameter Estimate	Standard Error	t value	Pr(>|t|)
Intercept (Dominant)	0.2981	0.0452	6.589	1.26e-06
AgeBH	-0.0056	0.0011	-5.196	3.28e-05
Co-dominant	0.0273	0.0173	1.579	0.1285
Suppressed	0.0667	0.0176	3.787	0.0010

There is an inverse gradient between age and breast height and JW percentage of 0.56% for every year older the tree is (starting at the minimum age in the data set, 29 years). Suppressed trees have a significantly different intercept to dominant trees ($p<0.01$) with a 6.67% larger JW percentage. There is no significant difference in the JW percentage of co-dominant and dominant trees (p=0.1285) despite the observed inverse relationship between dominance class and JW percentage in Figure 4.13a. With age at breast height accounted for in the model, the lack of significance between co-dominant and dominant trees is due to the large variation in JW percentage within each dominance class. This variation is most likely due to differences in growth rate (yield class): Experiment sites were deliberately chosen to provide the greatest contrast in values, *e.g.* only sites with high yield class ($\geq$18) or low yield class (=12) were selected and 4 sites were thinned and 6 unthinned (see Table 3.1 for more details, page 3-5).

It is unsurprising that thinning showed no effect on the proportion of JW as most thinning observed at the test sites was achieved by systematic or row thinning, with only a small proportion of later selective thinnings. This technique is likely to leave parts of the stand unaffected by thinning (Rollinson 1987) and therefore

have no effect on the proportion of JW for these trees. However, Brazier and Mobbs (1993) show that there is a pattern of growth, initially fast then slow before and after competition sets in, that is characteristic of unthinned stands. Therefore, a thinned stand of equivalent age to an unthinned stand should have a smaller proportion of juvenile wood as its growth rate would be improved through reduced competition for resources (Macdonald and Hubert 2002). This expectation can also be shown with the data collected here, with Figure 4.14 showing the difference in annual radial increment between mature wood (MW) and JW at breast height for thinned and unthinned stands.
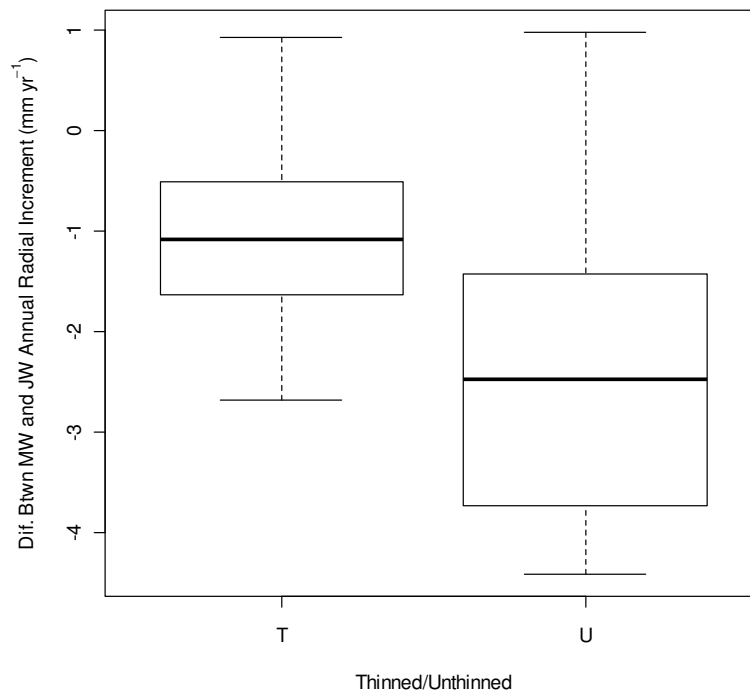
Figure 4.14. Difference between mature wood (MW) and JW growth rates at breast height for thinned (T) and unthinned (U) stands.

The thinned stands experienced a 1.08 mm drop in mean radial increment after the first 10 years of growth (COV = 94%), while the unthinned stands experienced a 2.36 mm drop in mean radial increment after the first 10 years of growth (COV = 68%).

The significant variations in the proportion of JW due to differences in growth rate have potentially important implications for the use of standing tree acoustic

tools; namely that they violate one of the assumptions implicit in their use (outlined in sections 3.4 and 4.1). This is because it is impossible to obtain a good measure of whole log stiffness from the stiffness of wood nearest the bark alone unless the stiffness of this material is proportional to inner-wood stiffness and inner-wood stiffness is partly controlled by the proportion of JW.

4.3.4 Using Density to Calculate Dynamic MOE for Logs and Trees

Section 4.3.3.1 showed that green disc density can vary by more than 5% of the mean 64% of the time in discs up to 160 mm top diameter. This can affect the accuracy of stress wave instruments (as outlined in section 2.4).

Figure 4.15a and b show how the relative estimation of bottom log stiffness changes with the inclusion of log density for each dominance class, *i.e.* log velocity^2 compared to log dynamic MOE.
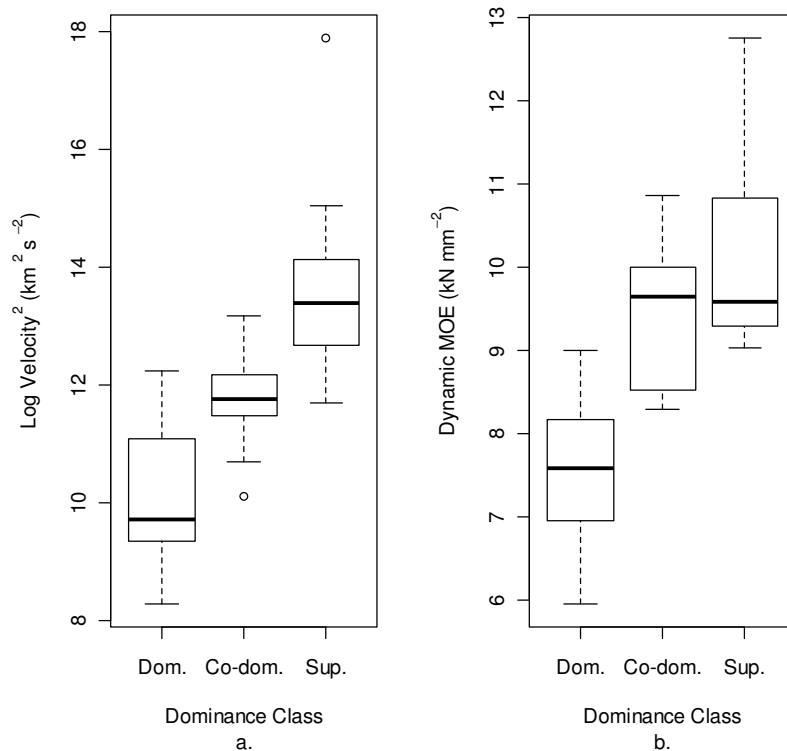
Figure 4.15. Comparison of relative stiffness between dominance class without the inclusion of density (a) and after the inclusion of density (b).

Instead of a discreet distribution of stiffness for each dominance class using log velocity^2 only, co-dominant and suppressed stiffness distributions overlap with the inclusion of green density. Significant differences between bottom log E_d were tested with ANOVA. There is no significant difference between the mean bottom log E_d of co-dominant and suppressed trees (p=0.17). There is a large, significant difference of 22.5% between the mean bottom log E_d of dominant trees and co-dominant and suppressed trees (p<0.01). This may be due to a decrease in oven dry density of dominant trees due to an increased proportion of earlywood in the stem. Figure 4.16 shows the mean oven dry density with height in the stem for each dominance class.
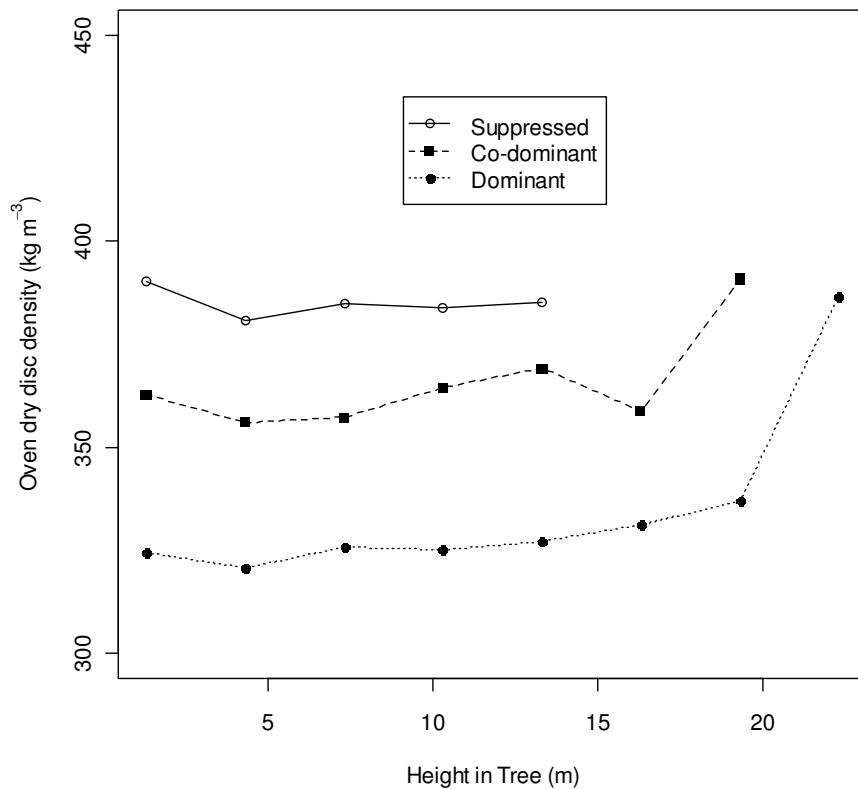
Figure 4.16. Mean oven dry disc density with height in stem for each dominance class.

The relationship between bottom log E_d with standing tree velocity^2 (*ST Velocity^2*), standing tree dynamic MOE (*ST Ed*) and standing tree MOE using the average effective density of the outer 30 mm of each tree (*ST Eff. Ed*) is shown in

Figure 4.17 a, b and c and summarised in Table 4.5. As with the analysis in Chapter 3, there is a highly leveraging data point. The R^2 values in shown on the graphs and in Table 4.5 were calculated with this point removed.
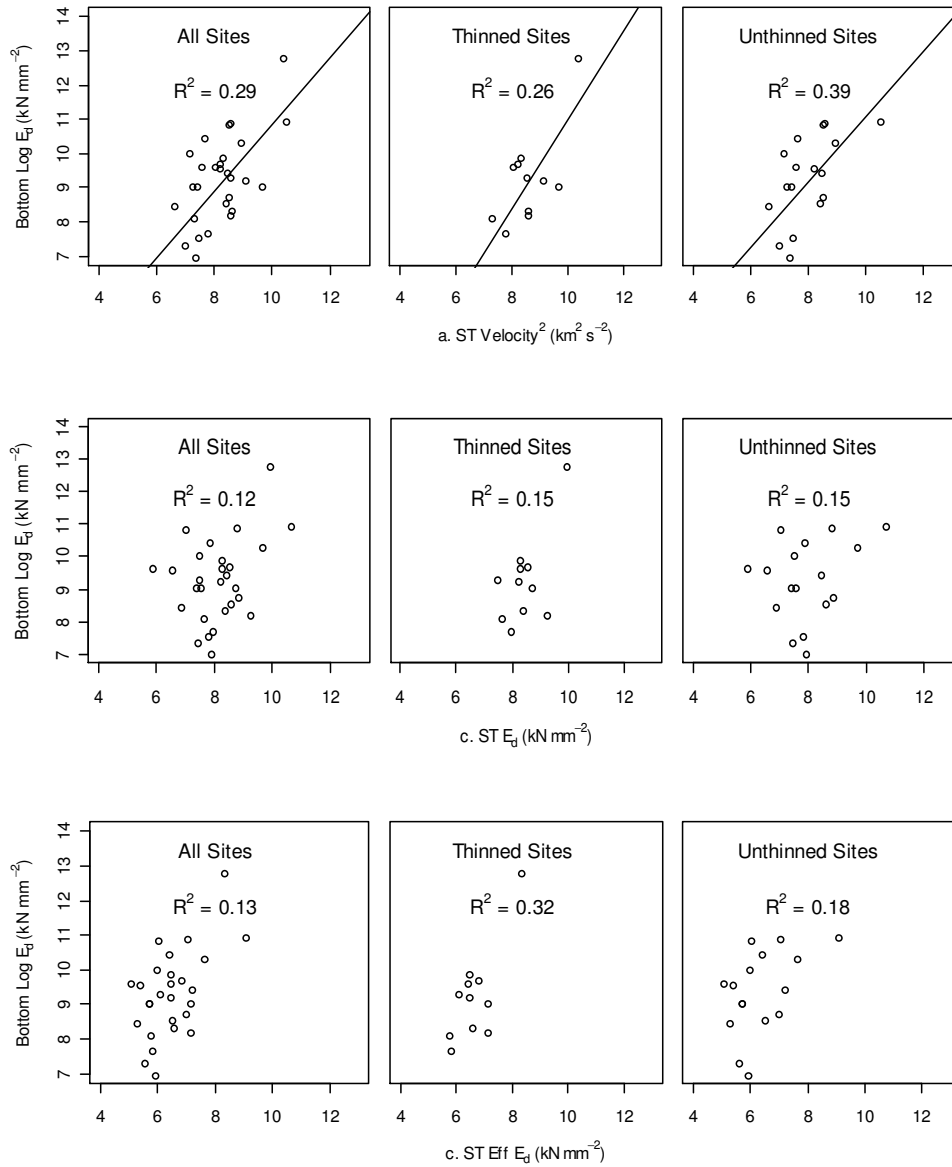
Figure 4.17. Relationship between bottom log dynamic MOE (Ed) with (a) standing tree velocity^2 (ST Velocity^2), (b) standing tree dynamic MOE (ST Ed) and (c) standing tree dynamic MOE using effective density (ST Eff. Ed).

Table 4.5. Calculated R^2 values for regression between log dynamic MOE and standing tree velocity^2, standing tree dynamic MOE and standing tree dynamic MOE using effective density.

Attribute	Overall	Thinned	Unthinned
ST Velocity^2	0.29	0.26	0.39
ST Dynamic MOE	0.12	0.15	0.15
ST Dynamic MOE$_{Eff}$	0.13	0.32	0.18

Using standing tree velocity alone provides a better measurement of bottom log dynamic MOE than standing tree dynamic MOE calculated using either normal green density or effective density. There was marginal improvement using effective density for thinned stands, with the R^2 changing from 0.26 to 0.32 (RSE is 0.95 and 0.9, respectively). Overall, correlations with log dynamic MOE were poorer than with log velocity^2.

The relationship between bottom log MOE with and live crown ratio (CR) and slenderness (HD) is shown in Figure 4.18 and summarised in Table 4.6. Again, the values in Table 4.6 were calculated after the removal of the highly leveraging data point.
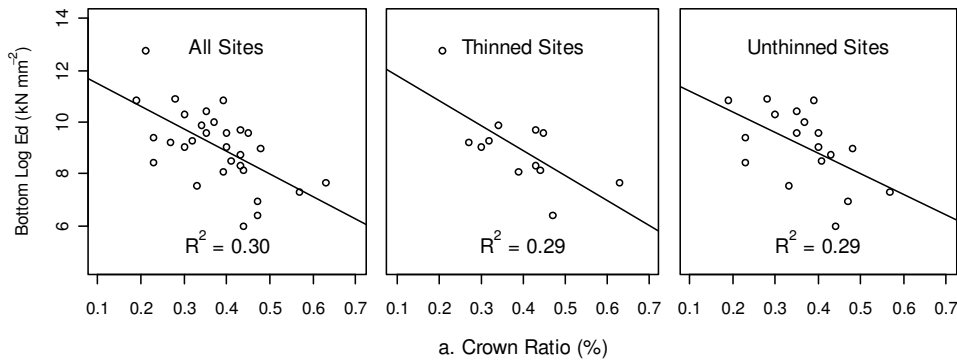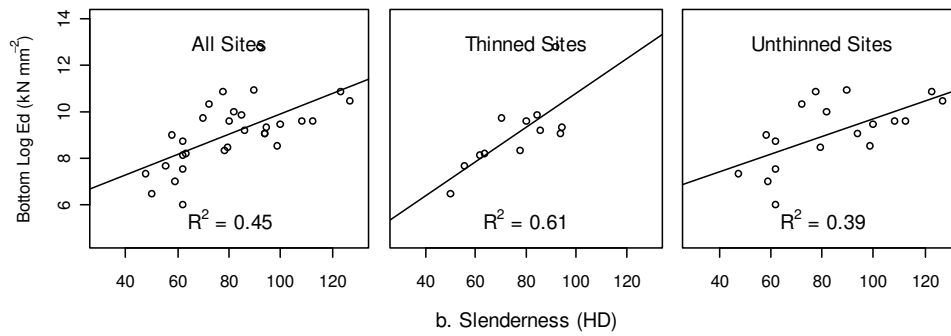
a. Crown Ratio (%)

Figure 4.18. Relationship between bottom log MOE (Ed) with (a) crown ratio and (b) slenderness.

Table 4.6. Calculated R^2 values for regression between bottom Log_{ED} and live crown ratio (CR) and height-diameter ratio (HD).

Attribute	Overall	Thinned	Unthinned
Live crown ratio (CR)	0.3	0.29	0.29
Height-diameter ratio (HD)	0.45	0.61	0.39

Again, there is a general deterioration in the relationship between these attributes when bottom log E_d is used instead of log velocity[2].

These results suggest that existing non-destructive measurement methods for standing tree stiffness are slightly less accurate at measuring the true dynamic stiffness of the logs. The inclusion of actual density or effective density to standing tree velocity did nothing to improve the accuracy of the method, indicating that factors such as variations in the proportions of JW and HW are the main cause of the poor relationship between standing tree velocity[2] and bottom log E_d. Interestingly, the height-diameter ratio was more effective at predicting bottom log E_d than the standing tree acoustic instrument.

Figure 4.19 shows the relationship between slenderness and bottom log E_d, highlighting dominance class.
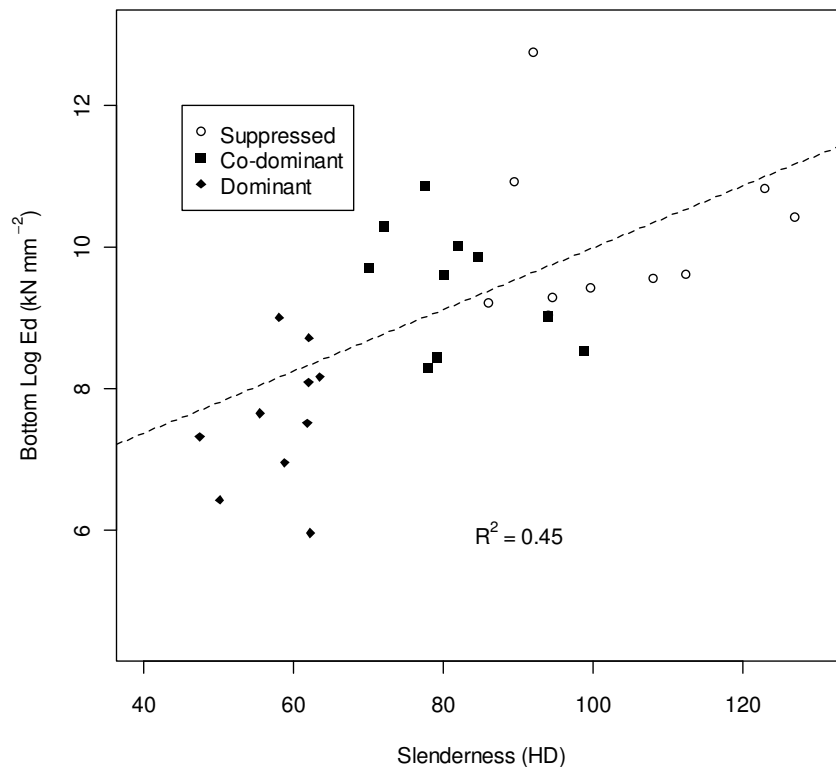
Figure 4.19. Relationship between bottom log E_d and slenderness showing the effect of dominance class.

When examining the variation of bottom log E_d by dominance class in Figure 4.19 and Figure 4.15b, dominant trees had a mean value 22.5% lower than the other classes. This is despite having the lowest proportion of JW. There are 2 mechanisms of tree growth that can account for this. The first; is that the JW percentage was defined as the area of the first 10 growth rings to the total disc area. The value of 10 years was chosen in this study because it was the value used in another experiment, presented in Chapter 6. Brazier and Mobbs (1993) and Cameron *et al.* (2005) used 12 years as their transition from JW to MW for Sitka spruce, whilst Larson *et al.* (2001) states that 10 years in loblolly pine is an acceptable for most purposes as the boundary changes depending on the criteria used to define it. Larson *et al.* (2001) also describes JW wood as synonymous with 'crown formed wood' because it is produced either within the living crown or in proximity to physiological processes emanating from the living crown. Dominant trees exhibit larger, deeper crowns that are slower to recede up the tree

than the trees surrounding them and it is therefore not unrealistic to expect that the juvenile wood zone would be extended as proximity to the crown is maintained for a longer period.

The second, is that growth rate is negatively correlated with basic density, as an increase in vigour results in an increase in earlywood width without a corresponding increase in latewood width (Brazier 1970). For Sitka spruce in the UK, Brazier (1970) and Petty *et al*. (1997) both show a pattern of decreasing density with increasing ring width. Earlywood, or spring wood, is characterised by trachieds (fibres) with wide lumens and thin walls to provide efficient transport pathways between the roots and the newly elongating shoots and needles. Latewood, or summer wood, is characterised by narrow lumens with thick cell walls to provide support for the expanding crown (Larson *et al*., 2001). The difference in function between the two fibre types result in latewood being much stiffer and stronger in bending than earlywood. Therefore, dominant trees will be composed of a high proportion of low stiffness, low density earlywood (*e.g.* Figure 4.16), resulting in logs of lower stiffness.

4.4 Conclusions

Before stating the conclusions of this study, it needs to be reiterated that the data presented here may not be entirely representative of the population as a whole; sites were chosen to provide contrasting combinations of altitude, yield class and silvicultural management. Trees within site were chosen to be the smallest, median and largest. The only other criteria for the trees were that they are capable of producing at least one sawlog, *i.e.* with a stem straightness score >2 and a diameter at breast height ≥200 mm.

The list below summarises the results of this chapter:
- The mean density variation of wood nearest the bark is not consistent between trees of different dominance classes.
- There is a large variation in density within a dominance class moving in from the bark.

- Density variation within and between dominance classes was greater in winter than summer.
- There were significant effects of freezing water within the wood nearest the bark during winter on standing tree velocity measurements.
- Heartwood variation at breast height was significant between trees of different dominance classes.
- There was significant variation in the green density of discs with height in the tree and dominance class.
- There was a significant variation in the JW percentage depending on age at breast height and dominance class.
- Including log density into the dynamic MOE calculation results in a general deterioration of the relationship between standing tree velocity, live crown ratio and height-diameter ratio compared to looking at log velocity^2 alone.
- Including density or effective density into the dynamic MOE equation for standing tree tools only improved the relationship with the dynamic MOE of logs for thinned stands.

Using standing tree instruments in winter months should be avoided as there are much larger variations in green density of the outer 30 mm in from the bark in winter compared to summer. Additional effects of freezing temperatures forming ice within the tree further complicate the relationship between standing tree velocity^2 and tree MOE.

The implication of these results is that the assumptions implicit in the use of standing tree acoustic tools for the accurate estimation of tree stiffness may not be valid when considering a population as a whole: different relationships between standing tree velocity and tree stiffness will exist depending on dominance class, silvicultural history and age of each stand because of the different proportions of JW and HW.

The variation in the green density of discs at breast height and up the tree's stem show that the assumption of constant density for using resonant acoustic tools on

logs will be have an error of over ±5% for 64% of measurements. The level of acceptable margin of error needs to be established to determine whether the green density of logs should be routinely measured when using acoustic instruments. Results from other studies around the world would suggest that including green density provides a much better prediction of the average stiffness of batten cut from a log.

5 Stress Wave Propagation in Standing Trees

5.1 Introduction

This chapter reports the results of an experiment which mapped the stress wave arrival times in three logs of varying diameters over a cross section at 0.5 m and 1.0 m from the stress wave initiation point. In this manner it is possible to both examine the rate at which the wave is expanding within a typical test span of a normal TOF measurement and determine how this expansion interacts with the density variation of wood nearest the bark in a tree as described in Chapter 4.

Furthermore, it is possible to compare the experimental wave behaviour with the proposed theoretical wave behaviour outlined in section 2.3. The basic fundamental concepts and theory behind wave mechanics are discussed and a distinction is found between what aspects of wave propagation in trees are covered by the theory and which are not. The implication of these findings on the accuracy of standing tree instruments is also discussed.

5.1.1 Objectives

The objectives of this chapter are to mimic a standing tree, time of flight acoustic test on three different size logs, ranging from 0.2 m to 0.46 m in diameter to determine:

1. The shape of the wave-front 0.5 m and 1 m from the stress wave initiation point to gain an understanding of how a wave spreads over a tree's cross section as it propagates.
2. To assess any possible impact of the wave propagation behaviour on the accuracy of time of flight stress wave instruments.

5.1.2 Background

Historically, the segregation of trees and logs has often been made on the basis of external characteristics. While this generally provides valuable information on the volume of timber that can be recovered, it is not a good indicator of the mechanical properties of this timber (Wagner *et al.* 2003). In recent years the use of acoustic (or stress wave) based instruments for segregating material based on wood properties, particularly modulus of elasticity, has become more common. With the development of portable and simple-to-use time-of-flight (TOF) and resonance-based tools, the use of acoustics in the forestry sector has increased, particularly in countries such as New Zealand (*e.g.*, Walker and Nakada 1999; Tseheye *et al*. 2000), Australia and the United States (*e.g*., Wang *et al*. 2000, 2001, 2002, 2004). This technology is beginning to be used more by the European forest industries.

For standing tree instruments, two transducers are placed on the standing tree a known distance apart and as the wave passes the first transducer, a timer is started. The timer is stopped when the wave reaches a second transducer. The velocity is calculated by dividing the distance travelled by the time taken. The distance between the two transducers is typically 1.0 m – 1.5 m. This approach is often referred to as time-of flight (TOF). Stiffness is then calculated using equation 2.1 (page 2-9) assuming a constant density because the stress wave is assumed to be travelling through the sapwood in the outer part of the tree. The assumed path of the stress wave is in the outer 20 mm – 30 mm of the tree, directly between the start and stop probes (Grabianowski *et al*. 2006). This region has been shown to be of relatively constant density (*e.g*., Weilinga *et al*. 2009) in radiata pine, however in Chapter 4 and in an earlier study by Chalk and Bigg (1956), this region was shown to be relatively variable in UK Sitka spruce, particularly in smaller diameter trees. The implication of these findings on the assumption of constant density for standing tree acoustic instruments depends on the behaviour of the stress wave between the impulse initiation and the stop probe.

Section 2.3 outlines some general theory behind two different types of wave propagation; dilatational waves and plane waves. Purely longitudinal, or dilatational waves, can only exist in an infinite, three-dimensional solid, *i.e.* where the medium is much larger than the wave front such that there are no boundary interactions. In finite beams and rods, if a stress wave is travelling down its long axis and the lateral contraction of the cross-section is constrained then stresses are introduced normal to the direction of the propagating wave, creating a three-dimensional instead of a one-dimensional stress condition (Cremer 2005). These stresses reduce the displacement in the longitudinal direction, thereby increasing the apparent stiffness, *i.e.* stress wave speed of the material (see section 2.3 for details). Andrews (2003) showed that over short distances, similar to test spans in live tree measurement, dilatational waves dominate and measurements can be quantitatively adjusted to the one-dimensional wave speed using equation 2.3 (page 2-13).

For the assumption of constant density to hold in Sitka spruce, stress waves would have to propagate in an essentially one-dimensional manner with very little outward spread over the TOF test span. However as Graff (1991) explains about the behaviour of stress waves:

"The interaction of one part of the system to the next is the interaction of one differential element on the next. Instead of the simple push pull motion along a series of springs and masses, the disturbance spreads outward in a three-dimensional sense. A wavefront will be associated with the outward spreading disturbance."

Andrews (2002) states that the disturbance that spreads from the excitation is not described by equation 2.1 until it has propagated a long way.

Relating this to standing tree TOF measurements, when the excitation is initiated, the stress wave starts propagating both up toward the top probe and outward across the tree's cross section. It is not yet a plane wave but possibly, by the time it arrives at the top probe 1.0 – 1.5 m away, a measure of more of the tree's wood properties than simply the area directly between the probes. If this

outward spread of the propagating wave is significant, then the variation in wood density from the bark inwards becomes an important factor in the error for the calculation of E_d for different diameter trees.

This chapter will take the analysis one step further and look at how the wave has propagated over a 1.0 m test span, typical of a standing tree TOF measurement. The extent of any three-dimensional wave propagation can be determined and the effect of any variation in density in the region examined.

5.2 Method and Materials

Three freshly cut Sitka spruce log billets were obtained from a test plot at Forest Research's Northern Research Station, Roslin, Midlothian. Each billet was approximately 1.2 m in length, centred at breast height and with diameters listed in Table 5.1. The stand was unthinned with a planting distance of 2.0 m and was approximately 40 years old.

Table 5.1. Diameter at breast height (DBH) and age of billets used in the stress wave path experiment.

Log Number	DBH (mm)
1	213
2	341
3	446

The experimental procedure consisted of two components:

1. Mapping the arrival time of the pulse at 0.5 m and 1.0 m from the point of stress wave initiation
2. Measuring the distribution of stiffness and density within each billet by reducing them to approximately 20 mm x 20 mm sections and measuring the dynamic MOE of each.

All TOF mapping was undertaken on the billets directly after felling. While one billet was being measured, the others were placed in cold storage (approximately

4˚C) to minimise any moisture loss. The distribution of stiffness and density were carried out at 12% MC.

5.2.1 TOF Mapping

A grid was drawn over the top end cross section of each billet to mark the TOF measurement locations. Each grid point was assigned a unique coordinate (in mm) with the origin at the top centre of the cross section, approximately 10 mm in from the bark, as shown in Figure 5.1.
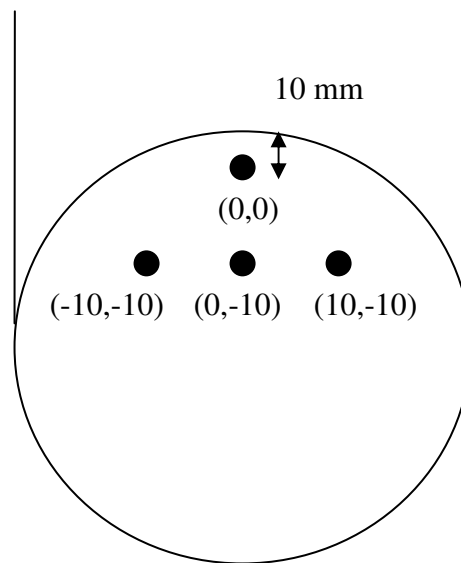
Figure 5.1. Location of origin in each test billet.

The grid pattern for each billet is shown in Figure 5.2. Each log was fitted with 4 rows of a 10 mm x 10 mm grid spacing at the top of the cross section to improve the resolution of the arrival times closest in radial distance to the stress wave initiation point. The grid was gradually spaced out as the radial distance increased.
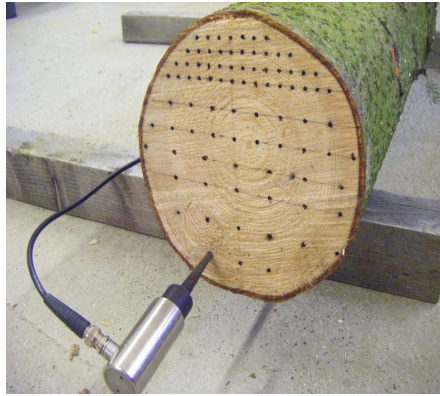
a. Small log   b. Medium log
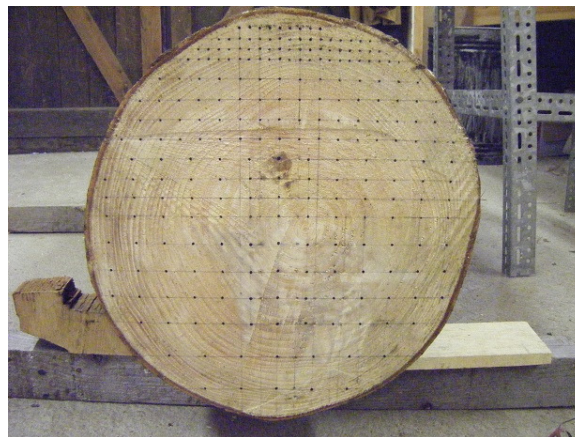
c. Large log.

Figure 5.2. Grid pattern for the a) small, b) medium and c) large logs.

The start and stop probes were those used for the IML Hammer (Instrumenta
Mechanic Labor GmbH, Germany) standing tree TOF instrument. However,
instead of using the impulse hammer supplied by IML, which is used to both
initiate the stress wave and start the timer, the experiment was set up similar to
the TreeTap TOF instrument (University of Canterbury, NZ) with an inert starter
probe and two active receiver probes placed further along the log a fixed distance
apart (*e.g.*, Toulmin *et al.* 2006). This setup was used to gain greater consistency
in the detection of the stress wave initiation, as the rise time of the impulse
hammer could change depending on how hard the probe was struck. The TOF
was calculated by measuring the difference in arrival times between the two
active receiver probes. The IML receiver probes consist of two spikes
approximately 70 mm long designed to hold a piezoelectric sensor. The first
receiver probe was placed directly in line (along the same azimuth) and a fixed
distance from the inert starter probe. The second receiver probe was placed on

each of the grid locations shown in Figure 5.2. Eight TOF measurements were recorded at each grid point using a Picoscope 2202 USB oscilloscope and analysed later using LabVIEW (National Instruments). The sample rate for the 1.0 m transit length was 2.5 MHz and the sample rate for the 0.5 m transit length was 5 MHz. A 400g hammer was used to initiate the stress wave.

a. 1.0 m TOF transit length   b. 0.5 m TOF transit length
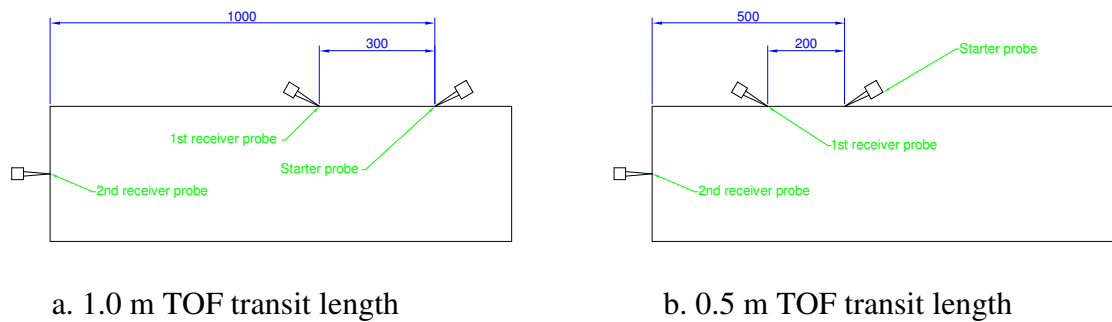
Figure 5.3. Probe layout for the a) 1.0 m transit length, and b) 0.5 m transit length.

Measurements were taken with the starter probe 0.5 m and 1 m from the top end of the log to measure the spread of the stress wave. When the starter probe was 1 m from the end of the log, the first receiver prober was placed 300 mm away along the same azimuth. When the starter probe was 0.5 m from the end of the log, the first receiver probe was placed 200 mm away along the same azimuth, shown in
Figure *5.3*.

An example waveform for a 1.0 m transit length measurement is shown in Figure 5.4. The signal in grey is the first receiver probe and the signal in red is from the second receiver probe.
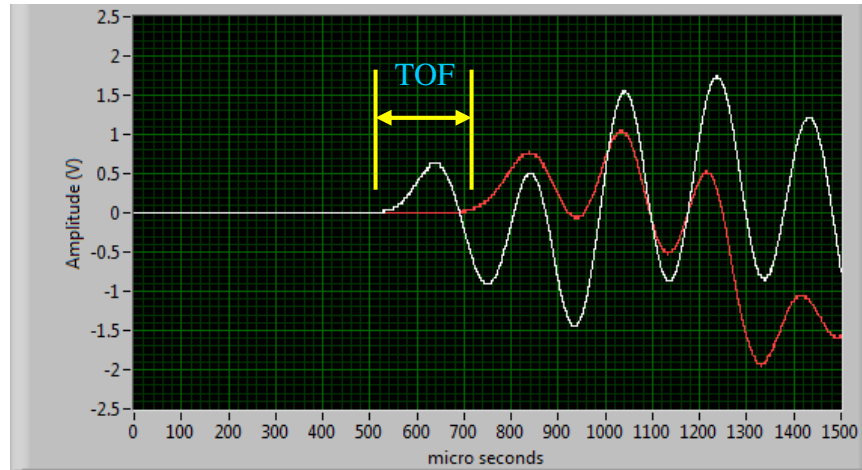
Figure 5.4. An example waveform showing the 1ˢᵗ (grey) and 2ⁿᵈ (red) receiver probe signals over a 1.0 m transit length.

The TOF for each grid location was calculated as follows:

.

- The first 800 measurements were used to find the level of background noise.
- The arrival time of the pulse was determined as the point where the signal exceeded 0.02V of the background noise.
- The TOF is the difference in the arrival time between the first and second receiver probe.
- Eight measurements per probe location were obtained and the median value was taken as the TOF value as it was the most stable.
- If erroneous measurements were obtained using this method, waveforms were re-examined and the TOF was determined manually.

5.2.2 Stiffness and Density Distribution

The billets used in the TOF mapping were cut into strips targeting approximate dimensions of 20 mm x 20 mm x 1000 mm in the radial (R), tangential (T) and longitudinal (L) directions, respectively. In reality, to try and gain as great a resolution as possible, dimensions down to 20 mm x 10 mm (R x T) were accepted. As each strip was cut, it was given a unique label so that it could be rearranged back into the exact position it came from within the log. A picture of

some of the resulting strips reassembled to their correct positions within the billet is shown in Figure 5.5.

Figure 5.5. Strips reassembled to their correct positions within the test billet.

The strips were conditioned to 12% moisture content before weighing and measuring its resonant acoustic velocity with a computer and microphone to obtain the dynamic stiffness as per equation 2.1. Dimensions were measured with digital callipers at 4 locations along the width and depth of each piece. A xylophone hammer was used to initiate the stress wave and upwards of 20 'hits' for each strip were recorded to a wav file with Audacity recording software (http://audacity.sourceforge.net) then analysed with LabVIEW. A Fast Fourier Transform (FFT) was carried out on the whole wav file to determine the main frequency components. An example sound recording and frequency spectrum is shown in Figure 5.6. The frequency with the greatest amplitude was recorded and the resonant velocity calculated using equation 2.2 (page 2-10).
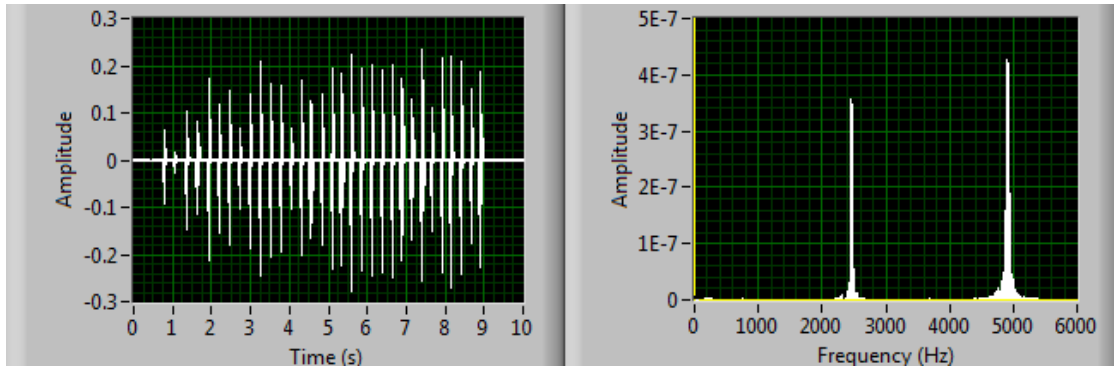
Figure 5.6. Example of resonant sound recording and its resulting frequency spectrum of a 1.0 m strip.

Each strip was then cut in half with the top and bottom pieces labelled such that the bottom piece was the section closest to the start probe and the top piece was the section that held the second receiver probe. Each half-length strip was then re-measured with the above procedure to determine resonant velocity and dynamic MOE.

The centre of each strip was given co-ordinates to correspond to its position within the log so that the density (at 12% moisture content) and dynamic MOE could be interpolated for the entire cross-section. Similar to the TOF mapping, the origin was located at the top of the log along the same azimuth as the starter probe. The distance to the centre of each strip was then calculated (accounting for the width of the saw) relative to the origin.

5.2.3 Data Analysis

LabVIEW was used to process signals from the PicoScope (Pico Technology Ltd) into TOF values and to determine the frequency components of each strip. Data were then analysed using R open-source statistical package (R Development Core Team 2010).

Interpolations were performed in R to obtain a smooth distribution of TOF, density and dynamic MOE over the cross section of each billet. Interpolated values were obtained using the 'interp' function within the Akima library (Akima *et al*. 2009).

5.3 Results

5.3.1 Wave propagation in each billet

Contour graphs of the TOF arrival times over the 0.5 m and 1.0 m transit lengths for each billet are shown in Figure 5.7.
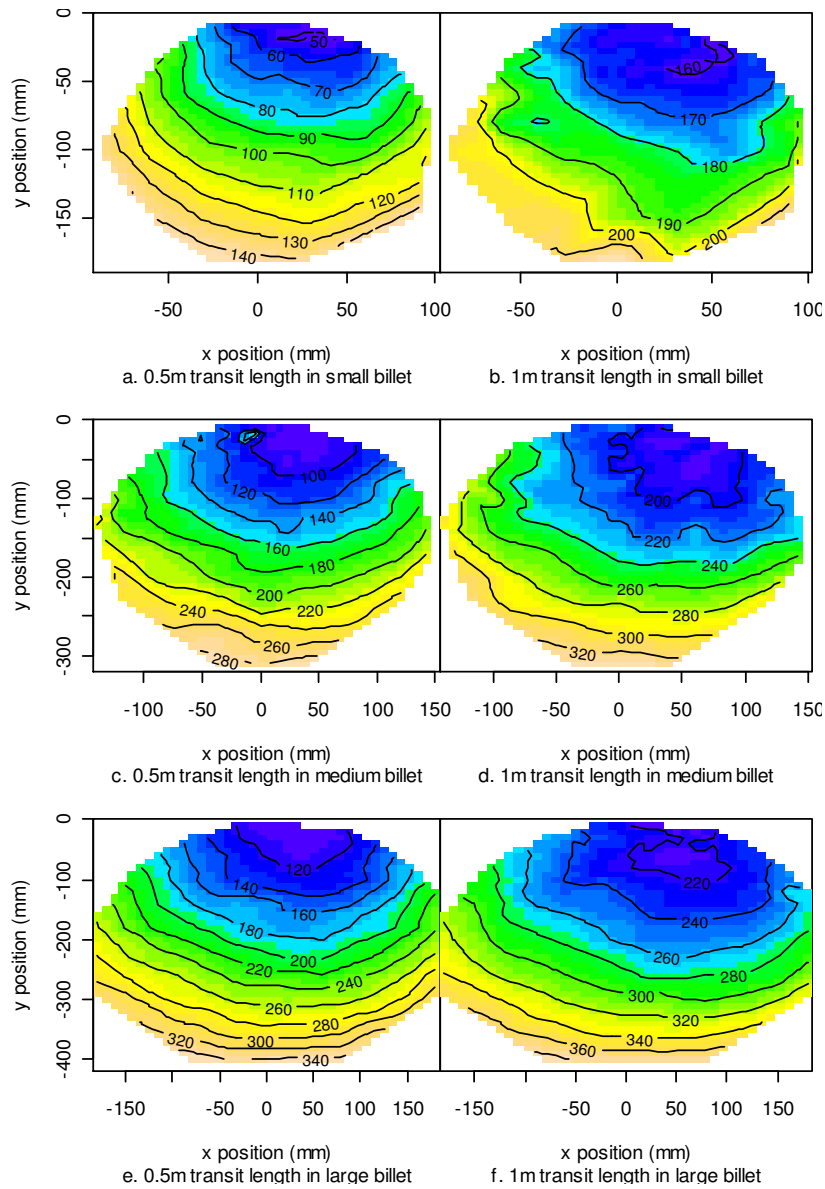
Figure 5.7.Contour graphs of the TOF arrival time for the 0.5 m and 1.0 m transit lengths. a and b, small billet. c. and d, medium billet. e. and f, large billet. The stress wave was initiated at the same azimuth as co-ordinate (0,0). Units of the contours are in microseconds.

The areas on the top of each graph near the origin that are contained within a single contour line show the extent of the radial and tangential wave propagation. In all instances with a 1.0 m transit length from the point of stress wave initiation, the wave has spread further than 30 mm.

There is a general pattern of increasing area of the billet being covered by a single contour line as the transit length is increased from 0.5 m to 1.0 m. There is also a consistent reduction in the gradient of TOF arrival times from the origin to the opposite side of the cross section when the transit length is increased. The fastest arrival times for each billet were biased to the right.

The stress wave speed for the 0.5 m and 1.0 m transit lengths of each log was calculated by dividing the respective lengths by the mean TOF of a 40 mm x 40 mm area with its top centred at the origin, $i.e.$, the approximate location of a TOF receiver probe in a standing tree measurement. The maximum velocities in the cross section did not occur in this 40 x 40 mm area. The estimated standing tree velocity, ST_{VEL}, and maximum velocity, Max_{VEL}, for each transit length and billet is shown in Table 5.2.

Table 5.2. The transit times to correspond to a standing tree tool velocity measurement, ST_{VEL}, and the maximum velocities, Max_{VEL}, for each billet and transit length.

Billet	Transit length (m)	ST_{VEL} (km s^{-1})	Max_{VEL} (km s^{-1})
Small	0.5	4.82	6.38
	1.0	4.10	4.30
Medium	0.5	2.89	3.72
	1.0	3.46	3.84
Large	0.5	2.70	2.96
	1.0	3.08	3.36

For the 0.5 m transit length, the difference between the standing tree and maximum velocities were 24.4%, 22.3% and 8.8% for the small, medium and

large billets, respectively. For the 1.0 m transit length, the difference between the standing tree and maximum velocities were 4.6%, 9.9% and 8.3% for the small, medium and large billets, respectively.

The minimum TOF for each y-position was obtained, normalised relative to its overall minimum and plotted. Figure 5.8 shows the relative TOF arrival times of the 0.5 m and 1.0 m transit lengths for each billet. The dotted line is the 0.5 m transit length and the solid line is the 1.0 m transit length.
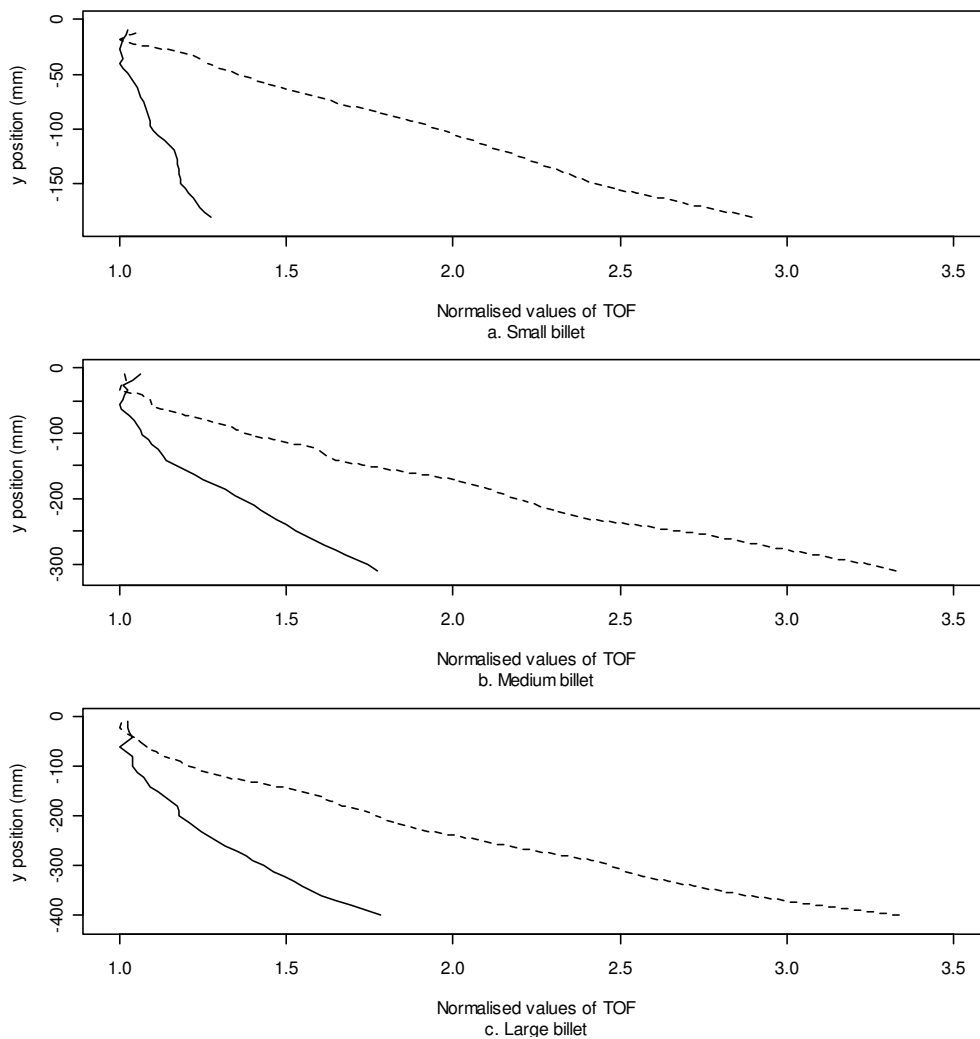
Figure 5.8. Minimum normalised TOF arrival times relative to the minimum for the 1.0 m (solid line) and 0.5 m transit lengths (dotted line). a) Small billet. b) Medium billet. c) Large billet.

For the small billet; the TOF for the 0.5 m transit length decreases for the first 20 mm near the origin then increases at a relatively constant gradient to the far side of the cross section. The maximum TOF time is 2.89 times larger than the minimum. For the 1.0 m transit length, the TOF pattern over the first 50 mm is erratic, with a sharply increasing and then decreasing gradient before briefly flattening. The TOF gradient then increases to the opposite side of the cross section. The maximum TOF time is 1.23 times larger than the minimum.

For the medium billet; the TOF for the 0.5 m transit length, has an almost constant gradient in TOF from the origin to the far side of the cross section apart from an initially decreasing TOF region 20 – 30 mm near the origin. The maximum TOF time is 3.32 times larger than the minimum. For the 1.0 m transit length, the TOF initially shows a decreasing gradient moving away from the origin to a flat area approximately 40 – 50 mm in length, before increasing again. The maximum TOF time is 1.77 times larger than the minimum.

For the large billet; the TOF profile for the 0.5 m transit length has an almost constant gradient in TOF from the origin to the far side of the cross section apart from a flat region 20 – 30 mm near the origin. The maximum TOF time is 3.33 times larger than the minimum. For the 1.0 m transit length, the TOF is initially relatively flat for approximately 30 – 40 mm before decreasing slightly, rising and flattening yet again before constantly increasing to the far side of the cross section. The maximum TOF time is 1.78 times larger than the minimum.

5.3.2 Density and dynamic MOE distribution in billets

The small, medium and large billets were converted into 35, 119 and 186 slices respectively, approximately 1.0 m long, to measure the distribution of density and MOE. The slices were then cut in half (length divided by 2) and re-measured to examine any longitudinal variation in these parameters. The density distribution within the top and bottom halves of each billet is shown in Figure 5.9.
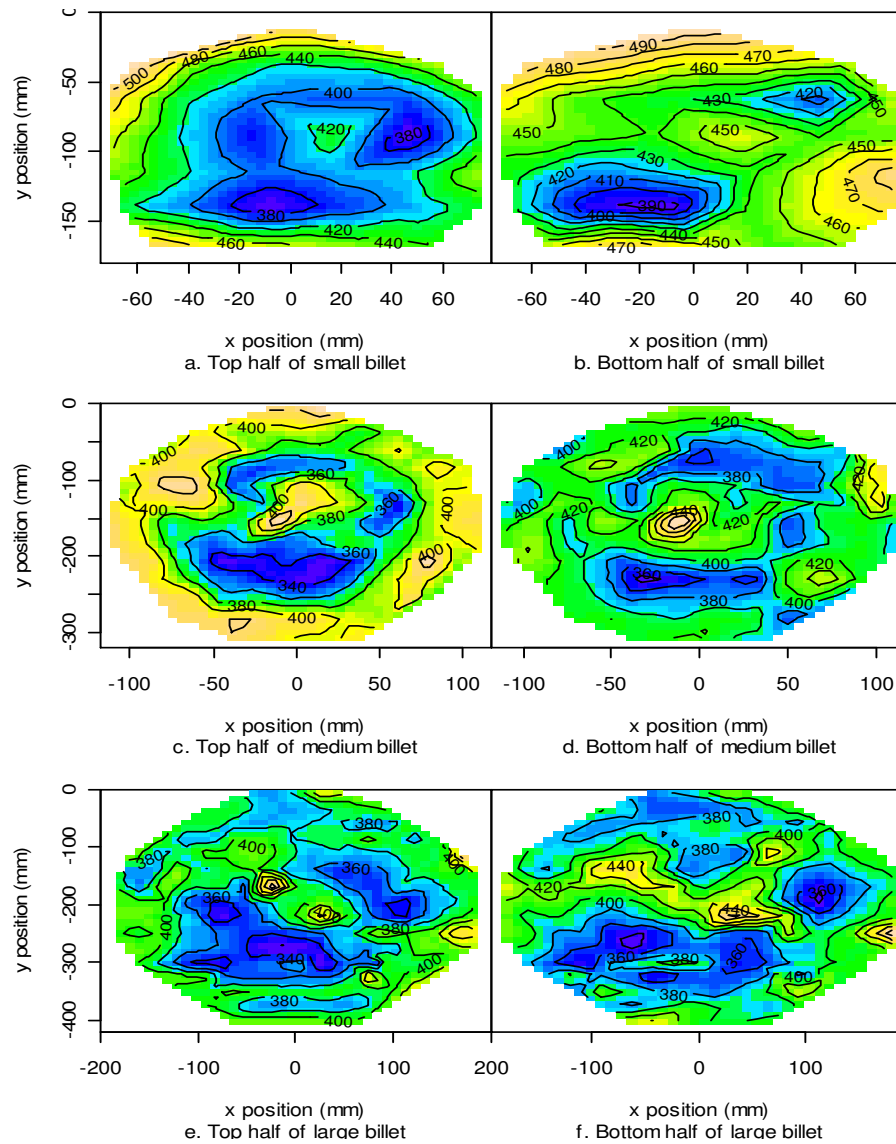
Figure 5.9. Density distributions (at 12% MC) within the top and bottoms half of each test billet. a and b, small billet. c and d, medium billet. e and f, large billet. Units of the contours are in kg m^{-3}.

All billets follow the general pattern of density variation expected for mature Sitka spruce; high density near the pith then decreasing in density, followed by a steady increase. However, the density pattern is in no way regular or symmetrical. Table 5.3 shows the mean and range of density for the top, bottom and whole sections of each billet. Density is at 12% moisture content.

Table 5.3 The mean and range of densities (at 12% MC) for the top, bottom and whole sections of each size billet. The value in parentheses is the standard deviation.

Billet Size	Region of billet	Min. density (kg m^{-3})	Mean density (kg m^{-3})	Max. density (kg m^{-3})
Small	Top half	360	430 (39)	499
	Bottom half	383	447 (25)	524
	Whole length	372	443 (31)	509
Medium	Top half	327	386 (27)	439
	Bottom half	323	406 (29)	534
	Whole length	337	398 (27)	484
Large	Top half	313	384 (29)	503
	Bottom half	331	394 (29)	519
	Whole length	331	391 (26)	484

The top half of each billet was always slightly less dense than the bottom half. Examining the mean densities of the whole length of each billet using t-tests, there was a significant difference between the small billet and the medium and large billets ($p<0.01$). There was also a significant difference between the mean densities of the medium and large billets ($p<0.05$). The small billet was 10.2% and 11.7% denser than the medium and large billets, respectively. The medium billet was 1.8% denser than the large billet.

The distribution of dynamic MOE, E_d, within each billet is shown in Figure 5.10.
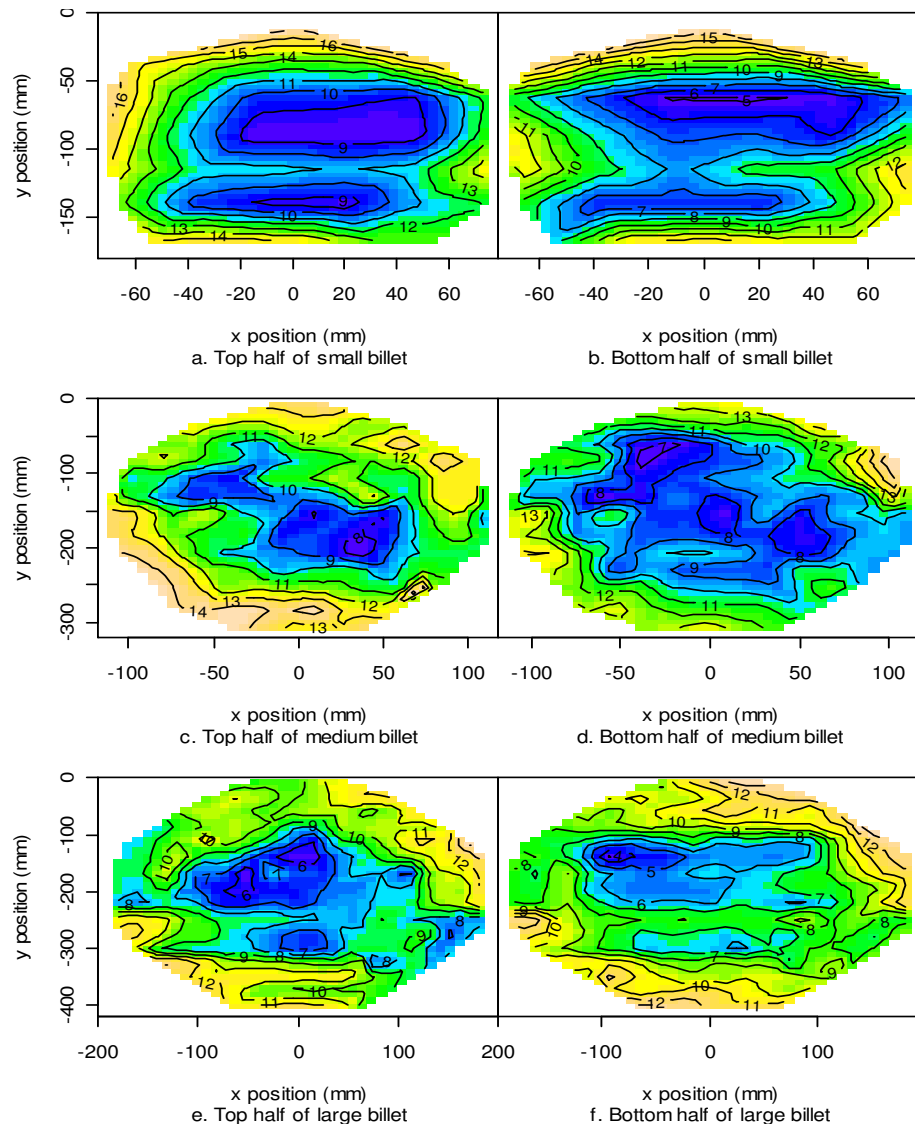
Figure 5.10. Distribution of dynamic MOE (at 12% MC) within the top and bottoms half of each test billet. a and b, small billet. c and d, medium billet. e and f, large billet. Units of the contours are in kN mm^{-2}.

There is a general pattern of increasing stiffness with distance from the centre of the log for all billets but it is not regular or symmetrical. Table 5.4 shows the mean and range of dynamic MOE for the top, bottom and whole sections of each billet.

Table 5.4. The mean and range of dynamic MOE (at 12% MC), E_d, for the top, bottom and whole sections of each size billet. The value in parentheses is the standard deviation.

Billet Size	Region of billet	Min. E_d (kN mm^{-2})	Mean E_d (kN mm^{-2})	Max. E_d (kN mm^{-2})
Small	Top half	8.18	12.34 (2.69)	17.66
	Bottom half	4.74	9.77 (3.18)	16.16
	Whole length	6.7	11.14 (2.79)	16.58
Medium	Top half	7.5	11.3 (1.82)	15.33
	Bottom half	6.56	10.42 (2.16)	17.14
	Whole length	7.51	10.7 (1.82)	14.51
Large	Top half	5.12	9.37 (1.91)	14.62
	Bottom half	2.84	8.65 (2.34)	13.83
	Whole length	5.05	8.84 (1.94)	13.75

The relationship between the dynamic MOE of the top and bottom halves, as well as the relationship between the average of the top and bottom halves versus the whole length is shown in Figure 5.11, Figure 5.12 and Figure 5.13.

5.3.2.1 Small Billet
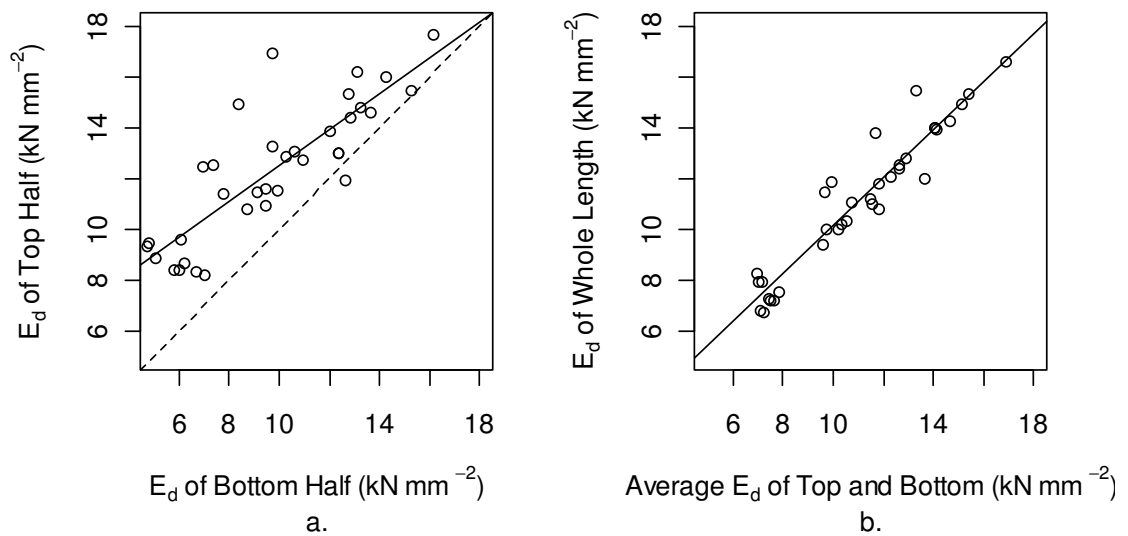
Figure 5.11. a. Relationship between E_d of top and bottom halves of the small billet. b. Relationship between the average E_d of top and bottom halves with E_d of whole length of the small billet

The top half of the billet is 1.11 times more stiff than the whole 1.0 m section (p=0.07). The R^2 between the top and bottom halves is 0.70. The relationship between the average dynamic MOE of the top and bottom halves and the dynamic MOE of the 1.0 m length almost 1:1 with an intercept value of 0.66 (p=0.26 and std err. = 0.59) and an R^2 of 0.91.

5.3.2.2 Medium Billet
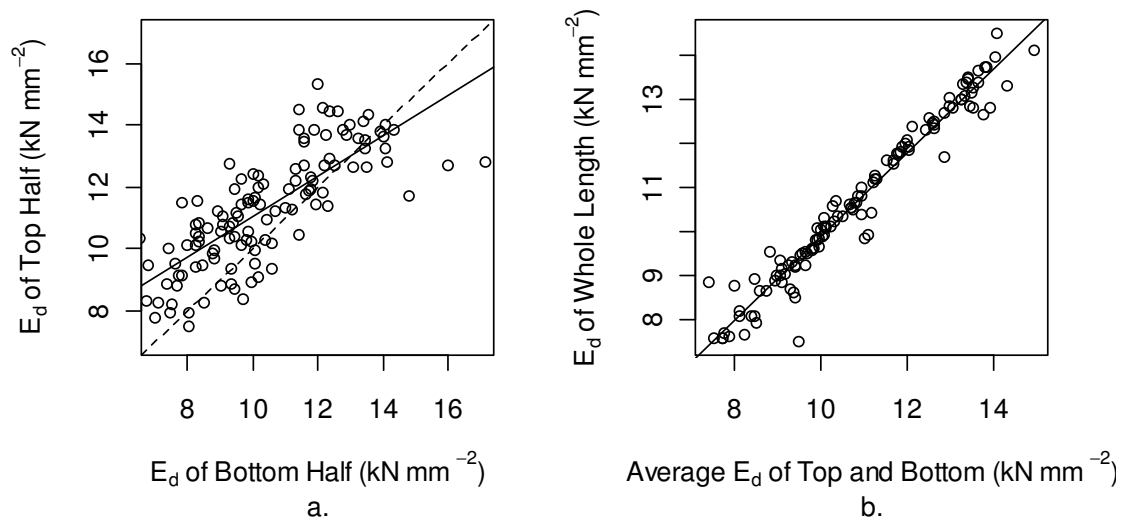
Figure 5.12. a. Relationship between E_d of top and bottom halves of the medium billet. b. Relationship between the average E_d of top and bottom halves with E_d of whole length of the medium billet.

The top half of the billet is 1.06 times more stiff than the whole 1.0 m section ($p<0.01$). The R^2 between the top and bottom halves is 0.59. The relationship between the average dynamic MOE of the top and bottom halves and the dynamic MOE of the 1.0 m length almost 1:1 with an intercept value of 0.41 ($p<0.05$) and an R^2 of 0.95.

5.3.2.3 Large Billet
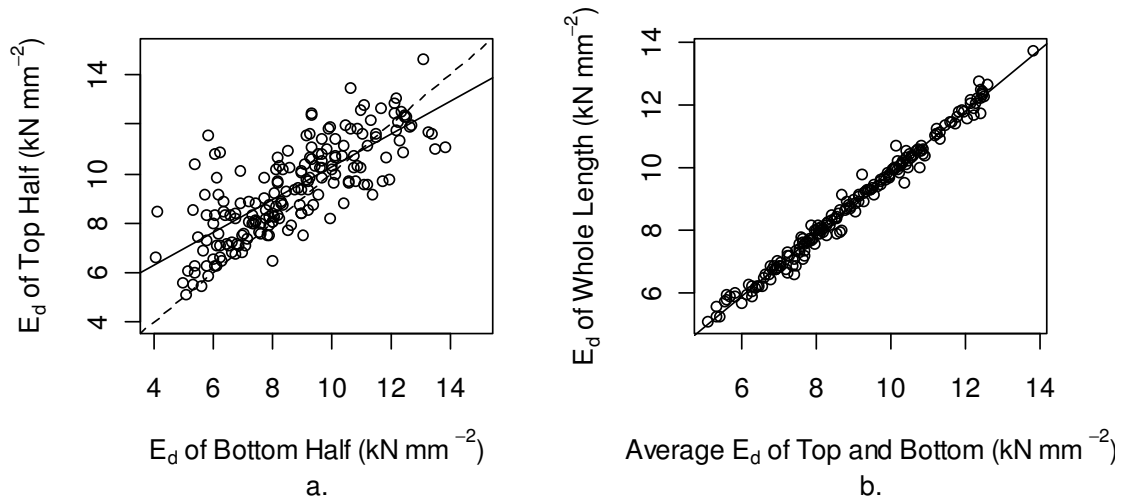
Figure 5.13. a. Relationship between E_d of top and bottom halves of the large billet. b. Relationship between the average E_d of top and bottom halves with E_d of whole length of the large billet.

The top half of the billet is 1.07 times more stiff than the whole 1.0 m section ($p<0.01$). The R^2 between the top and bottom halves is 0.6. The relationship between the average dynamic MOE of the top and bottom halves and the dynamic MOE of the 1.0 m length almost 1:1 with an intercept value of -0.07 ($p=0.35$ and std err. = 0.07) and an R^2 of 0.99.

5.3.3 Other required parameters

In order to discuss the effects of the wave propagation behaviour exhibited in this experiment, it is necessary to define a number of parameters. Firstly, the dilatational wave speed: The values estimated here are the Max_{VEL} for the 0.5 m transit length from each billet. This measurement represents the fastest possible sound wave in the billet as the transit length is assumed to be short enough that there are minimal boundary interactions and therefore almost purely dilatational (Meyers 1994, Andrews 2003). For comparison purposes, the Max_{VEL} over the 1.0 m transit length is also included in this table.

Secondly, the apparent wave speed, is the difference in the maximum arrival times of the 0.5 m and 1.0 m transit lengths divided by 0.5 m. These maximum arrival times occur on the opposite side of the cross section to the origin. For example, Figure 5.14 shows the TOF contour graphs for the large billet for the 0.5 m and 1.0 m transit lengths. The maximum TOF measurements at the opposite side of the cross-section are approximately 339 µs and 372 µs for the 0.5 m and 1.0 m lengths respectively, resulting in an apparent wave speed of 15.02 km s^{-1}.
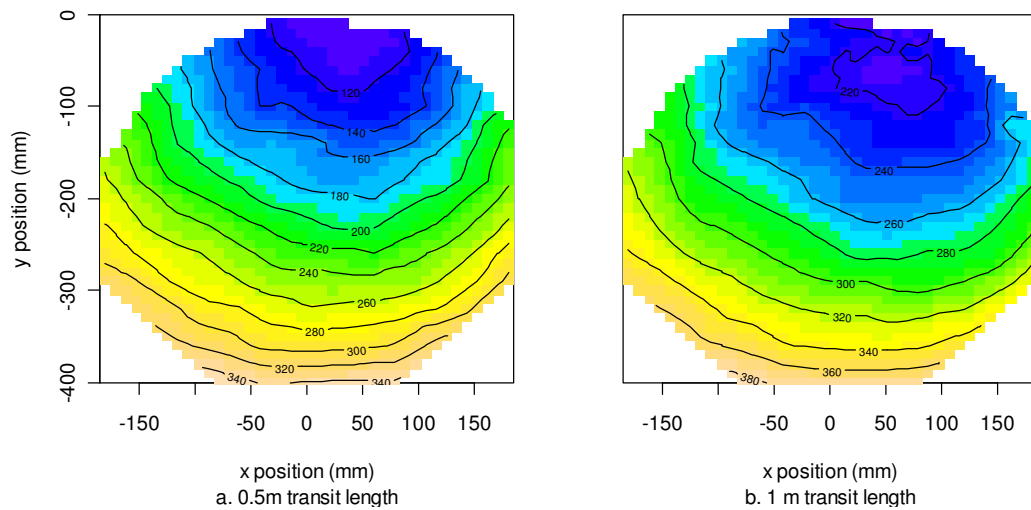
Figure 5.14. TOF contour graphs for the large billet for the a) 0.5 m transit length and b) 1.0 m transit length. The units for the contour lines are in microseconds.

The apparent wave speed is not a physical speed. It is only calculated to illustrate the properties of wave propagation within a standing tree during an acoustic measurement.

Thirdly, the extent of plane wave formation at 0.5 m and 1.0 m transit lengths, or quasi-plane wave size, is calculated as the distance from the origin before the minimum TOF arrival time maintains a consistently increasing gradient to the opposite side of the cross section. Table 5.5 shows the values of these parameters for each of the billets.

Table 5.5. Dilatational speed, apparent wave speed and quasi-plane wave size for each of the test billets.

Billet Size	Dilatational Speed (km s^{-1})	Fastest Wave Speed - 1 m Transit Length (km s^{-1})	Apparent Wave Speed (km s^{-1})	Quasi-plane wave size - 0.5 m transit length (mm)	Quasi-plane wave size – 1 m transit length (mm)
Small	6.38	4.29	8.07	18.7	40
Medium	3.72	3.84	10.37	20.0	64
Large	2.96	3.36	15.02	33.0	90

For the small billet, the dilatational wave speed was 1.49 times faster than the fastest wave speed over 1.0 m. For the medium and large billets, the dilatational wave speed was 0.97 and 0.88 times faster than the fastest speed over 1.0 m.

5.4 Discussion

Examining Table 5.5, two things are immediately obvious:
1. The apparent speed is greater than the dilatational wave speed (the maximum speed possible) for all billets.
2. For the medium and large logs, the wave speed over 1.0 m is faster than the dilatational wave speed.

These results can be explained by the three-dimensional spreading of the wave front and the interaction of the wave front with the boundary walls of the billet as opposed to the assumed one-dimensional path.

5.4.1 Wave Shape

The three-dimensional propagation of waves in a solid is most easily visualised by the Huygens' Principle (Christiaan Huygens 1629-1681). The Huygens' Principle states that "*all points on a wave front serve as point sources of spherical secondary wavelets. After time δt, the new position of the wavefront will be a surface tangent to the secondary wavelets*". This principle is illustrated in Figure 5.15.
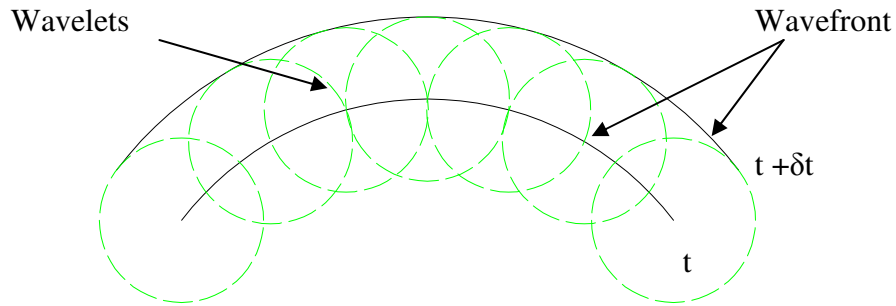
Figure 5.15. Illustration of the Huygens' Principle.

The illustration in Figure 5.15 is only meant as a visual aid and not as an accurate model to describe the wave propagation in a standing tree measurement; the anisotropy and inhomogeneity of material properties due to knots, compression wood grain angle, variation in moisture content, *etc.* will never allow for spherical wave propagation. However, Huygens' Principle does illustrate how a point-source impulse applied at the top edge of a cross section can spread to form a plane wavefront in a cylinder (neglecting boundary effects from the cylinder walls), *e.g.* Figure 5.16.
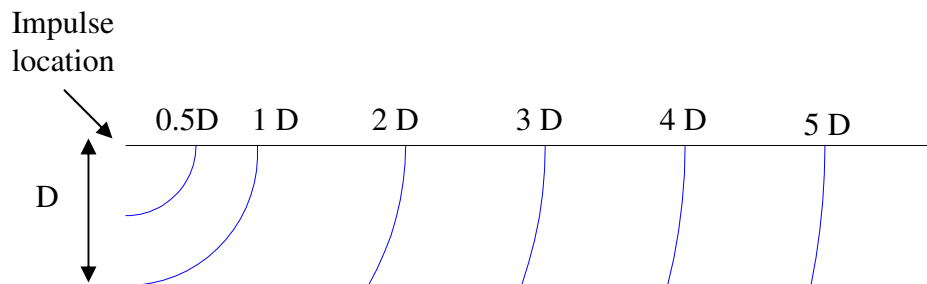
Figure 5.16. Spherical propagation of wavefront in a cylinder.

Davies (in von Karman, 1958) showed that in steel, when a bullet was fired against the lower end of the cross section, the stress from the impulse was evenly distributed over the cross section 4 – 5 diameters from the impact point. Similarly, Baker and Dove (1962) found that for a centrally located impact, stress was uniformly distributed after 2 diameters from the impact point. For wood,

Zhang *et al*. (2011) performed a similar experiment to that presented in this chapter, except over a larger range of transit lengths and found that the stress should be evenly distributed after approximately 10 diameters from the impact point. Closer inspection of the stress wave contours in Zhang *et al*. (2011) near the impact point show a similar distribution to the slowness plots of ultrasound propagation at various angles to the fibre direction in Bucur and Berndt (2001), where slowness is the inverse of speed in s m^{-1}. The results from Bucur and Berndt (2001) show an elliptical variation in slowness between the longitudinal and tangential planes, with the tangential plane for Douglas fir approximately 3 times slower than the longitudinal. The stress wave contours in Zhang *et al*. (2011) are approximately 2.5 times greater in the longitudinal than the radial direction after 100 μs for green (*i.e.* freshly felled) red pine. The difference in the transmission time between longitudinal and the tangential or radial directions, is due to the anisotropic nature of wood. Modelling the wave shape in a log based on these elliptical (rather than spherical) parameters estimated from Bucur and Berndt (2001) and Zhang *et al*. (2011), gives a reasonable approximation to the experimental findings in Zhang *et al*. (2011), shown in Figure 5.17. Figure 5.17 a uses the value obtained from Bucur and Berndt (2001) and Figure 5.17 b uses the value obtained from Zhang *et al*. (2011).
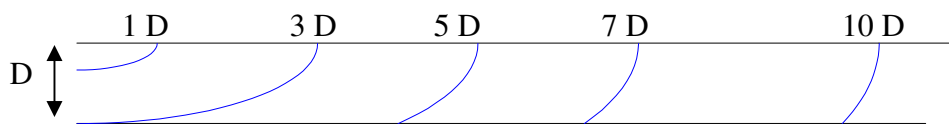
Figure 5.17a.
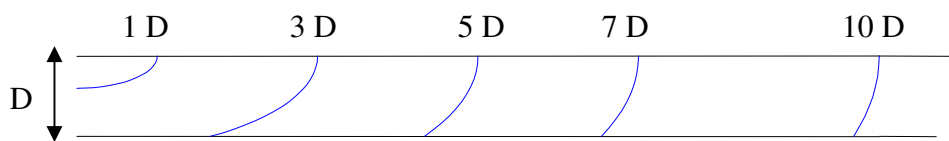
Figure 5.17b.

Figure 5.17. Model of wave shape using an elliptical rather than a spherical propagation shape. a. Value obtained from Bucur and Berndt (2001): longitudinal velocity 3 times faster than tangential. b. Value obtained from Zhang et al. (2011): longitudinal velocity 2.5 times greater than radial.

There are two aspects of the stress wave propagation in this experiment that are worth considering: Firstly, the outward propagation of the wave toward the opposite side of the cross section. The difference in size of the quasi-plane wave between the billets is shown in Table 5.5. This 'flattened' area of the wave extends more than twice as far into the large billet as the small, with the medium billet falling in between the two. This could be due to differences in stiffness between the billets, with the maximum dynamic MOE for each billet of 16.58 kN mm^{-2}, 14.51 kN mm^{-2} and 13.75 kN mm^{-2} for the small, medium and large billets, respectively. Putting this in terms of wave propagation by elliptical wavelets, differences in MOE could result in variations in the eccentricity of the ellipse, with stiffer material being more elongated in shape and less stiff material more circular. This effect also raises some interesting questions about how quickly the wave would spread outward when it reaches the lower stiffness core; minimum values of dynamic MOE ranged through 6.7 kN mm^{-2}, 7.51 kN mm^{-2} and 5.05 kN mm^{-2} for the small, medium and large billets respectively.

Importantly, the extent of the quasi-plane wave area changes with transit length. Table 5.5 shows size of the quasi-plane wave for both transit lengths on each billet, with the 1.0 m transit lengths 2.2 – 3 times larger than the 0.5 m transit length. If a quasi-plane wave behaves in a similar manner to a plane wave in that its speed is controlled by the entire area it covers, then the properties of a tree measured during a standing tree TOF test are not simply the area 20 – 30 mm wide, directly between the probes as is generally assumed. In this case the area controlling the speed of the wave would extend approximately 40 mm, 64 mm and 90 mm in the radial and tangential directions for the small, medium and large logs respectively.

The variation in size of the quasi-plane wave combined with the radial variation in density, examined in Chapter 4, makes this a potentially very complex problem to model. An examination of these combined properties will be undertaken in the general discussion (section 7.4).

The second property of the wave propagation of interest is that the fastest arrival times of the stress wave are distinctly concentrated to the right in all billets.

Andrews (2003) found a similar result; explaining that the stress wave was highly sensitive to the grain direction. Gerhards (1980) also showed that a stress wave will advance in the direction of the grain rather than normal to the long axis of the test specimen. The bias shown in this experiment is consistent with the left handed spiral grain growth pattern in Sitka spruce (Moore 2011). The implication of this is that the receiver probe in a standing tree TOF test is never aligned with the fastest arrival time as it is placed along the same azimuth as the starter probe. Therefore the accuracy of the instruments will be affected. If the grain angle were constant, this could be accounted for empirically. In this experiment the differences between minimum TOF and values that would be obtained in a standing tree TOF test were 4.6% 9.9% and 8.3% for the small, medium and large billets, respectively. However, even if the difference was consistent, the accurate placement of probes is essential for accuracy as misplacement will either overestimate or underestimate the TOF. This property of stress waves does raise the potential capability of being able to measure spiral grain on standing trees by finding the minimum TOF time and measuring the angle relative to the impact location.

5.4.2 Boundary Effects

The mathematical relations to give the speed of a stress wave in rods and in unbounded media are shown in Section 2.3. These relations correspond to plane waves, *i.e.* when the stress of the passing wave is applied evenly over the entire cross section, and to dilatational waves, *i.e.* when the stress has no interaction with the boundaries of the medium through which it travels. The ratio of dilatational to plane waves speed is given by equation 2.3 and is controlled by the Poisson's ratio. Values of Poisson's ratio in the longitudinal-radial (LR) direction given for Sitka spruce in the literature are given by Wang *et al*. (2007) with 0.33 and Bucur (2006, Table 4.1B) with 0.37. These values correspond to dilatational speeds being 1.22 and 1.33 times faster than the plane wave speed. For the experiment presented in this chapter, the greatest change in speed as the transit length increased from 0.5 m to 1.0 m occurred in the small billet. The fastest speed over 0.5 m was 1.49 times the fastest speed over 1.0 m. If this is a consequence of the transition from a dilatational to a plane wave, then it would

correspond to a Poisson's ratio in the LR direction of 0.404. This value is possible, though at the higher end of values presented for Sitka spruce. It should also be noted that the 3 dimensional expansion of the wave will result in stresses in the longitudinal-transverse (LT) direction as well as the LR direction. Bucur (2006) showed that the Poisson's ratio for Sitka spruce in the LT direction was 0.42.

With the leading edge of the wave 1.23 times further from the impact point than the trailing edge (Section 5.3.1), it is unlikely that the wave could be considered plane, yet it is unclear at what point wave interactions with boundaries start to significantly affect wave speed.

It is likely that there is some interaction between the stress wave and the walls of the billet with the net effect of slowing the wave down. This can be seen in the plots of the minimum TOF with distance from the origin in Figure 5.8a, b and c, where the minimum arrival time always occurs some distance away from the boundary walls for the 1.0 m transit length. Interestingly, this also appears to be true for the 0.5 m transit length in both the small and medium logs. It is unknown exactly how much this partial interaction with boundary walls of the billet will slow the wave propagation. Therefore, whilst the speed of a plane wave or a dilatational wave can be described by equations 2.1 and 2.3 respectively, it remains unclear how much the interaction of the stress wave with the boundaries will affect wave speed in the transition from a dilatational to a plane wave. This could be particularly important in analysing the wave speed in standing tree applications, where the impulse is applied very close to the boundary.

Zhang *et al*. (2011) showed that changing the distance between the transducers, equivalent to changing the test span in a standing tree TOF measurement, had no significant effect on the speed. Interestingly, this was also true for the small log tested in their experiment which had achieved a plane wave after 1.7 m (Figure *5.18*). If the transition from a dilatational to a plane wave resulted in an abrupt change in wave speed, then this would have been reflected in the results.

Instead, a linear relationship existed between transit length and TOF (Figure 5.19) with the transit length ranging from 0.6 m to 1.7 m.
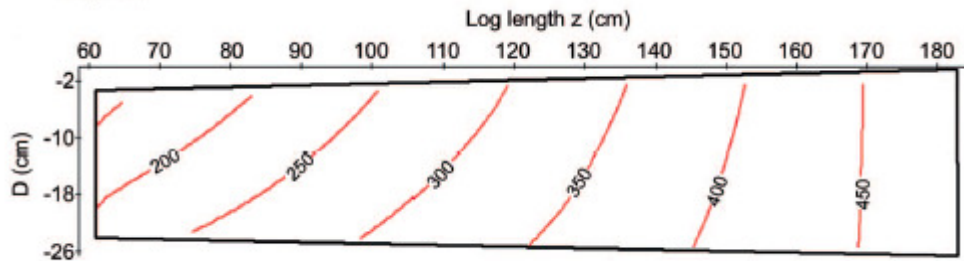
Figure 5.18. From Zhang et al. (2011). Small log stress wave contour maps in longitudinal-radial plane of red pine logs. Impacting point: z=0. Contour unit: microseconds (μs).

Andrews (2003) found in testing the change in the TOF over a 450 mm diameter, 6.0 m long radiata pine log that the velocity calculated using the resonant method is the slowest. The speed of the pulse in the early part of the log (exact length undefined), near the starter probe, was 1.29 times the resonance speed. Over the remaining length of the log, a linear relationship existed between transit length and TOF in the same manner reported in Zhang *et al.* (2011). Therefore, no change in velocity, either abrupt or gradual, due to a transition from a dilatational to a plane wave was recorded by Andrews (2003) either, even though the final transit length was 13.33 times the diameter, *i.e.* beyond the expected point of plane wave formation. Andrews (2003) also noted that the line of best fit for arrival times along the log had a negative intercept at the origin, implying that faster travel times occur closest to the excitation source. A negative intercept can also be inferred from the results of Zhang *et al.* (2011) for all log sizes, shown in Figure 5.19.
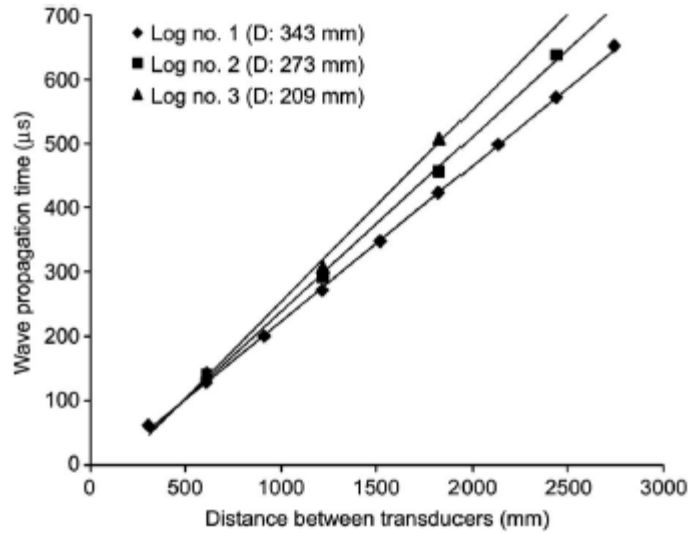
Figure 5.19. From Zhang et al. (2011). Relationship between wave propagation time and distance between two transducers.

Given the linear relationship between transit length and wave speed reported in Andrews (2003) and Zhang *et al.* (2011) up to and beyond the expected point of plane wave formation (*i.e.* at a length 10 times the diameter from the stress wave initiation point), it is possible to surmise that the dilatational speed only occurs over very short transit lengths. This conclusion was already reported in Andrews (2003) yet the difference now is that with the experiments reported in Zhang *et al.* (2011) and this chapter, it is possible to speculate that the effects of the boundaries on wave speed are imposed well before plane wave formation. Therefore, the speed along the length of the log and within a typical TOF test span is neither the dilatational speed nor the resonant speed.

The practical effect of this is that wave propagation behaviour could have a significant impact on standing tree TOF measurements where the transit length is in the region where significant change in the interaction between boundaries and the stress wave occurs. For example, the fastest wave speed of the small billet dropped by 33% as the transit length increased from 0.5 m to 1.0 m. Therefore, if it is assumed that the wave propagation time will have a linear relationship with the transit length from 1.0 m onward (as per Andrews (2003) and Zhang *et al.* (2011)) the measured wave speed will change with just the transit length and not due to differences in material properties. This is illustrated in Table 5.6.

Table 5.6. Illustration of how measured speed can change with transit length due
to the effect of boundary interactions only and not material properties.

Transit Length (m)	Measured Speed (km s^{-1})
1.0	4.29
1.1	4.16
1.2	4.06
1.3	3.99
1.4	3.93
1.5	3.89
1.6	3.85
1.7	3.82
1.8	3.79
1.9	3.77
2.0	3.74

The results from Table 5.6 show that if TOF were measured over a 1.0 m transit
length the measured velocity would be 12.8% higher than if the TOF were
measured over a 2.0 m transit length. This change in velocity would be due to a
change in wave propagation properties due to interaction with boundaries only
and have nothing to do with any change in material properties. Further
investigation is required to model the wave behaviour to determine optimal
transit lengths for a given tree diameter.

5.5 Summary and Conclusions

The results presented here suggest that the properties controlling the speed of a
stress wave in a standing tree are complex interactions between the radial and
tangential spread of the quasi-plane wave, the radial variation in density and the
unknown effect of boundary interactions. The understanding of these
interactions is the key to obtaining an accurate estimate of stiffness with standing
tree TOF instruments.

Understanding the distribution of stiffness in the test billets helped identify some of the causes of changing velocity along the billets length and perhaps, the rate of the radial expansion of the quasi-plane wave.

The commercialisation and use of standing tree, stress wave timers to estimate stiffness seems to have proceeded without a fundamental understanding of how they work, *i.e*., understanding exactly which material properties are actually being measured. Several attempts have been made, including the experiment presented in this chapter, to understand wave propagation behaviour (*e.g*., Andrews 2003, Chauhan *et al*. 2005, Grabianowski and Walker 2006, Wang *et al*. 2007, Mora *et al*. 2009, Zhang *et al*. 2011). However, a full understanding of the potential causes of error is still required

6 Cutting Pattern Experiment

6.1 Introduction

This chapter examines the effect of trying to improve the timber properties of structural battens produced at sawmills by altering the cutting patterns from those that would typically be used to produce structural dimensions. This experiment was undertaken in an attempt to find solutions to the current problem facing processors; increasing the proportion of higher quality construction timber from a resource that may be becoming less suitable for the task.

A number of factors were considered in the experiment that had previously only been considered either separately, theoretically or not at all. These include:

- The limitations imposed by a sawmill production line on the number of battens than can be produced and the location in the log from which they can be derived.
- Different log segregation techniques
- The pith-to-bark variation in stiffness and estimating the extent of the undesirable low stiffness region at the centre of a log.
- The effect of alternative cutting patterns on knot severity and distortion
- The effect of alternative cutting patterns on sawmill volume and value yields
- Evaluate the consequences of alternative cutting patterns on processing that may affect their implementation.

The consideration of these factors allows an accurate sawmill simulation to assess whether alternative cutting patterns can be practically and profitably implemented, should they be required.

6.1.1 Background

There are three factors, reviewed in section 2.1, which have prompted this investigation into cutting patterns:

1. Wood production is expected to increase to 10 million m^3 by 2020 (SFIC 2004)
2. The perception that the quality, of the Sitka spruce resource reaching harvestable age in the UK over the next 20 years is in decline (Macdonald and Hubert 2002). Quality of structural battens is defined here as the mechanical and physical properties, and the tree growth characteristics *e.g.* branching, that have the greatest effect on the use wood for structural applications.
3. The market for non-structural products, which account for approximately two-thirds of the market for British sawn timber, is saturated or likely to become saturated in the near future (McIntosh 1997, Cameron 2002).

This means processors will be required to increase the proportion of structural timber from a resource may be becoming less suitable for the task.

A reduction in the quality of the resource will correspond with a reduction in the pass-rate of structural battens at a sawmill's strength grading machine. Grading machines assign battens into strength classes based on a measured indicating property or properties such as density, knots, stress wave speed or reaction force in a non-destructive bending machine. These measured properties are related to the critical grade-determining parameter(s) such that on average, a package of timber should meet the required characteristics (EN14081:1-2005 CEN). For a particular species and grade combination, there is usually a limiting property that becomes the grade-determining parameter. In UK Sitka spruce, this is the stiffness, or MOE. The implication for sawmillers, is that a reduction in pass-rates at the grading machine will result in a loss of profitability due to incurred cost of kiln drying and planing material that will not make the required grade and the reduced sale price of reject battens. The reasons for this perceived reduction in quality arise from the proportion of juvenile wood in harvested trees

increasing due to genetic improvement for growth rate (*e.g.,* Cameron *et al.* 2005) and silvicultural practices such as shorter rotations (*e.g.*, Macdonald and Hubert 2002). The increase in the proportion of juvenile wood was reviewed in section 2.1 along with its detrimental effects on timber quality. Generally in British spruce, juvenile wood is of low stiffness and very likely to cause distortion. Therefore, to improve overall quality, processing techniques should focus on reducing the impact of the juvenile core.

6.1.2 Log segregation using acoustics

Using resonance based acoustic tools provides a means of measuring the volume weighted average of the material stiffness within a log (Chauhan *et al*. 2005). Studies using acoustics have shown that, by using either standard mill cutting patterns or cutting structural dimensions over the whole log cross-section, the yield of structural timber will improve if higher velocity logs are used. For UK Sitka spruce, a benchmarking study by Moore *et al.* (in press) showed that at a site level, the mean timber static MOE of structural battens from a site, $E_{0, mean}$, correlated well with the mean dynamic stiffness of logs (MOE_{dyn}) from that site, with an R^2 of 0.80 (Figure 6.1).
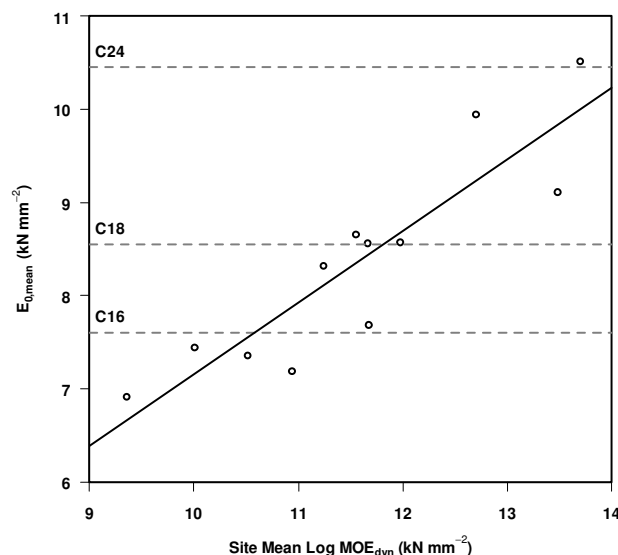
Figure 6.1. From Moore et al. (in press). Mean timber bending stiffness versus mean log dynamic stiffness for 12 sites around Scotland and northern England.

Note that the MOE_{dyn} in Figure 6.1 was calculated from equation 2.1 (page 2-9) assuming a constant density and is therefore log velocity^2 only.

Typical sawmill cutting patterns (in the UK and Europe) are designed to obtain maximum volume recovery (Kliger 2001) and make no adjustment for either the within-tree or between-tree variation in stiffness. A typical UK sawmill pattern is given in Figure 2.5 and Figure 2.6 in Chapter 2 (section 2.5) and shows that most battens of structural dimensions are cut from the centre of the log and can be completely or partially within the low stiffness juvenile core.

One approach to increasing the average stiffness of structural battens using conventional cutting patterns, could be to divert low stiffness logs to produce non-structural products. This would raise the average stiffness of the remaining logs and improve grading pass-rates. However, there is little overall benefit in rejecting logs to non-structural applications, as the market for this material is saturated or likely to become saturated in the near future (McIntosh 1997). In fact, since the overall target is to increase the proportion of structural timber produced, another strategy is required. It is possible that by utilising the predictable pith to bark variation in stiffness, structural battens of sufficient quality could be produced. Sitka spruce, like other plantation grown coniferous trees, has an average stiffness profile that runs in a predictable manner from the pith (lowest) to the bark (highest). Moore *et al*. (2009a, c, in press) has shown that between 36% and 50% of the variation in MOE of battens was due to within-log of within-tree variation for UK Sitka spruce. For radiata pine, Xu and Walker (2004) found that boards taken from near the bark were, on average, 50% stiffer than boards taken from the pith. This systematic and thus predictable stiffness variation within logs allows scope for more strategic log processing: rather than simply redirecting low stiffness logs to be processed purely into low value products, extract the higher stiffness sections by altering the cutting patterns currently used.

Therefore, whilst the mean values of the low stiffness logs shown in Figure 6.1 are below the minimum mean required for C16, high stiffness battens cut from

near the bark may well have been above the minimum required average stiffness for C16.

6.1.3 Segregation of logs accounting for density and growth rate

Using just acoustic velocity to segregate logs by stiffness has been shown to be successful by a number of researchers, *e.g*., Walker and Nakada, 1999; Tseheye *et al*. 2000, Dickson *et al*. 2004, Wang *et al*. 2000, 2001, 2002, 2004). However, the inclusion of density has been shown by Achim *et al.* (2009) and Jones and Emms (2010) to improve the prediction of average batten MOE. However, Chapter 4 of this thesis (section 4.3.3.1) showed that assuming a constant density resulted in an error of ±5% for 64% of discs sampled within and between trees. Therefore, the inclusion of this parameter should be included in a sawmill simulation to determine if it adds any overall benefit.

Even with the inclusion of density in the calculation of log stiffness, this value is a measure of the mean log stiffness across the entire cross section (Chauhan *et al*. 2005) (assuming the resonant technique is used). Therefore, the value gives no information about the proportion of very low stiffness material within the log. All that can be said for certain is that relative to another log of equivalent size, if one log has a lower value of dynamic MOE then its low stiffness zone will be larger. As such it would be useful to try and estimate the extent of this low stiffness area based on just the log velocity^2 or dynamic MOE information and several, simple assumptions. This is outlined later in section 6.2.1. Once this low stiffness area is estimated, then it is possible to adjust cutting patterns accordingly and avoid it.

Additionally, it would be useful to consider just how detrimental the juvenile core is to batten quality. Therefore, rather than basing cutting patterns on an estimated low stiffness area within a log, simply avoid the region that is most likely to produce poor quality battens based on knowledge about the growth rate of a log.

6.1.4 Distortion and knots

Whilst primarily investigating the effect of alternate cutting patterns on stiffness, consequent effects on other important batten properties should not be neglected. For example, it makes little sense to reduce the reject rate due to low stiffness only to increase it in another aspect such as distortion or knot severity.

Discussion with local sawmillers (SIRT conference 2011) has resulted in the conclusion that given the current quality of the resource (*i.e.* neglecting the possibility of any future decline in stiffness), distortion, particularly twist, is a greater cause of structural batten downgrade than low stiffness. Studies from around the world (*e.g.*, Cown *et al*. 1996 on radiata pine; Johansson *et al*. 2001 and Kliger 2001 on Norway spruce) also identify twist to be a major source of downgrade. Sawing pattern has a significant effect on the degree of twist and almost always develops on battens sawn from near the pith (Kliger 2001). Johansson *et al*. (2001) found that on Norway spruce, twist was most strongly correlated with ring curvature (*i.e.* inverse of the distance to the centre of the batten from the pith) ($R^2 = 0.52$) and spiral grain angle ($R^2 = 0.26$). Together, spiral grain and ring curvature explained about 70% of twist variation and the study recommended that a 75 mm x 75 mm region containing the pith should be avoided when producing structural material. Cown *et al*. (1996) attributes twist to the increased proportion of juvenile wood in fast grown plantations of radiata pine in New Zealand as juvenile wood exhibits features such as low density, high microfibril angle (low stiffness), spiral grain and compression wood.

Concerning knots: "*Most mechanical properties are lower in sections containing knots than in clear straight-grained wood because (a) the clear wood is displaced by the knot, (b) the fibers around the knot are distorted, resulting in cross grain, (c) the discontinuity of wood fiber leads to stress concentrations, and (d) checking often occurs around the knots during drying*" (USDA 1999). As trees grow in diameter, branches become incorporated in the stem (USDA 1999, Achim *et al*. 2006). If the branches are still alive they continue to increase in diameter as the tree increases in diameter, resulting in a conical shaped knot running from pith to bark resulting in larger knots at the bark than at the pith.

Most branches on Sitka spruce trees are in whorls. A whorl (or node) represents one year's growth by the apical meristem (*i.e.* growth in height). At the beginning of the following year, branches grow laterally from that apex, while the shoot continues upward. Therefore branches from the whorl or node will form clusters around the pith. Knot clusters affect the timber strength and need to be taken into account to comply with EN14081-1:2005 (CEN 2005) during visual override. Therefore it is unclear what the effect of moving structural battens away from the centre of the log will have on knot size in battens and needs to be taken into account.

6.1.5 Objectives

The objectives of this chapter are to:

- Test the effect of sorting logs on batten quality using various criteria: log velocity; log velocity and density; log velocity, density and proportion of juvenile core.
- Develop and test alternative log cutting patterns for lower stiffness logs, capable of being implemented within commercial scale mills that optimise for structural quality by taking into account the pith-to-bark variation in wood stiffness.
- Compare volume and value recoveries of the various cutting pattern approaches with typical sawmill patterns to examine the profitability of alternative patterns.
- Examine the effect mean cambial age relative to the juvenile core has on batten properties.

6.2 Method and Materials

Current pass rates of the basic construction grade of C16 are in excess of 90% for British spruce. Therefore to simulate a drop in the quality of the resource, the minimum required mean stiffness of the next highest construction grade, C18, was targeted. The minimum average batten stiffness required for C18 is 8.55 kN mm^{-2} and the minimum average batten stiffness for C16 is 7.6 kN mm^{-2} (these values take into account the 5% allowance below the actual mean target stiffness of 8 kN mm^{-2} and 9 kN mm^{-2} for the C16 and C18 grades, respectively (EN384 CEN 2010, EN14081:1 CEN 2005, EN338 CEN 2003)). Therefore targeting C18 represents a 12.5% drop in the mean stiffness of the resource.

To achieve a mean batten stiffness of 8.55 kN mm^{-2}, it is estimated that the minimum batten MOE threshold should be 5.9 kN mm^{-2}. This value is calculated assuming the population of Sitka spruce batten MOE is defined by a normal distribution with a mean of 8.2 kN mm^{-2} and a COV of 22%. This mean value is consistent with the values measured by Moore *et al.* (in press) and the COV is the variation in MOE assumed by EN338 (CEN 2003a). By removing all battens below 5.9 kN mm^{-2}, the mean MOE of the remaining battens becomes 8.55 kN mm^{-2}. This is illustrated in Figure 6.2.
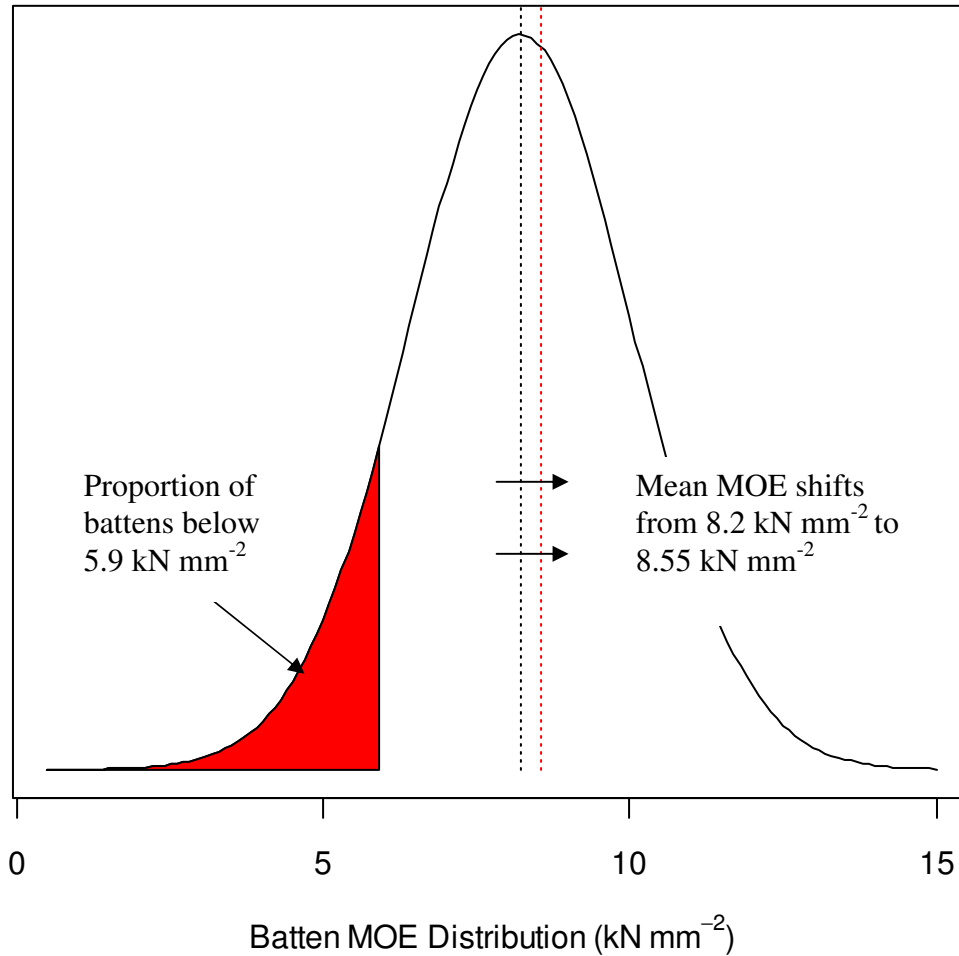
Figure 6.2. Illustration of how removal of all battens below 5.9 kN mm^{-2} results in the mean batten MOE shifting from 8.2 kN mm^{-2} to 8.55 kN mm^{-2}.

Therefore in effect, the value of 5.9 kN mm^{-2} represents a pseudo-machine control grader setting, assuming a perfect grader. A perfect grader is an idealised grader that would determine strength (MOR) and stiffness (MOE) exactly as a determined from a destructive 4-point bending test. In reality, grading machines are not ideal; they measure an indicating property or properties which are correlated to the grade determining property but not perfectly.

6.2.1 Log Selection and Sorting

For this experiment 155 logs were kindly donated by James Jones and Sons' Ltd Lockerbie sawmill in November 2010 with top end diameters that ranged from 220 mm to 320 mm. The forest (or forests) that the logs came from is unknown.

This is the most common log diameter range for structural batten production at this sawmill. It was chosen because it is the most representative of the available resource and it is theoretically the point of greatest cross-over between large diameter top logs having large proportions of juvenile wood and smaller, slower grown or suppressed logs and everything in between.

Resonant log velocity was measured with the Director HM200 (Fibre-gen NZ) after which, the density was obtained gravimetrically from a 50 mm thick disc from the end of each log less than a week after. The logs were then numbered and ranked in order of stiffness using equation 2.1. All logs were then divided into four roughly equal size groups, hereafter referred to as 'log groups', with almost identical dynamic stiffness distributions to test the various log segregation techniques and cutting patterns. Each log group was then further divided into low, medium and high stiffness logs using Figure 6.1 such that:

- The low stiffness logs corresponded to the logs with an average batten static global MOE of less than 8 kN mm^{-2}. Approximately 50% of the population fell into this category.
- The medium stiffness logs corresponded to the logs with an average batten static global MOE of between 8 kN mm^{-2} and 9 kN mm^{-2}. Approximately 33% of the population fell into this category.
- The high stiffness logs corresponded to logs with an average batten static global MOE of greater than 9 kN mm^{-2}. Approximately 17% of the population fell into this category.

The log groups were colour coded and had the bottom end painted to match with its colour code and stamped to match with its stiffness group. The first ten growth rings at the top end of the log were also coloured in orange to highlight the juvenile core. Logs marked according to segregation are shown in Figure 6.3.

Figure 6.3. Logs after being painted to identify log group and juvenile core.

6.2.2 Cutting Pattern Determination

Each log group represented a different sorting strategy and each stiffness group represented a different cutting pattern principle. The objective of each cutting pattern was to maximise the volume of structural dimension timber whilst adhering to the particular rules assigned to each log group. The cutting pattern description for each log group/stiffness group combination is shown in Table 6.1. Each log group in Table 6.1 has been labelled to correspond with its sorting and cutting strategy and will be used henceforth throughout the chapter:

1. '**Control**' is the control group using typical sawmill cutting patterns.
2. '**VelSort**' sorted logs by dynamic MOE assuming constant density and using log velocity^2 only.
3. '**DMOEsort**' sorted logs by dynamic MOE using density and velocity^2 in equation 2.1.
4. '**JWC sort**' sorted logs by dynamic MOE using density and velocity^2 and also accounts for the size of the juvenile wood content (JWC).

Table 6.1. Cutting pattern description for each log group/stiffness group combination.

Log Group	Label	Stiffness Group	Cutting Pattern Description
1. White Control Group	Control	Low, Medium and High	Typical sawmill cutting patterns for structural timber. Volume optimization.
2. Blue Sort using log velocity[2]	VelSort	Low	Estimate the size and extent of the low stiffness core and only cut structural dimensions from outside this region (same as DMOEsort low stiffness logs).
		Medium and High	Typical sawmill cutting patterns
3. Green Sort using dynamic MOE	DMOEsort	Low	Estimate the size and extent of the low stiffness core and only cut structural dimensions from outside this region (same as VelSort low stiffness logs)
		Medium and High	Typical sawmill cutting patterns
4. Red Sort using dynamic MOE and the size of the juvenile core.	JWCsort	Low	Only cut structural dimensions outside the first 10 growth rings.
		Medium	Only cut structural dimensions outside 75 mm x 75 mm box around the pith.
		High	Typical sawmill cutting patterns.

The MOE, distortion and knot measurements for the Control group are the values to which all other groups will be compared.

The VelSort and DMOEsort groups represented a pragmatic solution for sawmills and aimed to raise the average bending stiffness of their battens above a minimum of 5.9 kN mm^{-2}. To achieve this, cutting patterns must be altered such that structural dimensions are excluded from the least stiff part of the log. To estimate the extent of this low stiffness core, the following assumptions were made:

- Material from near the bark was 50% stiffer than the pith (*e.g.* Xu and Walker 2004).
- There was a linear increase in stiffness from pith to bark.
- The logs had a circular cross section
- The logs were a representative sample of the population.
- The pith was located in the centre of the log.
- The average stiffness of the battens from a log was related to the log velocity^2 by the regression equation in Figure 6.1:

$$E_{0,\ mean} = 0.616\ (LogVel^{\,2}) + 1.25$$

Where:
- $E_{0,\ mean}$ is the average batten stiffness from a log
- $LogVel^{\,2}$ is the log velocity^2

The solution results in a condition where the value of the average MOE of battens from a whole log occurs at two-thirds of the distance from pith to bark.

According to these assumptions, only the low stiffness logs possessed a low stiffness core incapable of reaching the minimum threshold of 5.9 kN mm^{-2}. Therefore, all medium and high stiffness logs within the VelSort and DMOEsort groups were cut with standard sawmill cutting patterns to maximise structural batten recovery. The inclusion of density in the calculation of dynamic MOE for the DMOEsort group should show whether the inclusion of this parameter adds any worthwhile improvement in the segregation of British spruce logs.

The JWCsort log group was the most cautious approach. Only the high stiffness logs were cut using standard mill cutting patterns. For the medium stiffness group, no structural dimensions were produced within a 75 mm x 75 mm box around the pith on the top end of the log (as per Johansson *et al.* (2001)). The low stiffness group was even more restricted with no structural dimensions cut from within the juvenile core (in this case the first ten growth rings) of the top end diameter.

A cutting pattern was determined for each log using the PowerSAW (SAATECHSystems Pty Ltd) simulation and analysis software. In order to obtain a statistically meaningful number of battens from each sort group/stiffness grade combination, structural dimensions were limited to the green nominal sizes of 103 mm x 49 mm (4" x 2"), 153 mm x 49mm (6" x 2") and 204 mm x 49 mm (8" x 2"). The 204 mm x 49 mm battens were then cut in half lengthways to produce two 103 mm x 49 mm battens after drying, just as a sawmill would. The optimal patterns were then transcribed onto the disc taken from the top end of each log and adjusted as required to account for each log's roundness, as shown Figure 6.4. This allowed for each log to be optimally rotated prior to cutting. Unfortunately it was not possible to measure log sweep on the logs and optimisation with PowerSAW was unable to account for this. If excessive sweep was encountered, adjustments to the cutting pattern were made *in-situ* which may have led to sub-optimal processing in a small number of cases.
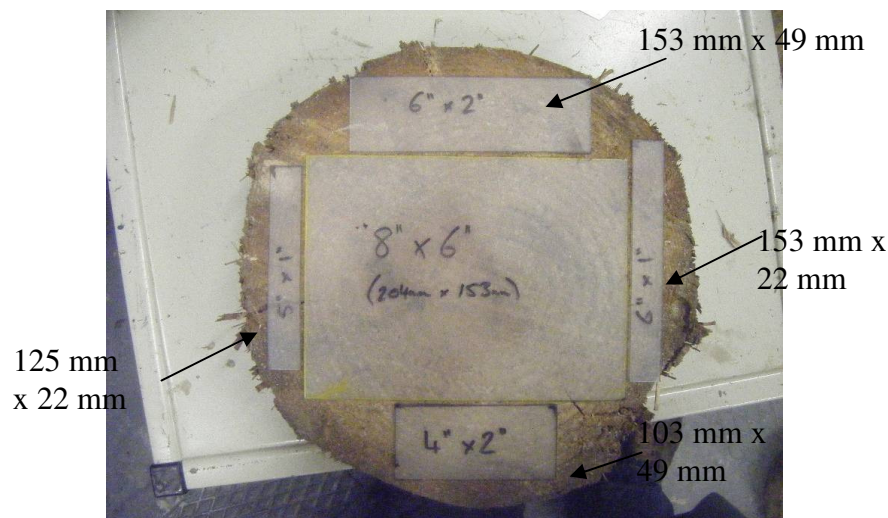
Figure 6.4. Example cutting pattern being transcribed onto a disc.

6.2.3 Log Processing

Obtaining structural dimensions from the higher stiffness areas near the bark must be done within the framework of what is possible within a sawmill if comparisons of volume recovery between various cutting patterns are to be valid. The framework used in this experiment was of a typical modern sawmill setup with the following (simplified) log breakdown sawing systems:

Primary breakdown: Quad-reducing bandsaws
This system consists of four bandsaws and a reducer (chipper) that can produce up to four side-boards and a central cant, *e.g*. Figure 6.5.
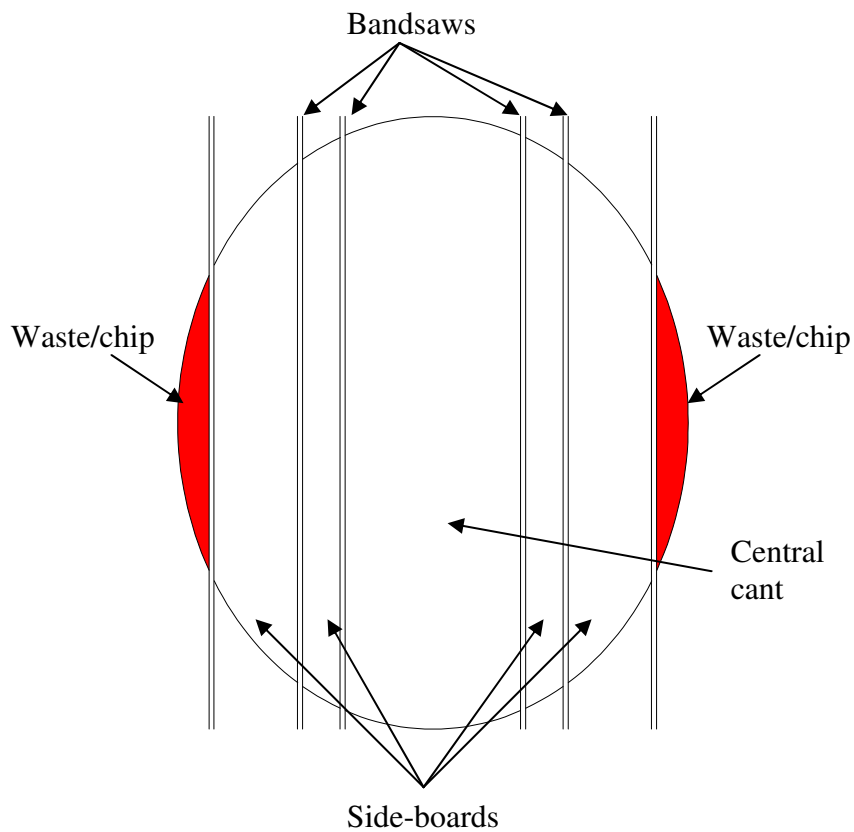
Figure 6.5. Log primary breakdown system.

Edging System

The side-boards are then send to an 'Edger' which removes the round portions remaining from the log and results in a complete batten with a rectangular cross section, *e.g*. Figure 6.6. An edging system can consist of up to four saws to produce up to three battens per side-board.
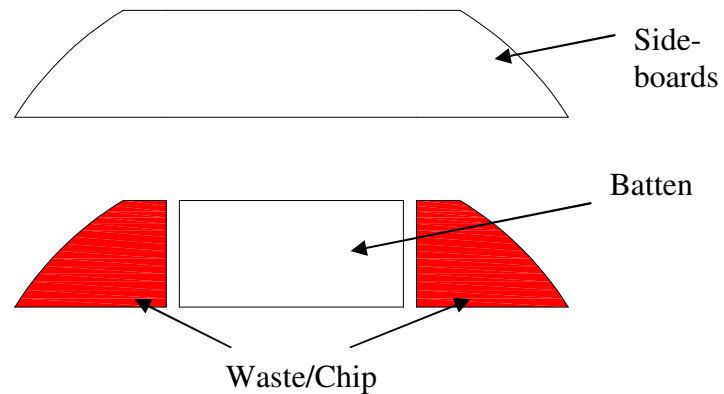
Figure 6.6. Edging system for slabs from primary breakdown.

Secondary breakdown: Quad-reducing bandsaws

This system consists of another four bandsaws and a reducer. The central cant is sent through the quad-reducer and can result in up to four more side-boards and a flitch, *e.g*. Figure 6.7.
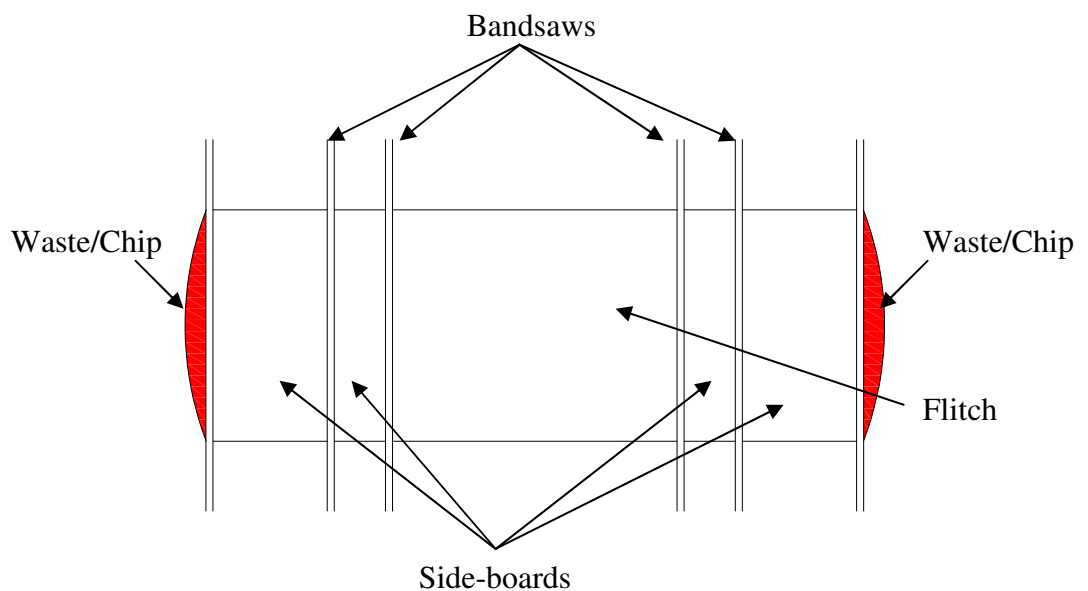
Figure 6.7. Secondary breakdown of the central cant.

<u>Final breakdown: Quad gang saw</u>

This system consists of four bandsaws to turn the flitch into up to five battens, *e.g.* Figure 6.8.
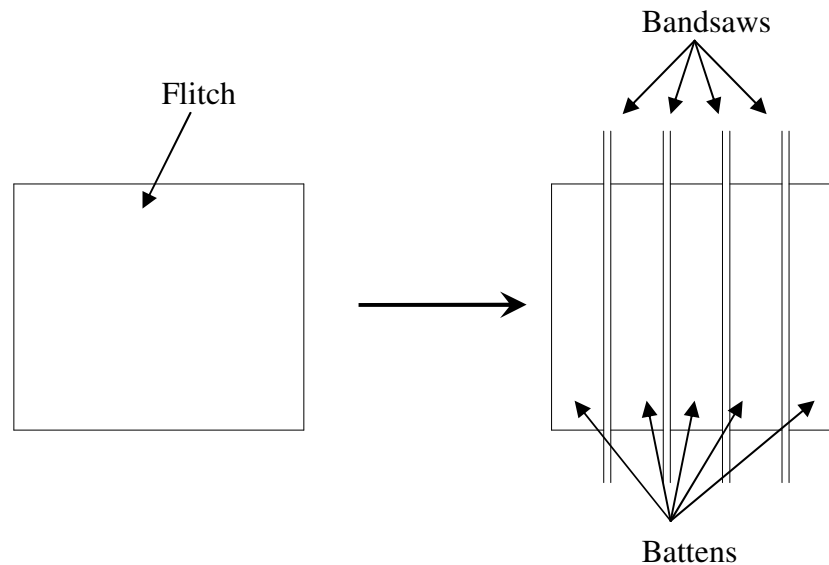
Figure 6.8. Final breakdown of a flitch.

In this way, up to 9 battens can be cut from the central cant (5 from the flitch and up to 4 from the side boards) with up to an additional 4 battens produced from the primary breakdown system. After all log breakdown systems have been used, some battens may still not have a completely rectangular cross section along its entire length, *i.e.* some of the round sections of the log are still visible. This is called wane. To remove wane, battens were cross-cut in multiples of 600mm (as per sawmill procedure) to remove affected areas, resulting in battens of reduced length. The minimum final batten length allowed in this experiment was 1.8 m.

The sawing system used to cut all the logs in this experiment consisted of:

- A single, portable horizontal bandsaw from Woodmizer (Wood-Mizer Industries) to act as the primary, secondary and final breakdown systems. The bandsaw thickness (kerf) of the bandsaws on the Woodmizer was 3 mm, the same as a commercial sawmill.
- A circular table saw to act as the edger
- A circular drop saw to remove wane.

All alternative cutting patterns are suitable for implementation in sawmills and no dimensions were produced that are not currently produced.

All battens were then dried to 12% moisture content using a Hydromat TK-MP4032 kiln (Gann Mess- u. Regeltechnik GmbH) at Forest Research's Northern Research Station, Scotland.

6.2.4 Batten Testing

A number of battens from each sort group/grade combination were taken for an in-depth analysis of knots, distortion and stiffness using a commercial grading machine. In total 147 (one hundred and forty seven), 103 mm x 49 mm and 74 (seventy four), 153 mm x 49 mm battens were selected. The approximate mean cambial ages of all 103 mm x 49 mm battens were also recorded. These battens were classified and labelled as either less than 10 years ('<10'), approximately 10 years ('10'), greater than 10 years ('>10') and much greater than 10 years ('>>10').

These battens were taken to Adam Wilson and Sons sawmill in Troon, Scotland and analysed using a MiCROTEC GOLDENEYE 702 x-ray grading machine to measure density, knot severity and knot location. MiCROTEC™ provided a ViSCAN unit to measure the resonant acoustic speed of each batten. Distortion was also measured using a FRITS (Freiburg's Improved Timber Scan) Frame (Seeling and Merforth, 2000). This uses a laser measurement system to measure the distance to the top of a batten from a datum point. Bow, twist and spring can be determined from the results. Four-point bending tests were conducted on a Zwick Z050 universal testing machine (Zwick Roell, Germany) to determine batten strength. Tests were performed in accordance with the procedures described in EN 408:2003 (CEN 2003) and EN384:2010 (CEN 2010). Global modulus of elasticity and modulus of rupture (MOR) were calculated from the data obtained during these tests using the equations given in EN 408 (CEN, 2003).

It should be noted that the knot values given by the GOLDENEYE 702 x-ray grading machine are not simply a measure of knot-area-ratio, and are non-dimensional values only. They do not have a scale but are the result of a well-defined but confidential algorithm from MiCROTEC (Bacher, personal communication). However, the knot severity values given by the GOLDENEYE do give an idea as to the relative scale of the knot size and frequency.

The dynamic stiffness was also measured on all battens (as per equation 2.1) by weighing each batten to determine its density and using the Director HM200 (Fibre-gen, NZ) to measure the resonant velocity. This was then converted to an estimated global MOE from the linear regression coefficients of the static global to dynamic MOE relationship (outlined later in section 6.3.3). Optimum pass rates (*i.e.* assuming a perfect grading machine) were calculated with 5.9 kN mm^{-2} as the machine grader threshold MOE.

6.2.5 Data Analysis

Data were analysed using the R open-source statistical package (R Development Core Team 2010). Linear models were examined with ANOVA to determine any significant effects on batten properties between all log groups which utilised alternative cutting patterns and the Control. This procedure was followed for each stiffness group within each log group. Additionally, linear models were examined with ANOVA to determine any significant effects on batten properties due to its cambial age relative to the juvenile core. A significance level of 0.05 was used.

6.2.5.1   Cost-benefit calculator to estimate value recovery

Further, a simple cost-benefit calculator was constructed in Microsoft Excel to examine the value recoveries of the various cutting pattern approaches. The calculator was created assuming the following illustrative values:

- Log cost is £34.56 m^{-3}, as per Cameron (2002).
- Drying cost was £15 m^{-3} and only structural dimensions were dried.

- The sale price of non-structural battens was £100 m^{-3}
- The sale price of battens with structural dimensions rejected at the stress grader was the same as for non-structural dimensions, £100 m^{-3}
- The sale price of structural battens above the minimum threshold of 5.9 kN mm^{-2} was £150 m^{-3}

Note: This model accounts for rejects due to low stiffness only and does not take into account fixed processing costs and revenue obtained from the sale of residues such as chip or sawdust. However it should provide an illustration of the effectiveness of alternative cutting patterns to improve value.

6.3 Results

The 155 logs came to an estimated volume of 31.27 m^3 which resulted in 1274 battens. The total volume of battens produced was 17.44 m^3 giving an overall volume recovery across all log groups of 55.8%.

6.3.1 Log Sorting

The mean log velocity^2 of the 155 logs was 10.85 km^2 s^{-2} (COV = 15.7%) corresponding to a mean log dynamic MOE of 8.97 kN mm^{-2} (COV = 16%). The mean top end diameter of the logs was 273 mm (COV = 13.5%) with a mean taper of 17 mm m^{-1} (COV = 73%). The distribution of log dynamic MOE, top end diameter and taper for each log group is shown in Figure 6.9.
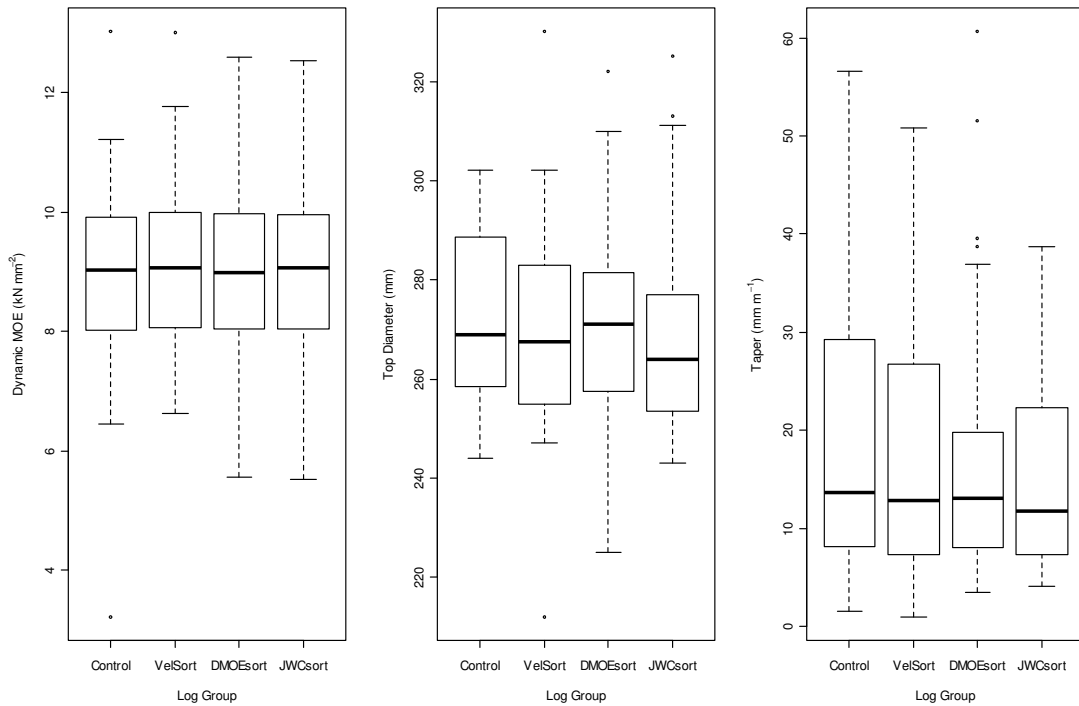
Figure 6.9. Distribution of properties among each log group.

Using ANOVA, there was no significant difference between log groups for any of the properties shown in Figure 6.9 (p=0.94, 0.5 and 0.2 for dynamic MOE, top diameter and taper, respectively).

The relationship between log velocity^2 and log dynamic MOE is shown in Figure 6.10a and the relationship between log velocity^2 and log density is shown in Figure 6.10b.
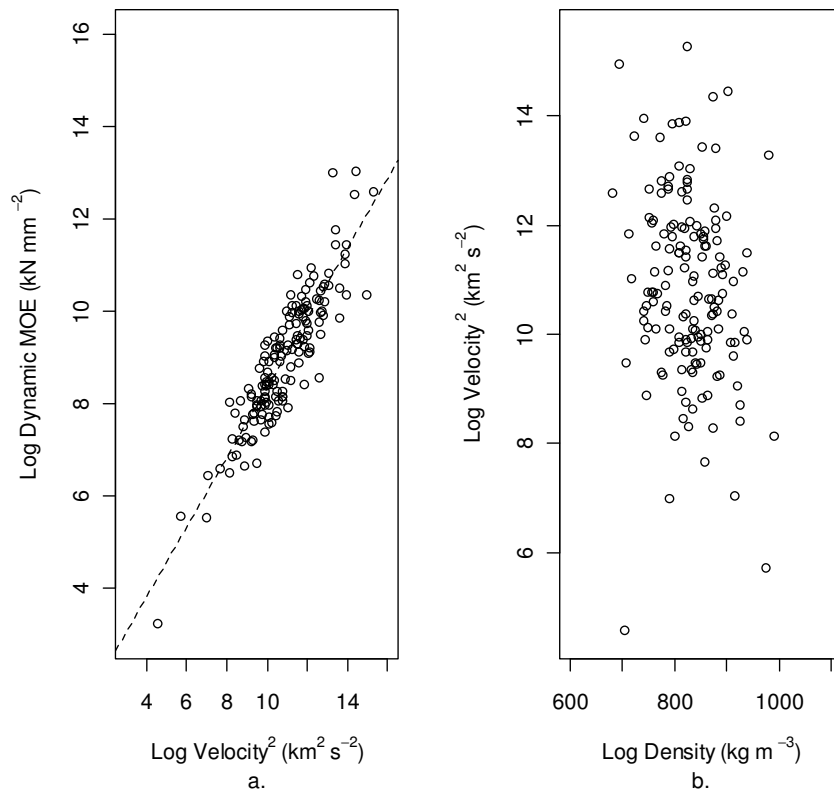
Figure 6.10. Relationship between log velocity^2 and (a) log dynamic MOE, (b) log density.

Using linear regression, the R^2 between log velocity^2 and log dynamic MOE was 0.81 with an intercept at 0.77 kN mm^{-2} ($p<0.05$) and a slope of 0.76 ($p<0.01$). The variation is due to the variation in log density. Log density ranged from 679 kg m^{-3} to 989 kg m^{-3} with a mean and COV of 828 kg m^{-3} and 7.1% respectively. There is no relationship between log density and log velocity^2.

6.3.1.1   Effect of assuming constant density on log sorting
The VelSort log group was sorted into stiffness groups by log velocity^2 and not dynamic MOE. This resulted in 6 logs (15.9%) allocated to incorrect stiffness grades:

- 1 log incorrectly downgraded from the high stiffness group into the medium stiffness group and 1 low stiffness log incorrectly upgraded to the medium stiffness group. These logs resulted in an

extra 6.4% and 7.8% of logs, respectively in the medium stiffness group.

- 3 logs incorrectly upgraded into the high stiffness grade from the medium stiffness grade. These extra logs resulted in an extra 41% of logs in the high stiffness grade.
- 2 logs incorrectly downgraded from the medium stiffness group to the low stiffness group. These logs resulted in an extra 11.3% of logs in the low stiffness group.

The effect of the miss-classification of logs on the proportion of logs within each log group is shown in Table 6.2.

Table 6.2. Summary of the number of logs in each log and stiffness group.

Log Group	Total No. of logs	Proportion of low stiffness logs (%)	Proportion of medium stiffness logs (%)	Proportion of high stiffness logs
Control	39	48.7	35.9	15.4
VelSort	38	47.4	26.3	26.3
DMOEsort	39	48.7	33.3	18.0
JWCsort	39	48.7	33.3	18.0

There is little difference in the proportion of logs within the low stiffness group yet the distribution of stiffness within the group will have been changed. The number of logs in the medium and high stiffness groups has changed by approximately 7% to 8% relative to the other groups.

6.3.2 Effect of alternative cutting patterns on the volume of structural battens produced

The overall volume recoveries and the proportion of structural battens produced from each log group are shown in Table 6.3.

Table 6.3. Overall volume recoveries and proportion of structural battens for each log group.

Sort Group	Overall volume recovery (%)	Proportion of battens cut to structural Dimensions (%)
Control	54.9	79.0
VelSort	55.2	73.8
DMOEsort	55.2	72.3
JWCsort	57.7	45.1

The JWCsort log group had the greatest volume recovery but the least proportions of structural dimensions produced. The volume recoveries of the Control, VelSort and DMOEsort log groups were very similar but the Control group produced the greatest proportion of structural battens.

A breakdown of the number of structural and non-structural battens produced from each log group as well as which position in the log they were produced from, *i.e.* whether they were produced from the central cant or side boards that went through the edger is shown in Table 6.4.

Table 6.4. Breakdown of the number of battens produced from each log group and position in log from which they were produced from.

	Structural			**Non structural**		
	Total	% battens from cant	% battens from edger	Total	% battens from cant	% battens from edger
Control	199	78.4	21.6	118	10.2	89.8
VelSort	173	65.9	34.1	144	41.0	59.0
DMOEsort	190	61.1	38.9	157	40.8	59.2
JWCsort	117	47.0	53.0	280	67.5	32.5

Table 6.4 shows that the implementation of alternative cutting patterns resulted in a reduction in the number of structural battens which are extracted from the central cant and an increase in the number produced at the edger. Conversely, this resulted in an increase in the number of non-structural battens produced in the central cant. Therefore, the total number of battens (both structural and non-structural) produced at the edger remains fairly similar with the VelSort, DMOEsort and JWCsort log groups producing 97%, 112% and 105% respectively, relative to the Control log group.

Table 6.5 shows the effect of alternative patterns on the proportion of log volume converted to structural dimensions for each log and stiffness group combination.

Table 6.5. Proportion of structural dimensions relative to log volume extracted from the each log and stiffness group.

Log Group	Proportion of structural dimensions from low stiffness logs (%)	Proportion of structural dimensions from medium stiffness logs (%)	Proportion of structural dimensions from high stiffness logs (%)
Control	42	45.1	44.6
VelSort	37.5	45.9	41.9
DMOEsort	34.3	45.7	47.0
JWCsort	15.2	31.9	50.3

For the low stiffness logs, excluding the juvenile core in the JWCsort log group only allowed 15.2% of a log's volume to be converted into structural dimensions. The reduction in the volume of structural dimensions for the VelSort and DMOEsort log groups was less severe, producing 37.5% and 34.3% respectively, compared to the Control log group's 42.0%.

For the medium stiffness logs, only the JWCsort log group implemented alternative cutting patterns. The JWCsort log group excluded a 75 mm x 75 mm box around the pith from producing structural dimensions, resulting in 13% to 14% less log volume converted to structural dimensions compared to any of the other log groups. The conversion rate for the Control, VelSort and DMOEsort were very similar. This was expected considering that they are applying the same cutting patterns.

In contrast, for the high stiffness logs, all log groups applied the same patterns yet the proportion of structural dimensions ranged from 41.9% for the VelSort to 50.3% for the JWCsort. The small number of high stiffness logs within each log group means that small variations in log shape (*e.g*., taper, sweep and top diameter) are likely to have an impact on yield of structural dimensions.

6.3.3 Effect of alternative cutting patterns on batten properties

A total of 679 structural battens were produced from all log groups. A sub-sample of 224 battens was taken for detailed assessment of bending stiffness (static and dynamic MOE), strength (MOR), distortion and knots. The number of battens from each log and stiffness group that was part of the sub sample is shown in Table 6.6.

Table 6.6. Number of battens from each log and stiffness group that were taken for detailed analysis of MOE, MOR, distortion and knots.

Log Group	Stiffness Group	No. Battens
Control	Low	21
	Medium	22
	High	13
VelSort	Low	24
	Medium	18
	High	13
DMOEsort	Low	29
	Medium	16
	High	14
JWCsort	Low	16
	Medium	13
	High	25

The relationship between the global MOE determined from EN408 bending test and the dynamic MOE from the MiCROTEC ViSCAN dynamic MOE is shown in Figure 6.11.
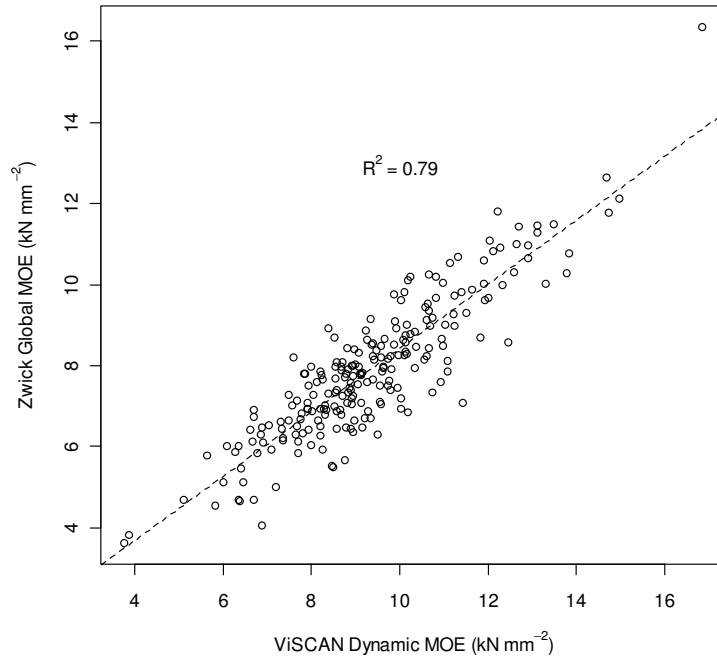
Figure 6.11. Relationship between global MOE and ViSCAN dynamic MOE

Using linear regression, the R^2 between the global MOE and the ViSCAN dynamic MOE was 0.79 with an intercept at 0.49 kN mm^{-2} (p=0.059, std err. = 0.26) and a slope of 0.79 (p<0.01). These regression coefficients were used to convert all the dynamic MOE measurements (calculated using acoustic velocity from the HM200) of the remaining battens to an estimated global MOE. Using the same relationship to convert the dynamic MOE measured with the HM200 to an estimated global MOE is possible as the relationship between ViSCAN and HM200 velocity is very good (R^2 = 0.9).

Of the sample of battens taken for further testing, none were rejected under the visual override criteria set in EN14081-1:2005 (CEN 2005) for bow or spring whilst 35.7% of all battens would have been rejected for visual override for twist. Therefore only results for twist type distortion are reported here. It needs to be noted that the battens were tested at 12% moisture content (MC) whereas sawmills only dry their battens to 20% MC. Reducing MC below the saturation point results in increasing distortion, so the values of twist reported here are higher than normal.

6.3.3.1 Results from detailed testing of MOR, MOE, distortion and knots

This section details the results from the detailed testing of MOR, MOE, distortion and knots for each of the low, medium and high log stiffness groups separately.

Low stiffness logs

The low stiffness logs have the greatest difference in cutting pattern approach between all log groups. A summary of the mean batten properties for the low stiffness logs of each log group is shown in Table 6.7. Because of the small sample size, values which were significant to $p<0.1$ were also included for consideration.

Table 6.7. Summary of the mean MOR, global MOE, twist and maximum knot severity for the low stiffness logs from each log group. The value in parenthesis are the standard deviations and significant difference relative to the control is indicated (calculated with ANOVA).

Log Group	No. battens	Strength (MOR) (N mm^{-2})	Global static MOE (kN mm^{-2})	Twist (mm per 25 mm width)	Overall knot severity
Control	21	30.5 (9.5)	6.74 (1.2)	1.92 (1.4)	10723 (3536)
VelSort	24	32.3 (11.5)^{ns}	7.11 (1.6)^{ns}	1.73 (0.9)^{ns}	9369 (3513)^{ns}
DMOEsort	29	29.7 (10.1)^{ns}	6.72 (1.2)^{ns}	1.58 (0.9)^{ns}	8663 (3284)*
JWCsort	16	32.2 (10.2)^{ns}	7.80 (1.0)*	1.30 (0.6).	6701 (3192)***

^{ns} is not significant
.is significant to $p<0.1$
*is significant to $p<0.05$
***is significant to $p<0.001$

There is no significant difference in MOR between log groups and only the JWCsort log group is significantly different from the Control group for MOE. The JWCsort group has a 15.9% greater MOE on average than the Control. For twist, the JWCsort log group was almost significantly different from the Control ($p=0.066$).

The JWCsort log group had 32.5% less twist on average than the Control. There was no significant difference in twist between the Control, VelSort and

DMOEsort log groups. For the overall knot severity, both the DMOEsort and the JWCsort log group were significantly different from the Control. There was a 19.2% and a 37.5% reduction in the value of mean overall knot severity for the DMOEsort and JWCsort log groups, respectively. There was no significant difference between the Control and the VelSort log group.

Medium stiffness logs

A summary of the mean batten properties for each log group for the medium stiffness logs is shown in Table 6.8. Only the JWCsort group did not utilise sawmill cutting patterns here.

Table 6.8. Summary of the mean MOR, global MOE, twist and maximum knot severity for the medium stiffness logs using standard sawmill patterns and alternative patterns. The value in parenthesis is the standard deviation and significant difference relative to the control is indicated (calculated with ANOVA).

Log Group	No. battens	Strength (MOR) (N mm^{-2})	Global static MOE (kN mm^{-2})	Twist (mm per 25 mm width)	Overall knot severity
Control	22	35.3 (9.7)	7.94 (1.3)	1.58 (0.7)	6936 (2638)
VelSort	18	35.9 (10.4) ^{ns}	8.19 (1.2) ^{ns}	2.22 (1.0)*	9465 (3188)*
DMOEsort	16	33.5 (11.1) ^{ns}	7.76 (1.5) ^{ns}	2.01 (1.5) ^{ns}	7729 (3948) ^{ns}
JWCsort	13	32.5 (11.9) ^{ns}	8.81 (1.8).	1.54 (0.6) ^{ns}	7483 (3232) ^{ns}

^{ns} is not significant
. is significant to $p<0.1$
* is significant to $p<0.05$

There was no significant difference in MOR between log groups. The VelSort log group was significantly different to the control for twist and overall knot severity. The twist and overall knot severity of the VelSort group were 40.5% and 36.4% greater than the Control. There was almost a significant difference in global MOE with the mean between the JWCsort and Control log groups. The JWCsort global MOE was 10.9% greater than the Control.

A summary of the mean batten properties for each log group for the high stiffness logs is shown in Table 6.9. All battens were produced using standard sawmill cutting patterns across all treatments for this stiffness group.

Table 6.9. Summary of the mean MOR, global MOE, twist and maximum knot severity for the high stiffness logs using standard sawmill patterns for each log group. The value in parenthesis is the standard deviation and significant difference relative to the control is indicated (calculated with ANOVA).

Log Group	No. battens	Strength (MOR) (N mm^{-2})	Global static MOE (kN mm^{-2})	Twist (mm per 25 mm width)	Overall knot severity
Control	13	48.1 (16.0)	10.10 (2.5)	1.65 (0.8)	5235 (2127)
VelSort	13	33.2 (12.8)**	8.70 (2.1).	1.58 (0.7) ^{ns}	8249 (2870)**
DMOEsort	14	36.5 (12.0)*	8.89 (2.0) ^{ns}	1.88 (1.0) ^{ns}	8195 (2815)**
JWCsort	25	34.4 (9.9)**	8.32 (1.4)**	2.37 (0.9)*	7373 (2288)*

^{ns} is not significant
.is almost significant $p<0.1$
*is significant to $p<0.05$
**is significant to $p<0.01$

There was a significant difference in the MOR between the Control and all the other log groups. The MOR for the Control group was 31%, 24.3% and 28.6% greater than the VelSort, DMOEsort and JWCsort groups, respectively. The global MOE for the Control group was significantly different to the JWCsort group and almost significantly different to the VelSort group. The global MOE for the Control group was 17.7% and 13.9% greater than the JWCsort and the VelSort groups, respectively. There was a significant difference in twist between the Control group and the JWCsort group. The twist for the Control group was 43.5% smaller than the JWCsort group. There was a significant difference in the overall knot severity between the Control and all the other log groups. The overall knot severity was 57.6%, 56.5% and 40.8% smaller than the VelSort, DMOEsort and JWCsort groups, respectively.

Considering that the battens from each log group were all produce using typical sawmill patterns from logs with a limited distribution in stiffness, the variation

seen here is not due to treatment. Rather it is random and due to small sample size and variation in branch size between logs which was not accounted for during log segregation.

6.3.3.2   Estimated Global MOE for each log and stiffness group

This section examines the estimated global MOE for all structural battens (including those taken for detailed testing) and compares it with the static global MOE from the detailed testing alone. A summary of the mean estimated global MOE for all structural battens for each log and stiffness group is shown in Table 6.10.

Table 6.10. Summary of mean estimated global MOE for each log and stiffness group. Value in parenthesis is the standard deviation and significant difference relative to the control is indicated (calculated with ANOVA).

Log Group	Low stiffness logs global est. MOE ($kN\ mm^{-2}$)	Medium stiffness logs global est. MOE ($kN\ mm^{-2}$)	High stiffness logs global est. MOE ($kN\ mm^{-2}$)	All stiffness groups combined global est. MOE ($kN\ mm^{-2}$)
Control	6.34 (1.3)	7.40 (1.0)	9.25 (1.8)	7.09 (1.6)
VelSort	7.04 (1.0)***	7.74 (1.1)^{ns}	8.32 (1.5)*	7.55 (1.3)**
DMOEsort	6.97 (1.0)***	7.78 (1.0)*	8.49 (1.4)^{ns}	7.56 (1.2)***
JWCsort	7.51 (0.9)***	8.00 (1.1)**	8.50 (1.5)^{ns}	8.02 (1.2)***

^{ns} is not significant
*is significant to $p<0.05$
**is significant to $p<0.01$
***is significant to $p<0.001$

For the low stiffness logs in Table 6.10, all log groups show a significant difference relative to the Control. The Control is 11.2%, 9.9% and 18.5% less than the VelSort, DMOEsort and JWCsort log groups, respectively.

For the medium stiffness logs in Table 6.10, there is a significant difference between the Control group and the DMOEsort and the JWCsort group. The Control is 5.3% and 8.1% less than the DMOEsort and JWCsort groups, respectively.

For the high stiffness logs in Table 6.10, there is a significant difference between the Control group and the VelSort log group. The Control group is 10% greater than the VelSort log group.

6.3.3.3 Comparison of global estimated MOE of all battens with those taken for detailed testing.

This section examines the mean estimated global MOE for each log group that was taken for detailed testing and compares it with the mean estimated global MOE of all battens produced from each log group (including those taken for detailed testing). This is shown in Table 6.11. A Wilcox rank sum test was used to test significant difference between means instead of a standard t-test as batten MOE was not normally distributed.

Table 6.11. Comparison of mean estimated global MOE of battens taken for detailed testing and mean global estimated MOE of all battens from each log group. Value in parenthesis is the standard deviation and significant difference in means between each log group is indicated (calculated with Wilcox rank sum test).

Log Group	Detailed testing - All stiffness groups combined global estimated MOE (kN mm^{-2})	All battens - All stiffness groups combined global estimated MOE (kN mm^{-2})
Control	7.94 (1.9)	7.09 (1.6)***
VelSort	7.77 (1.4)	7.55 (1.3)^{ns}
DMOEsort	7.61 (1.4)	7.56 (1.2)^{ns}
JWCsort	8.29 (1.1)	8.02 (1.2)^{ns}

^{ns} is not significant
***is significant to $p<0.001$

The Control group shows a significant difference in mean estimated global MOE between the battens taken for detailed testing and all battens. This is due to two factors; firstly, the high stiffness logs in the Control group produced battens of significantly higher mean MOE than the other log groups (Table 6.9). Secondly, the sample of battens from the Control group taken for detailed testing was not representative of its population. For example, the number of battens taken from low stiffness logs for detailed testing from the Control group accounted for

37.5% of the total number. In practice, the number of battens produced from low stiffness logs from the Control group accounted for 50.7% of the total. This misrepresentation is likely to significantly alter the mean MOE as seen in Table 6.11. This misrepresentation also precludes the overall comparison of mean knot severity and twist for each log group.

There is no significant difference between mean estimated MOE for the other log groups.

6.3.4 Grading Simulation

6.3.4.1 Grading with a perfect grader

This section examines the effect of alternative and conventional cutting patterns on the pass-rate, assuming a perfect grader and a minimum MOE threshold of 5.9 kN mm^{-2}. The pass-rate from each log group was inserted into the cost-benefit calculator outlined in section 6.2.5, along with their respective log volume recoveries and proportion of structural dimensions produced to examine the profitability of the alternative patterns relative to the Control.

The pass-rate is defined as the proportion of battens whose global estimated MOE exceeds 5.9 kN mm^{-2}. The pass-rate for each stiffness and log group is shown in Table 6.12.

Table 6.12. Proportion of structural battens exceeding 5.9 kN mm^{-2} for each stiffness group within each log group and the overall pass-rate for each log group.

Log Group	Low stiffness logs pass rate (%)	Medium stiffness logs pass rate (%)	High stiffness logs pass rate (%)	Overall pass rate (%)
Control	63.4	94.5	100.0	79.4
VelSort	88.9	96.2	97.5	93.1
DMOEsort	83.3	100.0	100.0	92.6
JWCsort	93.9	100.0	97.3	97.4

The overall pass rate for the Control group using typical sawmill patterns was 79.4%. This value is 13.7%, 13.2% and 18% below the VelSort, DMOEsort and JWCsort log groups, respectively. The cutting patterns for the VelSort and DMOE log groups were designed to raise the minimum batten stiffness above 5.9 kN mm^{-2}. The pass-rate for the low stiffness logs from these log groups was 88.9% and 83.3%, respectively. Clearly, the assumptions used to estimate the extent of the low stiffness core were inaccurate, yet they still succeeded in improving the pass-rate over the Control by 25.5% and 19.9% for the low stiffness logs in VelSort and DMOEsort log groups, respectively. The reason for the disparity in pass-rates between these groups could be due to the misclassification of logs due to the assumption of constant density when sorting the VelSort log group: from section 6.3.1, two logs were incorrectly downgraded from the medium stiffness log group to the low stiffness log group resulting in an extra 11.3% log volume.

6.3.4.2   Cost-benefit calculation for each log group

The cost-benefit calculation for each of the log groups are shown in Tables 6.13a,b,c and d. The input variables are highlighted in yellow and the output in green. The volume recoveries and proportion of structural dimensions produced for each log group were obtained from Table 6.3. The proportion of battens greater than 5.9 kN mm^{-2} for each log group were obtained from Table 6.12. The input and output variables are labelled A, B, C, *etc.* and the calculation performed to obtain each output is shown in the outermost column. The overall value is expressed per m^3 of all battens produced using the respective cutting patterns, *e.g.* the Control group produced 79% structural battens, therefore the overall value per m^3 is made up of 0.79 m^3 of structural battens plus 0.21 m^3 of non-structural battens.

The cost-benefit calculation for the Control log group is shown in Table 6.13.

Table 6.13. Control group cost-benefit calculator. Input variables are labelled A, B, C, *etc.* and highlighted in yellow, output variables in green. The calculation used to derive each output value is shown in the final column. The overall value is expressed per m^3 of all battens, both structural and non-structural, produced using typical sawmill cutting patterns.

I/O	Variable	Description	Value used	Calculation Used
Input	A	Log Cost (£ m^{-3}):	34.56	N/A
	B	Volume Recovery (%)	54.9%	N/A
	C	Volume of structural dimensions produced (m^3):	0.79	N/A
	D	Sale price structural (£ m^{-3}):	150	N/A
	E	Sale price reject (£ m^{-3}):	100	N/A
	F	Sale price non-structural(£ m^{-3}):	100	N/A
	G	Kiln drying cost (£ m^{-3}):	15	N/A
	H	Proportion > 5.9 kN mm^{-2} (%):	79.4%	N/A
Output	V1	Value of structural battens (£):	94.09	CxDxH
	V2	Value of non-structural battens (£):	21	(1-C)xF
	V3	Value of rejects (£):	16.27	(1-H)xExC
	C1	Actual log cost (£):	62.95	A/B
	C2	Cost of drying (£):	11.85	CxG
		Overall Value* (£ m^{-3}):	56.56	(V1+V2+V3)-(C1+C2)

*0.79 m^3 structural battens + 0.21 m^3 non-structural battens

The overall value using conventional sawmill cutting patterns in the Control group using a minimum MOE threshold of 5.9 kN mm^{-2} was £56.56 per m^3.

The cost-benefit calculation for the VelSort log group is shown in Table 6.14.

Table 6.14. VelSort log group cost-benefit calculator. Input variables are labelled A, B, C, *etc.* and highlighted in yellow, output variables in green. The calculation used to derive each output value is shown in the final column. The overall value is expressed per m^3 of all battens, both structural and non-structural, produced using alternative cutting patterns.

I/O	Variable	Description	Value used	Calculation Used
Input	A	Log Cost (£ m^{-3}):	34.56	N/A
	B	Volume Recovery (%)	55.2%	N/A
	C	Volume of structural dimensions produced (m^3):	0.738	N/A
	D	Sale price structural (£ m^{-3}):	150	N/A
	E	Sale price reject (£ m^{-3}):	100	N/A
	F	Sale price non-structural(£ m^{-3}):	100	N/A
	G	Kiln drying cost (£ m^{-3}):	15	N/A
	H	Proportion > 5.9 kN mm^{-2} (%):	93.1%	N/A
Output	V1	Value of structural battens (£):	103.06	CxDxH
	V2	Value of non-structural battens (£):	26.2	(1-C)xF
	V3	Value of rejects (£):	5.09	(1-H)xExC
	C1	Actual log cost (£):	62.61	A/B
	C2	Cost of drying (£):	11.07	CxG
		Overall Value* (£ m^{-3}):	**60.68**	(V1+V2+V3)-(C1+C2)

*0.738 m^3 structural battens + 0.262 m^3 non-structural battens

The overall value using alternative cutting patterns on low stiffness logs in the Velsort log group using a minimum MOE threshold of 5.9 kN mm^{-2} was £60.68 per m^3.

The cost-benefit calculation for the DMOEsort log group is shown in Table 6.15

Table 6.15. DMOEsort log group cost-benefit calculator. Input variables are labelled A, B, C, *etc.* and highlighted in yellow, output variables in green. The calculation used to derive each output value is shown in the final column. The overall value is expressed per m^3 of all battens, both structural and non-structural, produced using alternative cutting patterns.

I/O	Variable	Description	Value used	Calculation Used
Input	A	Log Cost (£ m^{-3}):	34.56	N/A
	B	Volume Recovery (%)	55.2%	N/A
	C	Volume of structural dimensions produced:	0.723	N/A
	D	Sale price structural (£ m^{-3}):	150	N/A
	E	Sale price reject (£ m^{-3}):	100	N/A
	F	Sale price non-structural(£ m^{-3}):	100	N/A
	G	Kiln drying cost (£ m^{-3}):	15	N/A
	H	Proportion > 5.9 kN mm^{-2} (%):	92.6%	N/A
Output	V1	Value of structural battens (£):	100.42	CxDxH
	V2	Value of non-structural battens (£):	27.7	(1-C)xF
	V3	Value of rejects (£):	5.35	(1-H)xExC
	C1	Actual log cost (£):	62.61	A/B
	C2	Cost of Drying (£):	10.85	CxG
		Overall Value* (£ m^{-3}):	**60.02**	(V1+V2+V3)-(C1+C2)

*0.723 m^3 structural battens + 0.277 m^3 non-structural battens.

The overall value using alternative cutting patterns on low stiffness logs in the DMOEsort log group using a minimum MOE threshold of 5.9 kN mm^{-2} was £60.02 per m^3.

The cost-benefit calculation for the JWCsort group is shown in Table 6.16.

Table 6.16. JWCsort log group cost-benefit calculator. Input variables are labelled A, B, C, *etc.* and highlighted in yellow, output variables in green. The calculation used to derive each output value is shown in the final column. The overall value is expressed per m^3 of all battens, both structural and non-structural, produced using alternative cutting patterns.

I/O	Variable	Description	Value used	Calculation Used
Input	A	Log Cost (£ m^{-3}):	34.56	N/A
	B	Volume Recovery (%)	57.7%	N/A
	C	Volume of structural dimensions produced:	0.451	N/A
	D	Sale price structural (£ m^{-3}):	150	N/A
	E	Sale price reject (£ m^{-3}):	100	N/A
	F	Sale price non-structural(£ m^{-3}):	100	N/A
	G	Kiln drying cost (£ m^{-3}):	15	N/A
	H	Proportion > 5.9 kN mm^{-2} (%):	97.4%	N/A
Output	V1	Value of structural battens (£):	65.89	CxDxH
	V2	Value of non-structural battens (£):	54.9	(1-C)xF
	V3	Value of rejects (£):	1.17	(1-H)xExC
	C1	Actual log cost (£):	59.90	A/B
	C2	Cost of Drying (£):	6.77	CxG
		Overall Value* (£ m^{-3}):	**55.30**	(V1+V2+V3) -(C1+C2)

*0.451 m^3 structural battens + 0.549 m^3 non-structural battens

The overall value for the JWCsort group using alternative cutting patterns on the low and medium stiffness logs using a minimum MOE threshold of 5.9 kN mm^{-2} was £55.30 per m^3.

The overall value for each log group is summarised in Table 6.17.

Table 6.17. Summary of overall values for each log group and difference relative to the Control, using the cost-benefit calculator.

Log group	Value (£ m^{-3})	% difference to Control
Control	56.56	-
VelSort	60.68	7.3%
DMOEsort	60.02	6.1%
JWCsort	55.30	-2.2%

The VelSort and DMOEsort log groups provide 7.3% and 6.1% respectively, greater value per m³ of battens produced than the Control. The cost of drying between these two log groups and the control is fairly similar; £11.07 m⁻³ and £10.85 m⁻³ for the VelSort and JWCsort groups respectively, compared to £11.85 m⁻³ for the Control. The increase in value relative to the Control is due to an improved pass-rate. This results in the value of structural battens improving to £103.06 and £100.42 for the VelSort and DMOEsort log groups respectively, compared to £94.09 for the Control.

For the JWCsort log group, Table 6.17 shows that despite producing 33.9% fewer structural dimensions (Table 6.3) than the Control group, its overall value is only 2.2% less. This is due the 18% difference in pass-rates (Table 6.12) between the two groups, resulting in a reduction in the cost of kiln drying; this was only £6.77 for the JWCsort group compared to £11.85 for the Control.

The values obtained using the cost-benefit calculator are very sensitive to the input values, *e.g.* the value of non-structural battens, the value of reject battens relative to non-reject battens and the cost of kiln drying. The cost-benefit calculator can be easily adjusted to enter values appropriate for each sawmill. However, using the values assumed here shows that the value of the VelSort and DMOEsort log groups becomes equivalent to the Control group when the pass-rate of the Control falls to approximately 90%. When the pass-rate of the Control falls below this point, the cutting patterns used in VelSort and DMOEsort log groups result in greater value than using conventional sawmill patterns.

6.3.4.3   Actual C18 pass-rates

When calculating the value of 5.9 kN mm⁻² as the minimum threshold batten MOE to achieve a mean batten stiffness of 8.55 kN mm⁻² required for the C18 strength grade, two assumptions were made about the stiffness of the logs *a proiri*:

1. The mean batten global MOE expected of the resource was 8.2 kN mm^{-2}

2. The COV of the global MOE was 22%

However, the mean batten estimated global MOE of the Control group is 7.09 kN mm^{-2}, 13% below the assumed value and approximately 7% below that required for C16. This indicates that the quality of the log population used in this study is below the mean value of the resource. Actual C18 pass-rates for each log group are shown in Table 6.18. Actual pass-rates are calculated by determining the actual proportion of battens that produced a mean batten global MOE of 8.55 kN mm^{-2}.

Table 6.18. Actual C18 pass-rates and pass-rates based on the threshold value of 5.9 kN mm^{-2} for each log group using the estimated global MOE.

Log Group	Actual C18 Pass rate (%)	Pass rate based on a 5.9 kN mm^{-2} threshold (%)
Control	39.7	79.4
VelSort	49.7	93.1
DMOEsort	47.9	92.6
JWCsort	72.6	97.4

Actual pass-rates are less than the threshold based pass-rate for all log groups. The actual pass-rates differ by approximately 40% for the VelSort, DMOEsort and JWCsort log groups. The actual pass-rate for the JWCsort log group differs by 24.8%.

Therefore, even with a 'perfect grader' being able to accurately measure batten stiffness, the threshold on a machine controlled strength grader remains constant while log stiffness can vary.

6.3.4.4   C16 pass-rate

Because the actual pass-rate for C18 was so poor, it was decided to re-examine the data and determine actual C16 pass-rates. Table 6.19 shows the actual C16 pass rate for each log group.

Table 6.19. Actual C16 pass-rate for each log group.

Log Group	C16 Pass rate (%)
Control	73.4
VelSort	94.2
DMOEsort	92.1
JWCsort	100.0

The VelSort and DMOEsort log groups have similar pass rates for C16 to what is currently experienced in sawmills indicating that the average log stiffness of the sample used in this experiment is less than the average of the overall population. The C16 pass-rates for each log group are very similar to the proportion of battens with a mean global MOE greater than 5.9 kN mm^{-2}, the expected threshold for C18.

6.3.5 Effect of cambial age on batten properties

This section examines the effect of cambial age on global MOE, MOR, knots and twist on all 103 mm x 49 mm battens that had undergone detailed testing. Therefore, rather than examining by log group, battens are now being examined by approximate cambial age relative to the juvenile core, *e.g.* less than 10 years (<10), approximately 10 years (10), greater than 10 years (>10) and much greater than 10 years (>>10). These are estimated values based on the proportion of juvenile wood in the top end of each 103 mm x 49 mm batten. The number of battens in each category is shown in Table 6.20.

Table 6.20. Number of battens in each cambial age category.

Cambial Age	No. battens
<10	36
10	31
>10	39
>>10	43

The effect of cambial age on wood properties is shown in Figure 6.12. The dotted lines in Figure 6.12b and c represent the 8.55 kN mm^{-2} mean batten MOE required to meet C18 and the maximum allowed twist for a batten to meet C18 in EN14081-1:2005 (CEN 2005), respectively.
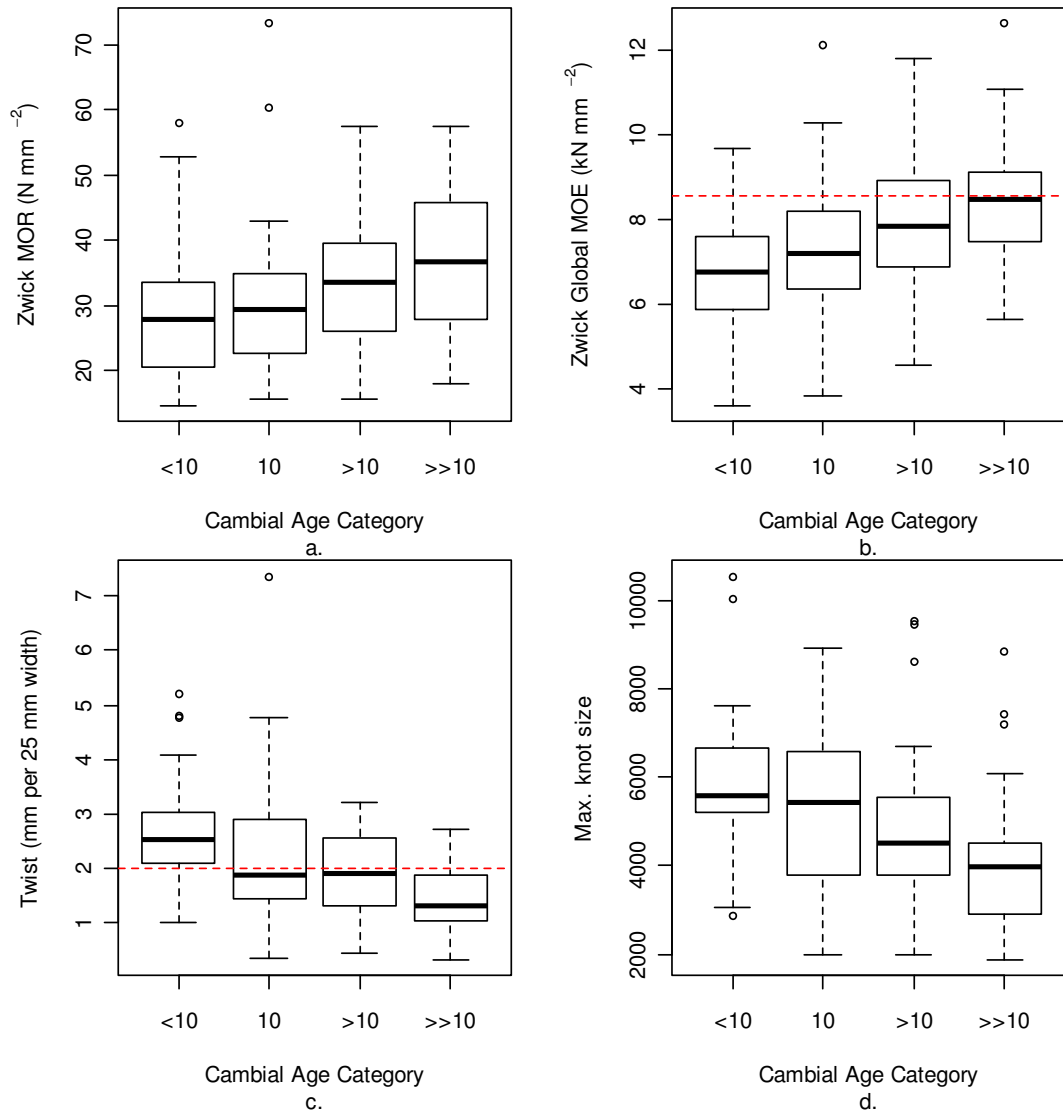
Figure 6.12. The effect of cambial age on (a) MOR, (b) Global MOE. The dotted line represents the average MOE required for C18. (c) Twist (at 12% MC). The dotted line represents the visual override grade limit for strength classes C18 and below. (d) Overall knot severity.

The mean batten properties and statistical significance between each cambial age group are summarised in Table 6.21.

Table 6.21. Summary of the mean MOR, global MOE, twist and maximum knot severity for each cambial age group, <10, 10, >10 and >>10. The values in parenthesis are the standard deviations and the letters shared in common between age groups indicate no significant difference (calculated with ANOVA).

Cambial age group	No. battens	Strength (MOR) (N mm^{-2})	Global static MOE (kN mm^{-2})	Twist (mm per 25 mm width)	Overall knot severity
<10	36	28.4 (10.8)a	6.61 (1.3)a	2.65 (1.0)a	10230 (2988)a
10	31	31.3 (12.3)a	7.36 (1.7)b	2.21 (1.4)ab	9164 (3634)a
>10	39	33.7 (10.7)b	7.98 (1.6)bc	1.92 (0.8)b	7007 (3330)b
>>10	43	37.0 (10.9)bc	8.50 (1.5)c	1.40 (0.6)c	5876 (2205)b

For MOR the general trend was that it increased form pith to bark. In ANOVA, battens >10 and >>10 years had significantly greater MOR than battens <10 years ($p<0.05$ and <0.01 respectively). The mean value for battens <10 years was 28.39 N mm^{-2} with the >10 and >>10 year categories 18.5% and 30% greater, respectively.

For static global MOE and using ANOVA, all other cambial age categories were significantly greater than battens <10 years ($p<0.05$, <0.01 and <0.01 respectively), in other words it increased from pith to bark. The mean value for battens <10 years was 6.61 kN mm^{-2} with the 10, >10 and >>10 year categories 11.2%, 20.7% and 28.6% greater, respectively.

Twist was observed to decrease from pith t bark. In ANOVA, battens >10 and >>10 had significantly less twist than battens <10 years ($p<0.01$ for both). The difference in twist with battens approximately 10 years in cambial age was almost significant with $p=0.069$. The mean value for battens <10 years was 2.65 mm per 25 mm, with the 10, >10 and >>10 year categories 16.2%, 27.3% and 47.2% less, respectively. There was also a significant difference in twist between battens >10 and >>10 years ($p<0.05$) with battens >>10 having 27.1% less twist than battens >10.

The knot severity parameter decreased from pith to bark. In ANOVA, battens >10 and >>10 had a significantly smaller overall knot severity than battens <10 years ($p<0.05$ and <0.01 respectively). The mean value for battens <10 years was 10230, with the >10 and >>10 year categories 31.5% and 42.6% less, respectively

The failure rate for twist by for each age group is shown in Table 6.22.

Table 6.22. Failure rate for twist by cambial age category.

Cambial Age	% of battens that fail C18 visual override for twist
<10	77.8
10	38.7
>10	46.1
>>10	13.9

The failure rate for twist by each age group is shown in Table 6.22. Failure rates are very high and it should be acknowledged that these battens were dried to 12% moisture content compared to current practice of 20%. It is expected, however, that the relative proportions between age groups would remain much the same.

6.4 Discussion

The discussion centres around four main points:

1. The ability of resonant acoustic instruments to measure log stiffness accurately without the inclusion of density.
2. How changes in the average log stiffness affects C16 and C18 pass-rate.
3. The effectiveness of the alternative cutting patterns at producing higher quality battens and increasing value.
4. The effect of alternative cutting patterns on processing logs.

6.4.1 Accuracy of acoustic measurements

Variation in log density is expected to produce a proportional error in the measurement of dynamic MOE if it is unaccounted for (section 2.4). The range of log density in this experiment was 679 kg m^{-3} to 989 kg m^{-3} with a mean of 828 kg m^{-3} (COV=7.1%). The range and COV of log densities measured in this experiment are very similar to that reported in Jones and Emms (2010). Yet while Jones and Emms (2010) found that the inclusion of log density in the calculation of log dynamic MOE improved the prediction of average batten MOE, the inclusion of density here did not result in a significant difference in estimated global MOE. This is despite 6 logs, or 15.9% of the number of logs sorted by log velocity alone, being misclassified. This apparent disparity could be explained by the different methodologies; Jones and Emms (2010) measured the mean batten MOE produced from each log whereas this experiment measured the mean batten MOE of a batch of logs.

It is also worth noting that there was no relationship between log velocity and log green density. As explained in Chapter 4 (section 4.1.2), the dynamic MOE is essentially constant above fibre saturation point when using resonant acoustic instruments. This means that a reduction in density due to reduced moisture content will result in a proportional increase in the velocity to compensate (*e.g.*, Chan *et al*. 2009, Ilic 2001). Therefore, no relationship between log velocity and green density indicates no systematic difference in moisture content between logs.

6.4.2 Effect of log stiffness on yield

The overall yield of C16 from the Control group was only 73.8%, well below the 90% currently expected from the resource. This indicates that the stiffness of the sample of logs used in this study was less than the overall average. Moore *et al*. (in press) achieved a C16 optimum pass rate of 97.7% after taking 301 logs from 120 Sitka spruce trees from 12 sites around Scotland and northern England. The overall log velocity^2 across the 12 sites in Moore *et al*. (in press) was 11.54 km^2 s^{-2}, or simply a velocity of 3.4 km s^{-1}. The overall log velocity^2 for the Control log group was 10.77 km^2 s^{-2}, or simply a velocity of 3.28 km s^{-1}.

The log velocity^2 from just the medium stiffness logs in this experiment was 11.42 km^2 s^{-2}, almost identical to that in Moore *et al.* (2011). The corresponding yield of C16 for the medium stiffness logs was almost identical too, with 97% of battens passing (using an optimum grader). If just the low stiffness logs from the Control group are examined, the mean log velocity^2 was 9.62 with a C16 yield of just 30.7%. These four values of log velocity^2 were plotted against C16 yield and shown in Figure 6.13.
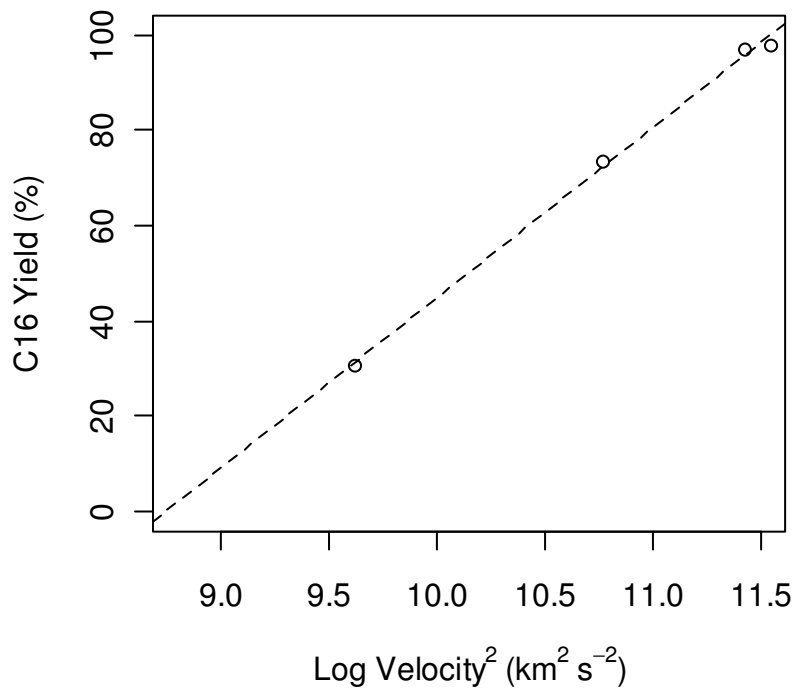
Figure 6.13. Relationship between log velocity^2 and C16 yield.

The linear regression equation for the relationship between log velocity^2 and C16 yield is given by:

$$\text{C16 Yield} = 35.7 \times \text{Log velocity}^2 - 312$$

Figure 6.13 shows that the optimum C16 yield will drop below 90% when the log velocity^2 drops below 11.26 km^2 s^{-2}. This corresponds to a 10% drop in pass-rate for a 2.46% drop in log velocity^2.

There are very few data points in Figure 6.13 yet this empirical result can be confirmed mathematically by examining the proportion of battens which pass C16 with a falling population mean batten MOE, shown in Figure 6.14. Optimum pass-rates in Figure 6.14 were calculated assuming an optimum grader and a normal distribution of batten MOE with a COV = 22%.
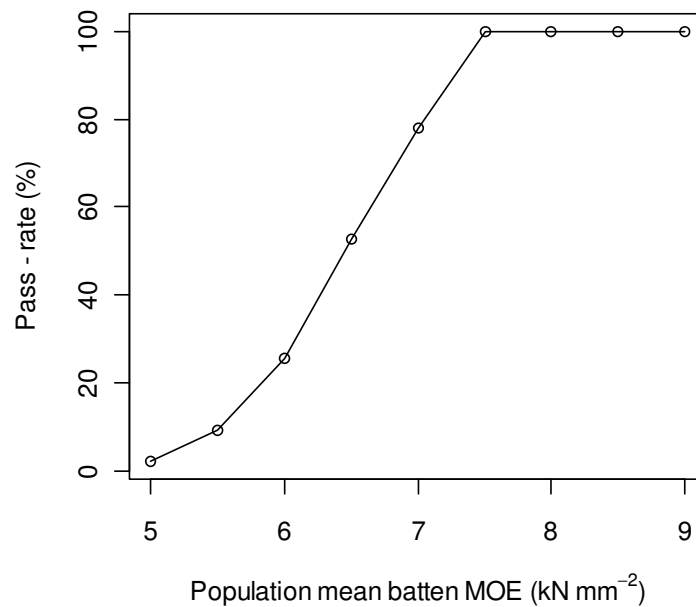
Figure 6.14. C16 pass-rate of battens with falling population mean MOE.

This would indicate that there is little room to manoeuver, in terms of log stiffness, before correctly graded pass rates fall dramatically and is of particular concern given that the quality of the resource is perceived to be in decline (Macdonald and Hubert 2002). Should the quality of the resource drop to levels seen in this experiment, implementation of the alternative cutting patterns used in the log groups segregated with resonance velocity or dynamic modulus log groups would provide an effective means of raising the pass rate above 90%.

However, the actual pass-rates in a sawmill will not drop as dramatically as shown in Figure 6.14, due to the machine grade threshold setting remaining constant despite a change in the population mean, as illustrated in section 6.3.4.3. It is very important to note that pass-rates will remain artificially high due to this

effect and the mean batten MOE of structural battens produced will be below that required by the standards (*e.g.* EN384 CEN 2010, EN14081:1 CEN 2005, EN338 CEN 2003).

Cutting patterns applied to log groups segregated with resonance velocity or dynamic modulus were meant to represent a pragmatic solution for sawmillers; balancing up potential loss in volume recovery and a reduced proportion of structural dimensions with alternative cutting patterns against an improved pass rate at the stress grader. Indeed, whilst approximately 5% less log volume was converted to structural dimensions using these patterns, there was no loss in overall volume recovery from a log and a 4% to 6% improvement in the proportion of a log that met the stiffness requirement for C16.

This is a far more efficient approach for sawmilling low stiffness logs and is reflected in the results from the cost simulation in section 6.3.4. The model used is very simple and the input parameters are entirely estimations, so it needs to be adjusted to current market values. The cost simulation has been presented in a way such that processors can recreate it and input their own values. However, if the current parameters can be considered representative, using the alternative cutting patterns for the log groups segregated with resonance velocity or dynamic modulus will result in an improved value per cubic metre of between 7.3% and 6.1%, respectively.

6.4.3 Effectiveness of alternative cutting patterns to improve batten quality

The improvement in all batten properties due to alternative cutting patterns can be explained by the effect of increasing the mean cambial age of the batten. Whilst the calculation of the low stiffness core did not achieve its aim of creating a minimum batten MOE of 5.9 kN mm^{-2}, the average batten MOE for the low stiffness logs segregated with resonance velocity or dynamic modulus resulted in a 12.1% and 10.8% improvement in stiffness respectively, over the Control log group. Table 6.12 shows that the vast majority of battens falling below this threshold for these log groups were produced from the low stiffness logs,

indicating that the assumptions used in the calculation of the low stiffness core were not conservative enough.

Despite the target minimum MOE not being reached, this experiment showed that a significant improvement in batten stiffness could be achieved as soon as production of structural dimensions was shifted slightly outside the centre of the log. Cutting patterns need to be further adjusted to exclude more of the centre of the log from producing structural battens to reach the desired threshold of 5.9 kN mm^{-2}.

Significant improvements in the other wood properties of interest were not achieved until the estimated mean cambial age of the batten was greater than 10 years. For distortion, Donaldson (1996 in Huang *et al.* 2003, Figure 6) reported a similar effect; showing that the 'warp prone zone' was larger than the very low stiffness zone at the centre of the log. The results reported here do somewhat contradict the findings of Johansson *et al.* (2001) who showed that twist was most strongly correlated with ring curvature (not juvenile wood) and spiral grain angle, stating that the easiest way to avoid twist was to avoid cutting structural dimensions from a 75 mm x 75 mm box around the pith. Cown *et al.* (1996) also showed that increasing log size (*i.e.* effectively reducing ring curvature) was the single most important factor explaining twist with spiral grain in the juvenile core also significant. Cown *et al.* (1996) acknowledged the difficulty of trying to separate the relative contributions of the proportion of juvenile wood and log size (as the two are strongly correlated), yet concluded that size does have an effect independent of the proportion of juvenile wood.

Whilst not measured in this experiment, it can be qualitatively stated that the first ten growth rings were definitely not contained within a 75 mm x 75 mm box around the pith for any of the logs in this experiment. The medium stiffness logs in the JWCsort log group avoided cutting from the region and found no significant difference in twist compared to typical sawmill cutting patterns. It was shown that cambial age (or proportion of juvenile wood) was by far the most significant factor in determining the magnitude of twist. The reject rate for twist on battens consisting entirely of juvenile wood (<10 years) is 77.8% and the

reject rate for battens consisting entirely of mature wood (>>10 years) was 13.9%. Even accounting for the effect of the drying practice employed in this experiment, this is very large difference.

The implication these findings have for processors is that the same variation in forest management practices that may be leading to a general decline in average log stiffness will most likely affect the same wood properties that increase twist, *i.e.* larger juvenile core. Therefore it is possible that reject rates due to twist will rise concurrently with reject rates due to low stiffness. Importantly however, given the results in this experiment, while it appears possible to make marginal adjustment to cutting patterns on logs of low average stiffness to improve overall batten stiffness, this has no significant effect on reducing twist.

For knots; the reduction in overall knot severity measured with the GOLDENEYE x-ray grader, with increasing cambial age was somewhat surprising. It was expected that battens from nearer the bark would have larger knots as branch size increases in a conical fashion with increased distance from the pith. It is probably due to a number of factors:

- The knot detection method was x-ray attenuation which measures wood density. The method does not distinguish between individual knots and knot clusters. Therefore we can state that knot clusters are more critical for the x-ray grading machine than the maximum knot size near the bark for Sitka spruce logs 220 mm to 320 mm in diameter.
- Although not measured explicitly, qualitatively there were a larger proportion of dead, or bark encased, knots on battens with a mean cambial age greater than 10. This is due to branches that are dead but not yet been self pruned. This is common under current silvicultural treatments (Achim *et al*. 2006).

6.4.4 Effect of alternative patterns on sawmill processing

The consequence to sawmill processing due to the implementation of any alternative cutting pattern would be to shift the production of structural dimensions away from the centre cant to the edge of the log. This will result in an increase in the number of structural battens produced at the edger (Figure 6.6). However, the actual total number of battens processed at the edger, both structural and non structural, with alternative patterns is not too dissimilar from typical patterns although some extra capacity at the edger may be required.

The main effect of the alternative cutting patterns on the sawmill process is to reduce the number of structural battens per volume of log, resulting in significant volumes of both structural and non structural dimensions being produced concurrently. This is different to the current batching process of producing structural or non structural and would require further modelling before implementation so that cutting schedules could be timed accurately. However, the cost simulation does show that alternative patterns will provide more value when pass-rates begin to fall.

6.5 Conclusions

Despite the misclassification of 15.9% of logs in the logs sorted by only using the MOE calculated from log velocity^2, there appeared to be no detrimental effect on the resulting mean batten stiffness. Results are not directly comparable to other studies which included density in the calculation as they matched each log with the mean batten stiffness from that log. This experiment only considered the mean batten stiffness from a batch of logs, so a lot of the resolution was lost.

It was estimated from the data that yield of C16 timber (maintaining grade properties) will decline steeply with a drop in average log stiffness when using conventional cutting patterns; for a 2.46% drop in log velocity^2 there is a 10% drop in C16 pass rate. Actual pass-rates will not fall as steeply due to the

machine grader threshold remaining unchanged with the variation in stiffness of the population. This is a consequence of machine control settings.

The alternative cutting patterns described in this experiment do offer a more profitable alternative to existing patterns if log stiffness drops to the levels seen in the sample population for this experiment. The effect of producing less volume of structural battens is mitigated by the much higher pass rate to either C16 or C18. However, these practical alternatives were aimed to increase the mean stiffness only. Analysis of average rates of twist show that it is little affected by changes in cutting pattern unless structural dimensions are not produced in the first 10 growth rings. This is of concern as the change in forest management practices and its effect on wood properties that are expected to drive the reduction in stiffness over the next 20 years though increasing the ratio of juvenile wood will probably also increase the proportion of twist. Therefore, if the average stiffness of the resource drops, then the degree of twist in battens is also likely to increase. Cutting patterns which only aim to raise stiffness a slight amount may not reduce the level of distortion in battens. This aspect needs further research.

7   Summary

7.1 Introduction

This thesis consists of two main themes:

1. Finding the range of error for using acoustic instruments on UK Sitka spruce with the assumption of constant density.
2. The ability of alternative cutting patterns to improve batten quality and value by accounting for the within-log variation in stiffness as well as the between-log variation in stiffness measured with acoustics.

There were 10 sites examined from mature stands around Scotland to determine variation in outerwood and whole tree density. Additionally, 155 logs were used in a sawmill simulation experiment to examine the effect of alternative cutting patterns.

7.2 Experimental review

The seasonal examination of the green density of wood near the bark did not use the same trees for summer and winter as it was feared that after taking a core in summer, any subsequent measurements would affected. Therefore seasonal variation in moisture content could only be examined using site averages. In one site, this procedure produced an inexplicably small change in velocity for a very large change in mean density. This most likely indicates that the range of densities was not adequately represented by the trees measured in summer. Also, only two seasons were examined; summer and winter, so it is unknown how the density changes throughout the year.

For stress wave path experiment, the wave propagation was only examined over a short distance, typical of what would be used in a standing tree TOF measurement. This resulted in an increased understanding of how the stress

wave spreads within the greatest area of interest. However it was not directly comparable with the two other major studies in this field, as it did not cover the same propagation lengths.

For the cutting pattern study, the battens produced were not traced back to the log they came from but rather only to their stiffness group. This allowed the examination of the effect of segregation technique on the corresponding batten properties but did not allow a direct comparison with two other studies which examined the effect of including density on the accuracy of acoustic sorting. By only tracing logs back to their stiffness groups, a significant amount of resolution was lost. As a result the full effects of misclassification can not be discussed fully. Also, the sample of battens taken away for detailed testing was not representative of the population. Further samples were required to conclusively determine the effect of cutting patterns on twist, knot severity and MOE. Twist should also be measured at 20% so that reject rates can be directly related to values expected in a sawmill.

7.3 Summary of results

7.3.1 Effect of season on standing tree acoustic measurements

There was shown to be considerable effect of season on standing tree acoustic measurements, with up to a 28.7% increase in velocity^2 for one site when sampling in winter. However, the change in velocity with season was not consistent, with another site showing a 5.1% decrease in velocity^2 from summer to winter. Examining the change in density from summer to winter at each site did not explain the change in acoustic speed. It is expected that freezing temperatures forming ice in the stem complicate the relationship between acoustic speed and density. Further, it is unknown whether the green density profiles obtained from wood near the bark in winter were normal or a result of desiccation brought on by abnormally cold weather.

7.3.2 Relationship between standing tree and log velocity

The relationship obtained between standing tree and log velocity in this thesis was quite poor compared to other studies. However, this thesis did target the extremes in growth rate at both a site and within-site level in order to amplify possible effects observed in Raymond *et al*. (2008). The study by Raymond *et al*. (2008) concluded that properties of wood near the bark are very poor predictors of whole tree or log properties in unthinned stands as the growth in the outer rings has been restricted by within-site competition. The dataset in this thesis was quite small though, so firm conclusions are impossible to make. Nonetheless it would appear that dominance class and thinning regime may affect accuracy of standing tree instruments. In fact, results suggest that using live crown ratio to estimate stiffness is just as accurate as standing tree velocity and slenderness is more accurate than both. The accuracy of standing tree tools appear to be affected by silviculture and differences in growth rate. This led to the formation of a number of assumptions implicit in their use that are required for accurate measurements. These are:

- Consistent relationship between outerwood stiffness and juvenile wood stiffness.
- Consistent ratio of mature wood to juvenile wood.
- Consistent ratio of heartwood to sapwood, *i.e*. tree density.

Overall, it would appear that tree level indicators such as slenderness and live crown ratio can estimate the stiffness of a tree either just as accurately, or even more accurately than standing tree velocity.

7.3.3 Variation in green density and the proportion of juvenile wood at breast height

The green density of wood in the outer part of the tree varies considerably both between and within dominance classes. On average however, suppressed trees have a 10.2% lower density than co-dominant trees over the first 60 mm in from

the bark. Dominant trees have a mean density 8.8% higher than co-dominant trees over the same range.

The variation in green disc density depended both on dominance class and height in the tree. Co-dominant trees had, on average, approximately 7% greater green density than suppressed and dominant trees. All dominance classes showed a consistent increase in green density with an increase in height.

The proportion of juvenile wood at breast height is greater in suppressed than either dominant or co-dominant trees. However, the dynamic stiffness of suppressed trees was greater than dominant trees which contained the lowest proportion of juvenile wood.

7.3.4 Stress wave propagation in standing trees

The extent of the radial and tangential propagation of a stress wave in a simulated standing tree TOF measurement showed that there is likely to be a complex interaction with density variation in the tree which will affect wave speed. The size of this quasi-plane wave was not consistent between test specimens, indicating that individual material properties will control this aspect. Also, it is unknown how boundary interactions affect the speed of the wave; there are two wave propagation behaviours that are clearly explained by theory, that of dilatational and plane waves and it would seem that in a normal standing tree test neither can explain the behaviour adequately. Dilatational waves appear to only exist for very short propagation distances in standing trees, while plane waves only form well outside the normal propagation distance for a standing tree TOF measurement.

7.3.5 Cutting pattern study

Alternative cutting patterns showed great ability to improve the mean MOE of resulting battens over standard sawmill patterns. The degree of improvement depended on the proportion of the juvenile core that was excluded from producing structural battens. Excluding the first ten growth rings from producing

structural dimensions showed an ability to reduce the overall knot severity measured by an x-ray grading machine and reduce twist. However, this resulted in a much reduced conversion rate into structural dimensions.

A pragmatic option for sawmills was also tested, which aimed at balancing the requirement for high yields of structural timber and increasing the mean MOE of battens. The target of this option was to increase the minimum global MOE of a batten above a minimum threshold of 5.9 kN mm^{-2} by assuming some basic properties about the distribution of stiffness within a log prior to cutting. This solution successfully managed to raise the mean batten MOE above that of sawmill cutting patterns, yet showed a non-significant difference in reducing knot severity or twist. However, this option was not conservative enough in its estimation of the extent of the low stiffness material within a log and produced a number of battens that fell below the target. Therefore, the assumptions used to estimate the size of the low stiffness area need to be revisited. Despite this, analysing the potential financial benefit of this option showed that its value exceeded that of standard sawmill patterns when the pass-rate of battens drops below 90%.

Examining batten properties by its age relative to the juvenile core showed that all properties relevant to structural timber improved with increasing cambial age.

7.4 General discussion

7.4.1 Accuracy of acoustic instruments

The majority of this thesis was devoted to determining the possible causes of error for stress wave instruments used to measure the stiffness of trees and logs. Chapter 3 determined a set of assumptions that were implicitly required for an accurate relationship between standing tree and log acoustics. Some of these assumptions were subsequently examined in Chapter 4 and considerable discrepancy was found between observed results and the assumptions. Firstly, a consistent ratio between mature and juvenile wood is required. The proportion of juvenile wood at breast height was found to be dependent on age at breast

height and dominance class, with suppressed trees containing approximately 6.6% greater proportion than dominant or co-dominant trees. Secondly, the assumption of constant, uniform density was also examined, both in logs and in the wood nearest the bark in standing trees. The density of freshly felled Sitka spruce logs across ten geographical locations around Scotland had a mean of 810 kg m^{-3} (COV=11.2%) with an overall range of 610 kg m^{-3} to 1064 kg m^{-3}. This range is greater than that seen in the log population used in the cutting pattern experiment; 679 kg m^{-3} to 989 kg m^{-3} with a mean of 828 kg m^{-3} (COV=7.1%). This indicates the possible effects of drawing logs from a reduced geographical region and normalization of density due to the delay between harvesting and processing. The overall variation in log density suggests that considerable improvement in the prediction of log stiffness could be made with its inclusion.

There is very little literature discussing the implications of variation in green log density on acoustic measurements. Achim *et al*. (2009) states that the relationship between the static MOE of battens and the dynamic MOE of logs could be improved from R^2 = 0.41 to R^2 = 0.69 with the inclusion of log density for white spruce. The trees in this study were approximately 73 years old and came from a thinning trial which produced stands of a wide range of basal areas; from control through 18 m^2 ha^{-1}, 25 m^2 ha^{-1}, 32 m^2 ha^{-1}. This combination of age and stocking would result in a very broad range of HW/SW ratios and therefore significant differences in log density. Wang *et al.* (2003, 2004) reports green density for a number of species; jack pine, red pine, Douglas-fir and ponderosa pine, with density that ranges from -29% to +32.3%, -9.4% to +7.1%, -15.2% to +18.2% and -16.9% to +10.8% for each species respectively. There was no discussion in Wang *et al.* (2003, 2004) on the implications of using velocity^2 only.

Due to the relatively young harvest age, the assumption of constant density in green logs is routinely used in papers from Australia and New Zealand (*e.g*., Tseheye *et al*. 2000, Matheson *et al*. 2002, Dickson *et al*. 2004). However, Jones and Emms (2010) showed that the inclusion of log density in the calculation of dynamic MOE provided a significant improvement in the prediction of kiln dried batten MOE measured by a machine stress grader; R^2 improved from 0.49 to

0.68. This study was conducted on the second and third logs in the stem and interestingly showed that the HW varied from 11% to 60% with a mean of 20%, resulting in a green log density variation between 695kg m^{-3} and 1012 kg m^{-3} with a mean of 913 kg m^{-3}. The magnitude of this improvement is similar to that seen in Achim *et al*. (2009), despite the obvious differences in age of trees. Overall, it would appear that HW variation is significant in mature trees for many species of harvest age green density should be accounted for in the calculation of log MOE. This was not observed in the cutting pattern experiment as battens were not traced back to each log, yet both Achim *et al*. (2009) and Jones and Emms (2010) showed the scale of the possible improvement.

The variation in the density of wood nearest the bark was also examined to determine its effect on the assumption of constant density when using standing tree acoustic instruments. The mean density between dominance classes was found to vary considerably from about 20 mm in from the bark onward toward the pith. Additionally, the variation at each successive location within each dominance class was very large in the transition zone between sapwood and heartwood. This indicates that it is not possible to simply apply an adjustment on density by dominance class as the variation within each dominance class is also large. Therefore using standing tree instruments on British spruce will result in stress waves passing through regions of variable density, resulting in a reduced accuracy.

It was not possible to examine the true effect of the variation in density without understanding the path/trajectory of the stress wave within the TOF test span. Chapter 5 examined the stress wave propagation in a representative suppressed, co-dominant and dominant tree. From these results, it is possible to speculate on how the maximum wave speed in the medium and large billets was larger than the dilatational wave speed. This is achieved by examining the size of the quasi-plane wave and viewing it in parallel with the moisture content profiles of the wood nearest the bark in Chapter 4. The moisture content in the co-dominant and dominant stems of UK Sitka spruce trees begin to decrease rapidly from about 40 mm in from the bark. The wave expansion measured in this experiment was 64 mm and 90 mm for the co-dominant and dominant billets respectively,

placing it well into the lower density region. Wang and Chaung (2000) have shown how velocity increases with decreasing moisture content. Therefore a wave expanding into material with similar mechanical properties (*i.e.* mature wood) with less density, will travel faster than a wave still confined to the outer parts of the billet, which are higher in density.

Whilst the radial density variation was able to explain the increase in wave speed for the medium and large billets, it was unable to account for the 33% drop in wave speed for the small billet. This result is inconsistent when viewed in conjunction with the typical density profile of a suppressed tree; suppressed trees show a much faster transition to low density heartwood when moving in from the bark. Therefore, it was expected that the wave speed would increase for suppressed trees as well, as the size of the quasi-plane wave increased. However, the reason for this change in wave speed can be explained by the interaction of the stress wave with the boundaries of the billet. Section 2.3 outlines some general theory behind dilatational wave propagation and explains that dilatational waves can only exist in an infinite, three-dimensional solid, *i.e.* where the medium is much larger than the wave front such that there are no boundary interactions. Inspection of the propagation pattern for the small billet clearly shows a large portion of the circumference interacting with the quasi-plane wave, indicating that boundary interactions are occurring and that the wave is no longer dilatational.

Consequently, the results presented in Chapter 5 suggest that inaccuracy of TOF instruments could be due to the summation of errors from:
- The assumption of constant density when there may be a complex interaction of the wave with density variation in the tree.
- Variation in grain angle affecting the location of the fastest TOF arrival time relative to the placement of the sensor.
- Unknown effects of boundary conditions on the stress wave speed.

Therefore, the following questions remain:

- Do the differences in mechanical properties, growth properties and boundary conditions between trees cause variation in wave propagation?
- How does the radial variation in density interact with the stress wave?

A quantitative analysis of wave propagation in trees was not permitted given the time constraints, however it is of great necessity than one is developed to gain a full understanding of the causes of error with this technique. The 'elliptical model' of wave propagation presented in Chapter 5 is a generalisation only as it does not account for any of the possible causes of variation presented here.

This discussion is not to suggest that standing tree acoustic instruments do not work all of the time; some excellent correlations with resonant log velocity and wood stiffness have been obtained elsewhere, *e.g.* Wang *et al*. 2001, Grabianowski and Walker 2006, Mora *et al*. 2009. However, papers by Raymond *et al*. (2008), Moore *et al*. (2009) and the results from Chapter 3 of this thesis would suggest that variations in silviculture and environment between stands adversely affect the accuracy of these instruments. This may therefore affect the potential uses of these instruments, *e.g.* to compare silvicultural treatments, different age stands and different dominance classes within an even age stand. Therefore, as Zhang *et al*. (2011) states: "One of the key issues is to fully understand the stress wave behaviour in standing trees so that measured stress wave parameters can be correctly interpreted and wood properties of the trees can be predicted with a high accuracy".

7.4.2 Alternative cutting patterns and batten quality

The second major component of this thesis was the examination of how alternative cutting patterns can improve the quality of battens and the profitability of processors. The results show that pragmatic cutting patterns designed to maximise the yield of structural battens whilst accounting for the low stiffness area at the centre of the log significantly increased the mean stiffness of battens over typical sawmill cutting patterns. However, these patterns showed no

significant effect in reducing twist, a major cause for downgrade in sawmills. Twist was significantly reduced when battens were extracted from outside the juvenile core, which in this case, was defined as the first ten growth rings. This is consistent with results in radiata pine in Donaldson (1996 in Huang *et al*. 2003), which showed that the low stiffness zone within a log is smaller that the area prone to distortion.

The effect of excluding the juvenile core from producing structural dimensions on sawmill production was to reduce the yield of structural battens from 45% of log volume for conventional sawmill patterns to 15%. The net effect of forest practices on the quality of the resource outlined in section 2.1, has been to increase the proportion of the juvenile core. Therefore, avoiding the juvenile wood completely will most likely reduce the yield of structural battens even further.

If the failure rate due to twist does increase with the decline in resource quality, avoiding juvenile wood for producing structural dimensions is not a practical solution for reducing its occurrence. The quality of the juvenile core can change between trees. Suppressed trees have the greatest proportion of juvenile wood, yet they are also the trees that have the highest log velocity[2] and slenderness (section 3.4.2). Watt *et al*. (2006) and Lassere *et al*. (2009) both describe how slenderness can improve the stiffness of the juvenile wood material and Cameron *et al*. (2005) showed that the microfibril angle of slower grown trees was consistently lower than for fast grown trees, even in the first ten years. Further work is required to determine the region within a log that will produce battens prone to twist, *i.e.* instead of calculating a low stiffness core as in Chapter 6, the size of a 'high twist' core needs to be calculated instead. Johansson *et al*. (2001) found that approximately 70% twist was explained by a combination of ring curvature (50%) and spiral grain (20%) in Norway spruce. The authors calculated that a 75 mm x 75 mm box around the pith should be avoided to reduce twist. This was trialled on one group of logs and did not produce a significant change in twist relative to sawmill patterns, indicating that this exclusion zone does not work for British spruce. This is most likely because the juvenile wood zone in the UK is larger.

In any case, applying an arbitrary exclusion zone is unlikely to be efficient; either producing too much distorted material or converting too much of a log into non-structural product. A working model to predict the size of the 'high twist' core on a dynamic basis using parameters measureable in a sawmill environment is required.

7.5 Further work

1. A full seasonal audit of the variation in outerwood density is required to determine the full error range for standing tree TOF measurements due to this effect.

2. A thorough examination of the ability of slenderness and live crown ratio to measure stiffness in UK Sitka spruce as per Watt *et al.* (2006) and Lassere *et al.* (2009). Establishing whether the relationship observed here is consistent will give researchers, foresters and industry another (possibly more accurate) method to determine stiffness of standing trees.

3. The dynamic stiffness of suppressed trees is greater than for dominant or co-dominant trees, yet it contains the largest proportion of juvenile wood. It needs to be established whether the juvenile wood in suppressed trees is of sufficiently superior quality to produce structural timber with adequate stiffness and dimensional stability. Knowing this could help reduce the proportion of the log from a suppressed tree that needs to be avoided, thereby increasing the yield of structural dimensions.

4. The relationship of tree stiffness with slenderness and live crown ratio should be examined further to confirm whether they are superior to standing tree instruments.

5. The occurrence of compression wood is likely to be a confounding effect on all measurement methods and needs to be investigated further.

6. The proportion of UK Sitka spruce logs whose density varies by more than 5% from the overall mean is large. It needs to be established whether this variation has a significant effect on the utility of acoustic velocity on logs using resonant instruments. Achim *et al.* (2009) and

Jones and Emms (2010) have both shown that including density improves the ability to predict mean batten stiffness, yet no practical improvement was seen with its inclusion in the cutting pattern experiment reported here.

7. A fundamental understanding of the behaviour of stress waves in a standing tree TOF measurement is required so that measured values can be correctly interpreted. This will improve the accuracy of the technique and potentially uncover new applications. A vast amount of work exists in the field of the dynamic behaviour of materials outside the wood science literature. Some of the experimental techniques and theory can be readily adapted to wood. For example:

   a. Baker and Dove (1962) studied the wave behaviour in plastic bars with strain gauges placed at various lengths from the point of stress wave initiation to determine how quickly the wavefront spread over the entire cross section. This could be adapted for small wood samples of various stiffness and moisture contents to build a model of how a stress wave will propagate through a tree.

   b. Berryman (1999) explains the influencing material properties affecting the transmission of stress waves in porous rock at various levels of saturation. Rather than explaining that the effect of water wave speed as the proportion that vibrates in phase with the passing wave, it is explained in terms of pore size and permeability. These properties also exist in wood and an investigation is required to determine its applicability here.

8. The prediction extent of the low stiffness core using simple assumptions about the distribution of stiffness within a log listed in Chapter 6, underestimated its size. Further work is required to refine these assumptions to determine if the size of the low stiffness core can be accurately measured based on a single measure of dynamic log stiffness without knowing the variation in growth rate within a log. This is essential for the refinement and efficient implementation of alternative cutting patterns, such that optimal pass-rates can be maximised while minimising its effect on the conversion rate of a log into structural battens.

9. If twist is a greater cause of batten failure than stiffness, a model is
    required that can predict the size of the area within a log that is most
    likely to produce battens that will distort.

7.6 Concluding remarks

This thesis has shown that there is considerable variation in density, both in the
outer part of a tree and between whole logs which will affect the accuracy of the
stiffness measurement obtained from acoustic velocity. The poorly understood
behaviour of stress waves in standing trees may result in additional errors due to
the unknown extent to which density variation effects wave speed and
interactions of the wave with boundaries. As a result, standing tree acoustic
instruments should be treated with caution when used in British spruce.

The implementation of resonance based acoustic instruments within a sawmill
simulation to segregate low stiffness logs to be processed with alternative cutting
patterns showed a definite ability to add value by improving mean batten MOE.
Significant improvements in knot and twist measurements were not observed
until the mean cambial age of battens was greater than ten years.

References

Achim, A., Carter, P. 2005. Assessing the potential of acoustic tools to predict wood stiffness in Sitka spruce. Forest Research report, Forestry Commission, UK, 7pp.

Achim, A., Gardiner, B., Leban, J-M., DaQuitaine, R. 2006. Predicting the branching properties of Sitka spruce in Great Britain. New Zealand Journal of Forestry Science 36: 246–264

Achim, A., Paradis, N., Salenikovich, A., Power, H. 2009. Using acoustic tools to improve the efficiency of the forestry wood chain in eastern Canada. The Future of Quality Control for Wood & Wood Products', 4-7th May 2010, Edinburgh. The Final Conference of COST Action E53.

Akima, H. Interpolation of irregularly spaced data. R port by Albrecht Gebhardt aspline function by Thomas Petzoldt <petzoldt@rcs.urz.tu-dresden.de> enhancements and corrections by Martin Maechler, 2009.

Andrews, M. 2002. Wood quality measurement – son et lumiere. New Zealand Journal of Forestry.

Andrews, M. 2003. Which acoustic speed? Pages 159–165 in Proc. 13th International Symposium on Nondestructive Testing of Wood, August 19–21, 2002, Berkeley, CA.

Auty, D., Achim, A. 2008. The relationship between standing tree acoustic assessment and timber quality in Scots pine and the practical implications for assessing timber quality from naturally regenerated stands. Forestry. 81: 475:487.

Auty, D., Weiskittel, A. R., Achim, A., Moore, J. R., Gardiner, B. A. 2012. Influence of early re-spacing on Sitka spruce branch structure. Annals of Forest Science. 69: 93-104.

Baker, W. E., Dove, R. C. 1962. Measurement of internal strains in a bar subject to a longitudinal impact. Experimental Mechanics. 2: 307-311.

Beauchamp, K. 2011. The Biology of Heartwood Formation in Sitka Spruce and Scots Pine. PhD Thesis, School of Geosciences, University of Edinburgh.

Berryman, J. G. 1999. Origin of Gassman's equations. Stanford Exploration Project, Report. 102: 187–192

Brazier, J. D., Mobbs, I . D. 1993. The influence of planting distance on structural wood yields of unthinned Sitka spruce. Forestry. 66: 333-352.

Brüchert, F., Gardiner, B. 2006. The effect of wind exposure on the tree aerial architecture and biomechanics of Sitka spruce (*Picea sitchensis, Pinaceae*). American Journal of Botany 93: 1512–1521.

Bucur, V. 2006. Acoustics of Wood. Springer – Verlag, Berlin, Germany. 393 pp.

Bucur, V., Berndt, H. 2001. Ultrasonic Energy Flux Deviation and Off-Diagonal Elastic Constants of Wood. IEEE Ultrasonics Symposium, 697.

Burdon, R.D., Kibblewhite, R.P., Walker, J.C.F., Megraw, R.A., Evans, R., and Cown, D.J. 2004. Juvenile versus mature wood: a new concept, orthogonal to corewood versus outerwood, with special reference to *Pinus radiata and Pinus taeda*. Forest Science. 50: 399–415.

Cameron, A. D. 2002. Importance of early selective thinning on the development of long-term stand stability and improved log quality: a review. Forestry 75: 25-35.

Cameron, A. D., Lee, S. J., Livingston, A. K., Petty, J. A. 2005. Influence of selective breeding on the development of juvenile wood in Sitka spruce. Canadian Journal of Forest Research. 35: 2951-2960.

CEN, 2003b. Structural timber—Strength classes. EN338:2003. European Committee for Standardisation, Brussels. 14 p.

CEN, 2003a. Timber structures – Structural timber and glued laminated timber – Determination of some physical and mechanical properties. EN408:2003. European Committee for Standardization, Brussels. 13 p.

CEN, 2005. Timber structures - Strength graded structural timber with rectangular cross section. Part 1: General Requirements. EN 14081-1:2005. European Committee for Standardization, Brussels, 30 p.

CEN, 2010. Structural timber – determination of characteristic values of mechanical properties and density. EN 384:2010. European Committee for Standardization, Brussels. 19 p.

Chalk, L., Bigg, J. M. 1956. The distribution of moisture in the living stem in Sitka spruce and Douglas fir. Forestry, 29: 6-21

Chan, J. M. 2007. Moisture content in radiata pine wood: Implications for wood Quality and water-stress response. PhD thesis, School of Forestry, University of Canterbury, NZ.

Chan, J. M., Walker, J. S., Raymond, C. A. 2009. Effects of moisture content and temperature on acoustic velocity and dynamic MOE of radiata pine sapwood boards. Wood Science and Technology. 45: 609-626.

Chauhan, S. S., Entwhistle, K.M., Walker, J.C.F. 2005. Differences in acoustic velocity by resonance and transit time methods in an anisotropic laminated wood medium. Holzforschung. 59: 428-434.

Chauhan, S. S., Walker, J. C. F. 2006. Variations in acoustic velocity and density with age, and their interrelationships in radiata pine. Forest Ecology and Management. 229: 388–394.

Cown, D. J. 1992. New Zealand pine and Douglas-fir: suitability for processing. Bulletin 216, Forest Research, Rotorua, New Zealand. 72 p.

Cown, D. J., Hasslet, A. N., Kimberly, M. O., McConchie, D. L. 1996. The influence of wood quality on lumber drying distortion. Annales des Sciences Forestierer. 53: 1177-1188.

Crawley, M. J. 2007. The R Book. John Wiley and Sons Ltd, London. 942 pp.

Cremer, L., Heckl, M. & Petersson, B. A. T. 2005 Structure borne sound: structural vibrations and sound radiation at audio frequencies. Berlin, Germany: Springer. 607 pp.

DeBell, J.D., Lachenbruch, B., 2009. Heartwood/sapwood variation of western redcedar as influenced by cultural treatments and position in tree. Forest Ecology and Management. 258: 2026-2032.

Dickson, R. J., Joe, B., Harris, P., Holtorf, F., Wilkinson, C. 2004. Acoustic segregation of Australian-grown *Pinus radiata* logs for structural board production. The Journal of the Institute of Foresters of Australia. 67: 261-266.

Dinwoodie, J. M. 2000. Timber: its nature and behaviour. 2nd Edition. E & FN Spon, London. 257 pp.

Evans , R. and Ilic , J. 2001 Rapid prediction of wood stiffness from density and microfibril angle . Forest Products Journal. 51: 53-57.

Fonweban, J., Mavrou, I., Gardiner, B., MacDonald, E. In press. Modelling the effect of spacing and site exposure on spiral grain angle on Sitka spruce *(Picea sitchensis* (Bong.) Carr.) in Northern Britain.

Forestry Commission. 2010. Forestry statistics 2010 – a compendium of statistics about woodland, forestry and primary wood processing in the United Kingdom. 150 p. Available at: www.forestry.gov.uk/statistics.

Gjerdrum, P., 2003. Heartwood in relation to age and growth rate in Pinus sylvestris L. in Scandinavia. Forestry. 76: 413-424.

Goncalves, R., Costa, O. A. L. 2008. Influence of moisture content on longitudinal, radial, and tangential ultrasonic velocity for two Brazilian wood species. Wood and Fiber Science. 40: 580-586

Grabianowski, M., Manly, B., Walker, J. C. F. 2006. Acoustic measurements on standing trees, logs and green lumber. Wood Science and Technology. 40: 205-216.

Graff, K. F. 1975. Wave motion in elastic solids. New York, NY:Dover. 649 pp.

Herrick, G. T., Friedland, A. J. 1990. Winter desiccation and injury of subalpine red spruce. Tree Physiology. 8: 23-36.

Hillis, W., 1987. Heartwood and Tree Exudates. Springer-Verlag, Berlin, New York.

Huang, C. L., Lindstrom, H., Nakada, R., Ralston, J. 2003. Cell wall structure and wood properties determined by acoustics – a selective review. Holz als Roh- und Werkstoff. 61: 321-335.

Ilic, J. 2001. Variation in the dynamic elastic modulus and velocity in the fibre direction with other properties during the drying of *Eucalyptus regnans* F. Muell. Wood Science and Technology. 35: 157-166.

Johansson, M., Perstorper, M., Kliger, R., Johansson, G. 2001. Distortion of Norway Spruce Timber. Part 2: Modelling Twist. European Journal of Wood and Wood Products. 59: 155-162.

Johansson, M., Kliger, R., Perstorper, M. 1994. Quality and performance of structural timber. New Zealand Timber Design Journal. 9: 11-20.

Jones, T. G., Emms, G. W. 2010. Influence of acoustic velocity, density, and knots on the stiffness grade outturn of radiata pine logs. Wood and Fiber Science. 42: 1-9.

Karman, T. von. 1958. Advances in Applied Mechanics, Vol 5 pp 134. Academic Press, New York, NY.

Kliger, I. R. 2001. Spiral grain on logs under bark reveals twist-prone raw material. Forest Products Journal. 51: 67-73.

Kolsky, H. 1963 Stress waves in solids. New York, NY: Dover. 212 pp.

Larson, P. R., Kretschmann, D. E., Clark, A. III., Isebrands, J. G. 2001. Formation and properties of juvenile wood in southern pines. Forest Products Laboratory, USA. 46 pp.

Lassere, J. P., Mason, E. G., Watt, M. S. 2005. Influence of genotype and spacing on *Pinus radiata* [D. Don] corewood stiffness in an 11-year old experiment. Forest Ecology and Management. 205: 375-383.

Lassere, J. P., Mason, E. G., Watt, M. S., Moore, J. R. 2009. Influence of initial plant spacing and genotype on microfibril, wood density, fibre properties and

modulus of elasticity in *Pinus radiata* D. Don corewood. Forest Ecology and Management. 258: 1924-1931.

Lee, S. J. 1999. Improving the timber quality of Sitka spruce through selection and breeding. Forestry. 70: 123-133.

Macdonald, E., Hubert, J. 2002. A review of the effects of silvaculture on timber quality of Sitka spruce. Forestry 75: 107:138.

Macdonald, E., Mochan, S. & Connolly, T. 2001. Protocol for stem straightness assessment in Sitka spruce. Forestry Commission Information 39. Forestry Commission, Edinburgh. 8 p.

McIntosh, R. 1997. Timber quality creates marketing challenge. Forestry and British Timber, August: 17–20.

McLean , J.P. 2008 Wood properties of four genotypes of Sitka spruce . Ph.D. thesis. Department of Analytical and Environmental Chemistry, University of Glasgow, Glasgow, UK. 269 pp.

Malcolm D. C. 1997. The silviculture of conifers in Great Britain. Forestry. 70: 293-307.

Mason W. L. 2007. Changes in the management of British forests between 1945 and 2000 with possible future trends. Ibis, 149: 41–52.

Matheson, A.C., Dickson, R.L., Spencer, D.J., Joe, B. & Ilic, J. 2002. Acoustic segregation of *Pinus radiata* logs according to stiffness. Annals of Forest Science. 59: 471-477.

Meyers, M. A. 1994. Dynamic behavior of materials. John Wiley & Sons, Inc., New York, NY. 668 pp.

Mochan, S., Moore, J., Connolly, T. 2009. Using acoustic tools in forestry and the wood supply chain. Forestry Commission. FCTN018. 6 pp.

Mochan. S., Moore, J., Leslie, D. 2007. What's all the noise about? Forestry and British Timber, October, 22-24.

Moore, J. 2011. Wood properties and uses of Sitka spruce in Britain. Forestry Commission Research Report. Forestry Commission, Edinburgh. i–vi + 1–48 pp.

Moore, J. R., Achim, A., Lyon, A., Mochan, S., Gardiner, B. 2009a. Effects of early re-spacing on the physical and mechanical properties of Sitka spruce structural timber. Forest Ecology and Management 258, 1174-1180.

Moore, J. R., Lyon, A. J., Searles, G. J., Lehneke, S. A., Ridley-Ellis, D. J. In press. The effects of site and stand factors on selected properties of Sitka spruce sawn timber in the United Kingdom

Moore, J. R., Lyon, A. J., Searles, G. J., Vihermaa, L. E. 2009b. The effects of site and stand factors on the tree and wood quality of Sitka spruce growing in the United Kingom. Silva Fennica 43: 383-395.

Moore, J. R., Mochan, S. J., Bruchert, F., Hapca, A. I., Ridley-Ellis, D. J., Gardiner, B. A., Lee, S. J. 2009c. Effects of genetics on the wood properties of Sitka spruce growing in the UK: bending strength and stiffness of structural timber. Forestry. 82:491-501.

Mora, C. R., Shimleck, L. R., Isik, F., Mahon, J. M. Jnr., Clark, A. III., Daniels, R. F. 2009. Relationship between acoustic variables and different measures of stiffness in standing Pinus taeda trees. Canadian Journal of Forest Research. 39: 1421-1429.

R Development Core Team 2010. R: A language and environment for statistical computing. R Foundation for Statistical Computing, Vienna, Austria. ISBN 3-900051-07-0, URL http://www.R-project.org.

Raymond, C. A., Joe, B., Anderson, D. W., Watt, D. J. 2008. Effect of thinning on relationships between three measures of wood stiffness in Pinus radiata: standing trees vs. logs vs. short clear specimens. Canadian Journal of Forest Research. 38: 2870-2879.

Ridoutt B. G., Wealleans, K. R., Booker, R. E., McConchie, D. L., Ball, R. D. 1999. Comparison of log segregation methods for structural lumber yield improvement. Forest Products Journal. 49: 63-66.

Rollinson, T. J. D. 1987. Thinning control of conifer plantation in Great Britain. Annales des Sciences Forestières. 44: 25-34.

Ross, R. J., Pellerin, R. F. 1994. Non destructive Testing for Assessing Wood Members in Structures. A Review. Forest Products Laboratory General Technical Report, FPL-GTR-70. 42 pp.

Roth, B. E., Li, X., Huber, D. A., Peter, G. F. 2007. Effects of management intensity, genetics and planting density on wood stiffness in a plantation of juvenile loblolly pin in the southeastern USA. Forest Ecology and Management. 246: 155–162.

Sakai, A. 1970. Mechanism of Desiccation Damage of Conifers Wintering in Soil-Frozen Areas Ecology. 51: 657-664.

Saranpää, P. 2003. Wood density and growth. In: Wood Quality and its Biological Basis. Edited by J.R. Barnett and G. Jeronimidis. Blackwell Publishing Ltd. Oxford. UK: 87-117.

Seeling, U. and Merforth, C. "FRITS – a new equipment to measure distortion" European Journal of Wood and Wood Products, 2000. 58: 338-339.

SFIC. 2004. Scotland's forest industries. Scottish Forest Industries Cluster, Edinburgh. 52 p.

Simpson, H. L., Denne, M. P. 1997. Variation of ring width and specific gravity within trees from unthinned Sitka spruce spacing trial in Clocaenog, North Wales. Forestry. 70: 31-45.

Stirling, G., Gardiner, G., Connolly, T., Mochan, S., Macdonald., E. 2000. A survey of Sitka spruce stem straightness in south Scotland. Forest Research, Northern Research Station, Scotland. 56 pp.

Tseheye, A., Buchanan, A.H. and Walker, J.C.F. 2000. Sorting of logs using acoustics. Wood Science and Technology. 34: 337-344.

USDA 1999: Wood handbook — Wood as an engineering material. U.S. Department of Agriculture, Forest Service, Forest Products Laboratory, Madison, WI. FPL-GTR-113. 463 p.

Wagner, F. Gorman, T. and Wu, S. 2003. Assessment of intensive stress-wave scanning of Douglas-fir trees for predicting lumber MOE. Forest Products Journal. 53: 36-39.

Waghorn, M. J., Watt, M. S., Mason, E. G. 2007. Influence of tree morphology, genetics, and initial stand density on outerwood modulud of elasticity of 17-year-old *Pinus radiata*. Forest Ecology and Management 244, 86–92.

Walker, J. C. F. and Nakada, R. 1999. Understanding corewood in some softwoods: a selective review on stiffness and acoustics. International Forestry Review. 1:251-259.

Wang, S. Y., Chiu, C. M., Lin., C. J. 2002. Variations in ultrasonic wave velocity and dynamic Young's modulus with moisture content for Taiwania plantation lumber. Wood and Fiber Science. 34: 370-381.

Wang, S. Y., Chuang, S. T. 2000. Experimental data correction of the dynamic elastic moduli, velocity and density of solid wood as a function of moisture content above the fibre saturation point. Holzforschung. 54: 309-314.

Wang, S. Y., Lin., C. J., Chiu, C. M. 2003. The adjusted dynamic modulus of elasticity above the fiber saturation point in Taiwania plantation wood by ultrasonic-wave measurement. Holzforschung. 57: 547-552.

Wang, X. Ross, R.J., Carter, P. 2007. Acoustic evaluation of wood quality in standing trees. Part 1. Acoustic wave behavior. Wood and Fiber Science, 39: 28-38.

Wang, X., Ross, R. J., Green, D. W., Brashaw, B. K., Englund, K., and Wolcott, M. 2004. Stress wave sorting of red maple logs for structural quality. Wood Science and Technology. 37:531-537.

Wang, X., Ross, R. J., Mattson, J. A., Erickson, J. R., Forsman, J. W., Geske, E. A., and Wehr, M. A. 2001. Several non-destructive evaluation techniques for assessing stiffness and MOE of small-diameter logs. USDA Forest Service Forest Products Laboratory, Research Paper, FPL-RP-600. Madison, WI. 12 pp.

Wang, X., Ross, R. J., Mattson, J. A., Erickson, J. R., Forsman, J. W., Geske, E. A., and Wehr, M. A. 2002. Nondestructive evaluation techniques for assessing modulus of elasticity and stiffness of small-diameter logs. Forest Products Journal. 52:79-85.

Wang, X., Ross, R. J., McClellan, M., Barbour, M. J., Erickson, J. R., Forsman, J. W., and McGinnis, G. D. 2000. Strength and stiffness assessment of standing trees using a non-destructive stress wave technique. USDA Forest Service, Forest Products Laboratory Research Paper, FPL-RP-585. Madison, WI. 9 p.

Waring, R. H., Running, S. W. 1998. Forest Ecosystems: Analysis at multiple Scales. Academic Press, San Diego. 370 pp.

Watt, M. S., Moore, J. R., Facon, J-P., Downes, G. M., Clinton, P. W., Coker, G., Davis, M. R., Simcock, R., Parfitt, R. L., Dando, J., Mason, E. G., Brown, H. E. 2006. Modelling the influence of stand structural, edaphic and climatic influences on juvenile *Pinus radiata* dynamic modulus of elasticity. Forest and Ecology Management. 229: 136-144.

Wielinga, B., Raymond, C.A., James, R., Matheson, A.C. 2009. Effect of green density values on *Pinus radiata* stiffness estimation using a stress-wave technique. New Zealand Journal of Forestry. 39:71-79.

Xu, P., Walker, J. C. F. 2004. Stiffness gradients in radiata pine trees. Wood Science and Technology. 38: 1-9.

Zhang, H., Wang, X., Su, J. 2011. Experimental investigation of stress wave propagation in standing tree. Holzforschung. 65: 743-748.

Zwick Roell, http://www.zwick.co.uk/en/products. (last accessed 10/6/2011)